ADIPOGENESIS WITHIN A HOLLOW FIBER-BASED, THREE-DIMENSIONAL DYNAMIC PERFUSION BIOREACTOR

by

Danielle Marie Minteer

B.S. in Bioenginering, University of Pittsburgh, 2010

Submitted to the Graduate Faculty of

Swanson School of Engineering in partial fulfillment

of the requirements for the degree of

PhD in Bioengineering

University of Pittsburgh

2015

UNIVERSITY OF PITTSBURGH

SWANSON SCHOOL OF ENGINEERING

This dissertation was presented

by

Danielle M. Minteer

It was defended on

March 2, 2015

and approved by

Jorg C. Gerlach, MD/PhD, Professor, Departments of Surgery, Bioengineering,

University of Pittsburgh

David Kaplan, PhD, Professor and Chair, Department of Bioengineering, Professor,

Department of Chemical Engineering, Tufts University

J. Peter Rubin, MD, Endowed Professor and Chair, Department of Plastic Surgery,

Professor, Department of Bioengineering, University of Pittsburgh

Yadong Wang, PhD, Professor, Departments of Bioengineering, Chemical Engineering,

Mechanical Engineering and Materials Science, and Surgery, University of Pittsburgh

Dissertation Director: Kacey G. Marra, PhD, Associate Professor, Departments of Plastic

Surgery and Bioengineering, University of Pittsburgh.

ADIPOGENESIS WITHIN A HOLLOW FIBER-BASED, THREE-DIMENSIONAL DYNAMIC PERFUSION BIOREACTOR

Danielle Marie Minteer, PhD

University of Pittsburgh, 2015

Adipose-derived stem cells (ASCs) represent a promising cell source in the field of tissue engineering and regenerative medicine. Due to the wide availability and multipotent ability of ASCs to differentiate into tissues such as bone, cartilage, muscle, and adipose, ASCs may serve a wide variety of regenerative medicine applications. Accordingly, ASCs have been utilized in studies addressing osteoarthritis, diabetes mellitus, heart disease, and soft tissue regeneration and reconstruction after mastectomy and facial trauma. Traditional, static, two-dimensional cell culture of ASCs do not allow for mature adipocyte differentiation or long-term maintenance of adipocytes *in vitro*. In order to study metabolic diseases, such as type II diabetes mellitus, a three-dimensional scaffold for *in vitro* adipocyte maintenance is necessary.

In collaboration with the Bioreactor Laboratory at the McGowan Institute for Regenerative Medicine, our laboratory has developed the use of a hollow fiber-based bioreactor for three-dimensional, dynamic perfusion of ASCs and adipose tissue formation *ex vivo*, creating a stable system in which long-term culture of adipocytes is

possible, providing a model useful for potential drug discovery and tissue engineering applications, specifically those addressing type II diabetes mellitus. The studies presented in this dissertation aim to assess metabolic activity and differentiation of ASCs from patients with or without type II diabetes in the bioreactor system; engineer a long-term culture environment relevant to physiological type II diabetic and non-diabetic conditions *ex vivo*; optimize tissue growth homogeneity; enhance adipogenesis within the bioreactor culture with the use of a decellularized adipose extracellular matrix (ECM) hydrogel.

ASCs derived from patients with type II diabetes at time of isolation were found to behave metabolically similar and appear architecturally comparable to those derived from patients without type II diabetes mellitus when differentiated and maintained as adipocytes in the bioreactor system. When cultured at a physiologically relevant glucose level matching that of healthy patients or patients with type II diabetes, ASCs were able to proliferate, differentiate into adipocytes, and be maintained within the bioreactor system for at least one week. A decellularized adipose ECM hydrogel was established and applied to the bioreactor cultures; however, due to technical challenges, no firm conclusions can be made.

The microenvironment by which ASCs are surrounded is critical for cell differentiation and growth. Engineering and control of such microenvironment is possible within the hollow fiber-based, three-dimensional, dynamic perfusion bioreactor culture system, proving to be a promising model for potential drug discovery and therapeutics. Future directions include further evaluation of ASC differentiation and adipocyte metabolism within type II diabetic environments, application of established

decellularized adipose ECM hydrogels to wound healing treatments and adipose graft volume retention.

TABLE OF CONTENTS

LIST OF TABLES

LIST OF FIGURES

ACKNOWLEDGEMENTS

Thank you to Dr. Kacey Marra, my primary PhD advisor, PI over the past eight and a half years, and mentor. Not only has Dr. Marra contributed to the work presented in this dissertation, but has allowed me countless opportunities within the laboratory to grow as a student, scientist, and team leader. I owe infinite gratitude towards Dr. Marra for taking me in as a nineteen year-old undergraduate student and immediately challenging me to develop my own protocols, mentor fellow students, and assist with several different projects, then eventually inviting me to join the laboratory for my Ph.D. studies. For the better part of the past decade, Dr. Marra has taught me how to think independently and scientifically, and what it takes to be a strong, encouraging, and passionate leader and mentor. Without her, this dissertation could never have existed.

I would like to acknowledge the Department of Bioengineering for providing me with the opportunity to study at the University of Pittsburgh as an undergraduate student in 2006 and to continue my studies as a Ph.D. student. In particular, I want to thank Dr. Borovetz and Dr. Shroff for the incredible amount of support and guidance they provide to all students in the department and for constantly striving towards making the department the best it can be. Additional thanks are due to graduate student administrator, Nick Mance, for all of the helpful assistance he has provided over the past four and a half years. I am extremely grateful for the immense project guidance and mentorship of my committee members: Dr. J. Peter Rubin, Dr. Jorg Gerlach, Dr. David Kaplan, and Dr. Yadong Wang.

1.0 INTRODUCTION

1.1 ADIPOSE TISSUE

1.1.1 Adipose Tissue Biology and Function

Understanding of adipose-derived stem cell (ASC) biology is imperative to advance adipose-based therapies into clinical practice. Adipose tissue is present in all mammalian species and some non-mammalian species, and is located in: subcutaneous tissues, the intraperitoneal compartment (visceral fat surrounding organs), and diffusely throughout the body as padding for vital structures [1]. Brown adipose tissue is highly functionally specialized and abundant in mammalian infants where it functions to maintain body heat. This mitochondria rich brown fat is sparse in adults but can be found in the thorax and neck [2, 3]. This thesis will focus on white adipose tissue. Components of adipose tissue involve mostly mature lipid laden adipocytes, and supporting tissue types: blood vessels, lymph nodes, nerves, and stromal-vascular cells.

Adipose tissue is derived from the mesoderm, along with other migratory cells, including the dermis, bone and cartilage, and the circulatory system [Fig. 1]. Adipogenesis the process of adipocyte maturation and subsequent fat tissue generation – involves proliferation of adipose stem cells (adipose precursor cells also known as preadipocytes) followed by the differentiation of the cells into mature adipocytes.
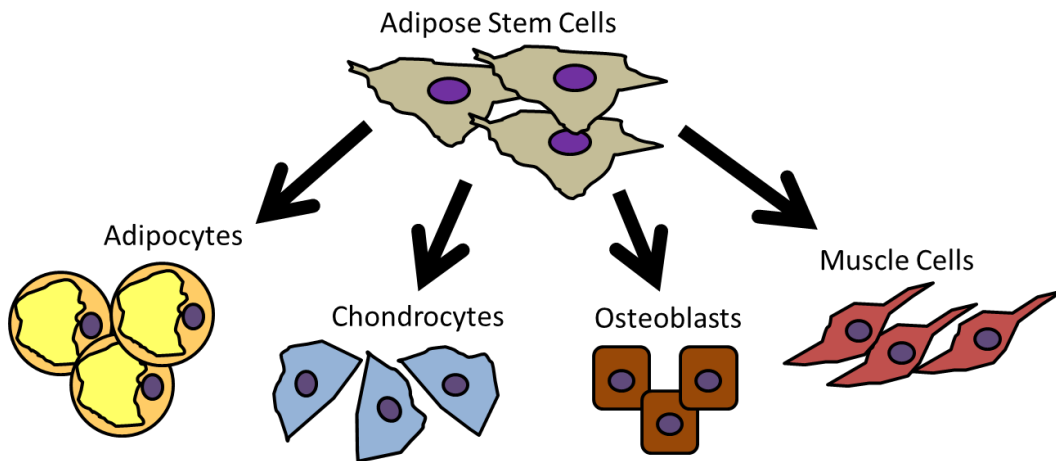
Figure 1. Multilineage Capacity of ASCs. Derived from th emesenchymal germ line, adipose stem cells hold the multipotentiality to differentiate into adipocytes, chrondrocytes, osteoblasts, or muscle cells with the addition of proper growth factor and under appropriate culture conditions. Image from Minteer, et al. [4].

Proliferation and differentiation of ASCs are controlled via hormonal, neuronal, and paracrine pathways [1]. Specifically, thyroid hormones and glucocorticoids have been found to enhance development of adipocytes in rats [5, 6] and porcine, which are more comparable to human fetuses during development [7-9]. Furthermore, a glucocorticoid analogue, dexamethasone, is a widely accepted enhancer of preadipocyte recruitment and differentiation when incorporated with insulin [7]. The use of insulin and dexamethasone is currently being studied as a method of inducing regenerating adipose tissue for reconstructive surgeries at the University of Pittsburgh [10]. The main paracrine signal, which triggers adipocyte proliferation and differentiation, is insulin-like growth factor-1 (IGF-1) [7]. IGF-1 has been proven to directly increase preadipocyte

replication and differentiation in cell lines and neutralizing IGF-1 antibodies blocks adipogenesis in primary cultures [11-17].

Adipose tissue is critical for maintaining energy metabolism through storage of lipid, a task carried out by the mature adipocytes as a response to specific circulating hormones. Adipose function is multifactorial, encompassing endocrine functions, glucose metabolism, and lipid metabolism. These functional mechanisms overlap and interact with surrounding tissues and capillaries in addition to influencing energy homeostasis throughout the entire organism [18]. Over fifty biochemical products are secreted by adipocytes, often with factors characteristic to different fat depots. The endocrine function of the adipocyte releases factors important to steroid metabolism such as tumor necrosis factor-α (TNF-α), interleukin-6 (IL-6), monocyte chemotactic protein (MCP-1), plasminogen activator inhibitor-1 (PAI-1), adiponectin, resistin, leptin, and angiotension. Several receptors are expressed on adipocytes for proteins involved in endocrine metabolism as well [19, 20].

Adipocytes store lipid in the form of triglycerides, which are presented to the adipocyte in the form of a glycerol molecule and three fatty acid chains. Once the free fatty acids are transported into the adipocyte, triglycerides are reformed and stored inside the lipid droplet. Hormone sensitive lipase and lipoprotein lipase regulate triglyceride entry, storage, and release in the adipocytes. Knowledge of adipocyte biology and function, in addition to the key factors involved with endocrine, glucose, and lipid metabolism is necessary for the study of obesity and the several chronic diseases associated with adipose tissue [4].

3

1.1.2 Obesity and Ties to Chronic Diseases

Obesity remains an ever-growing pressing health issue in developed countries and is rapidly approaching epidemic status in the United States. Using body mass index (BMI) [Eqn. 1], "overweight" describes those with a calculated BMI between 25 and 30, while "obese" classifies those bearing a BMI greater than 30:

$$BMI = \frac{mass(kg)}{(height\ (m))^2}$$ [Equation 1]

According to the United States Centers for Disease Control and Prevention, approximately 35.8% of American adults and 18% of adolescents ages 6-11 years were obese in 2010, a steady increase since 1962 when 13% of Americans were obese [21]. Including obesity, 69% of American adults over the age of 20 were overweight in 2011 [21].

It is known that obesity can induce chronic diseases such as coronary artery disease, degenerative arthritis, type 2 diabetes mellitus, gall bladder disease, gout, hypertension, infertility, restrictive lung disease, stroke, and various types of cancers [22-26]. Diseases influenced by obesity are characterized by abdominal, visceral fat deposits, causing an "apple shape" [26] (Fig. 2). Such an effect is known as the metabolic syndrome.

Figure 2. Metabolic Syndrome. Derived from [26].

Adipose tissue does function as an endocrine organ in addition to its glucose and lipid storage functions. As adipocytes increase in size and a person gains weight, several molecular and cellular changes occur and ultimately influence whole-body metabolism. Horowitz et al., identified higher free fatty acid (FFA) and glycerol levels in obese women compared to lean women, suggesting a promotion of insulin resistance – the primary cause of type 2 diabetes [27, 28]. In addition to FFAs, several proinflammatory factors are secreted by adipose tissue, with especially strong presence in those with obesity. TNF-α, IL-6, MCP-1, transforming growth factor-β (TGF-β), plasminogen activator inhibitor type I, tissue factor and factor VII are all elevated in obese individuals as compared to those with lean BMIs (< 20) [22, 29].
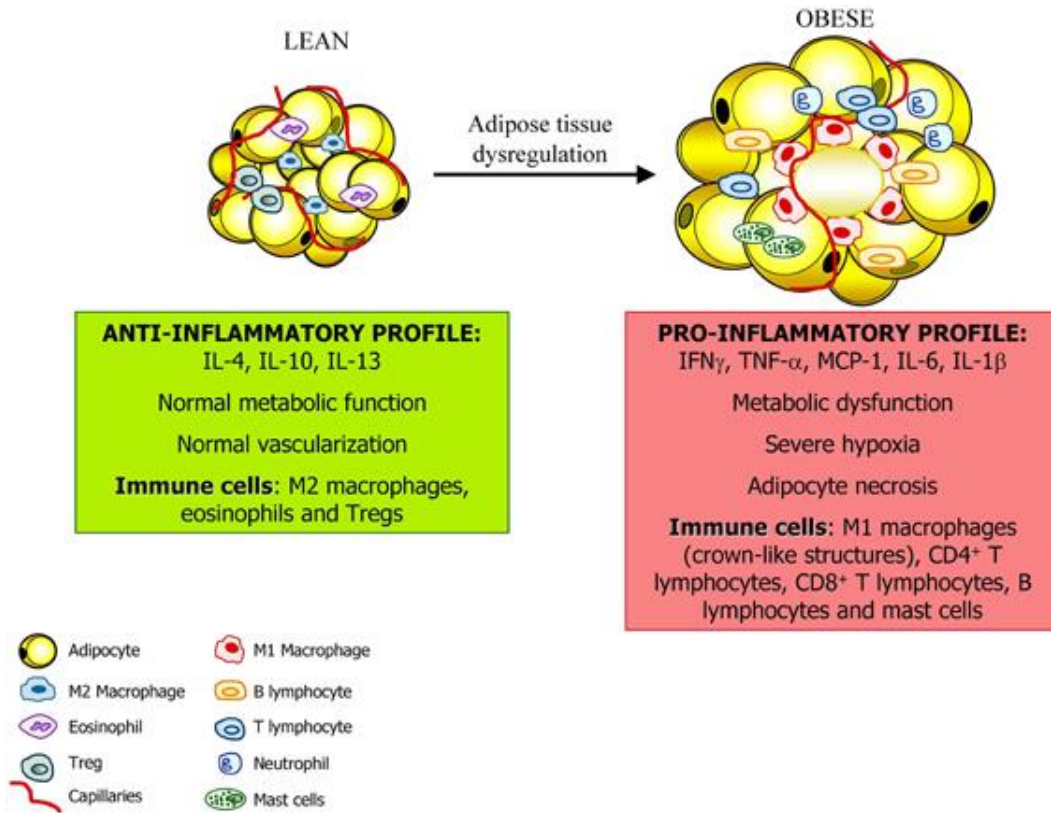
Figure 3. Endocrine Organ Functions of Adipose Tissue. Derived from Catalan et al. [29].

Adipose tissue is present throughout the mammalian body, whether under the skin to provide insulation, or surrounding organs serving as padding and protection. While diseases such as type 2 diabetes and degenerative arthritis were traditionally thought to be diseases of the pancreas and heart, respectively, relatively recent discoveries of fat additionally functioning as an endocrine organ, it is clear that expansion and proliferation of adipose tissue indeed affects whole-body homeostasis.

1.1.3 Clinical Applications

ASCs can be isolated from human adipose tissue and hold high potential to differentiation into mature adipocytes and other tissue types along the mesenchyme lineage, including chondrocytes, osteoblasts, skeletal and cardiac muscle [30-52]. Differentiation of ASCs into mature adipocytes has been studied in bioreactors – rotating wall (with and without microcarriers) and three-dimensional hollow fiber membrane-based – as methods of long-term adipocyte culture and high throughput screening tools for drug discovery [53, 54]. However, one of the most promising and rapidly advancing clinical applications of ASCs lies in the field of clinical soft tissue regeneration and reconstruction [55-62].

1.1.4 Diabetes Mellitus

Two types of diabetes mellitus exist: type I and type II. While this thesis focuses on type II diabetes mellitus rather than type I, it is important to acknowledge the differences between the two diseases. Broadly, patients with type I diabetes have a lack of insulin as a result of an autoimmune disorder which destroys the pancreatic β-cells that release insulin. Eventually, insulin production from the body is eliminated, leaving the adipose, liver, and muscle unable to consume glucose used to create energy. Patients with type I diabetes are typically diagnosed in childhood and must take insulin, either via injection or pump, throughout their lifetimes in addition to testing their blood sugar multiple times per day. Type I diabetic patients are encouraged to carefully balance their diet and exercise to aid in blood sugar level regulation.

Unlike type I, type II diabetes mellitus may develop at any age and accounts for 95% of diabetic patients. Type II diabetes is characterized by insulin resistance, a condition in which the body is able to produce insulin but the adipose, liver, and muscles are unable to absorb glucose [Fig. 4]. This results in an elevated level of blood glucose, signaling β-cells to increase insulin production. Over time, the β-cells cannot maintain the amount of insulin necessary for glucose uptake; additionally, the insulin receptors on adipocytes become exhausted. Insulin resistance is further described in section 3.1.1. of this thesis. Type II diabetes is preventable and reversible through lifestyle changes including diet and exercise regulation. Patients diagnosed with prediabetes and type II diabetes are prescribed to first make the necessary lifestyle changes, then to combine with oral medications. If blood sugar control is not improved, oral medication in combination with insulin is prescribed.
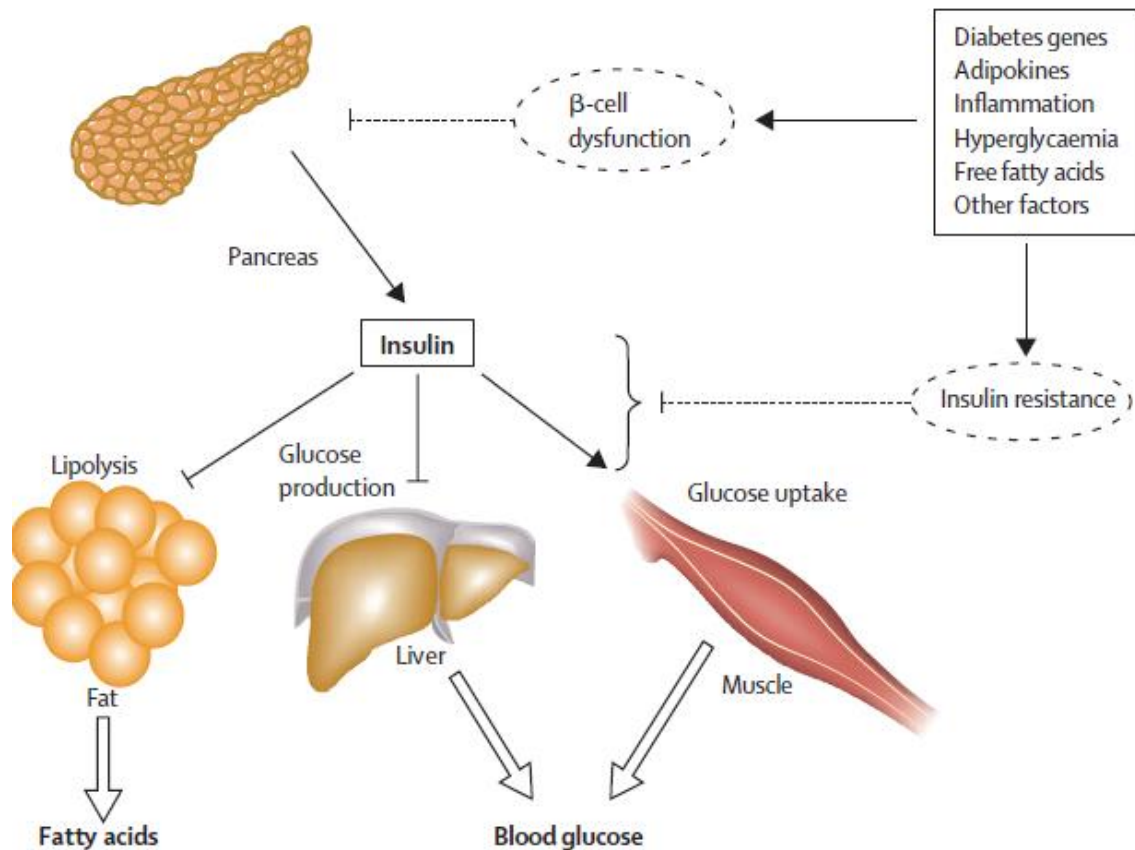
Figure 4. Physiology of insulin resistance in type II diabetes [63]. In healthy patients, insulin secretion from the pancreas reduces glucose output by the liver and increases glucose uptake by the skeletal muscle and adipose tissue. Less insulin secretion reduces insulin signaling in target tissues, leading to an increase in fatty acid circulation and elevated blood glucose levels.

1.2 ADIPOSE-DERIVED STEM CELLS

1.2.1 ASC Isolation and Culture Conditions

Standardized protocols to isolate adipose-derived stem cells from human adipose tissue are in place in many laboratories, including the Adipose Stem Cell Center at the University of Pittsburgh [55, 56]. Discarded adipose tissue from elective surgeries is

collected from the operating room. Whole fat tissue is chopped by hand with sterile scissors until finely minced. The mechanical processing step is not necessary for lipoaspirate, which is already in particulate form following harvest. To remove the fibrous, collagen content of the tissue, a collagenase solution is added to the minced fat and shaken at 37 °C until a fatty supernatant is clearly visible within the solution. Typically, after 25-30 minutes, a fatty layer rises and the tissue-collagenase solution should be centrifuged for 10 minutes at 1000 rpm at 4 °C. Next, the supernatant/fatty layer is aspirated and the pellet resuspended in an erythrocyte lysing buffer to remove any red blood cells. Filtering and washing steps are performed with centrifugation at 1000 rpm, 4 °C, for 10 minutes. The resultant SVF pellet is can be re-suspended, cultured, and assessed for functional capacity [62]. ASCs will adhere to the surface of an untreated flask after approximately 6 hours incubation at 37 °C and 5% CO_2. Once ASCs have adhered to the culture flask surface, non-adherent populations are washed away with sterile phosphate buffered solution and fresh culture media added to the flask. Essential points in the ASC isolation protocol are highlighted in Figure 5.

A commonly used ASC expansion media consists of a DMEM and DMEM/F12media combination, with 10% serum, some form of antibiotic (typically penicillin/streptomyocin), and typically a miniscule amount of dexamethasone, which prevents any differentiation into another mesenchymal lineage, such as osteoblasts.
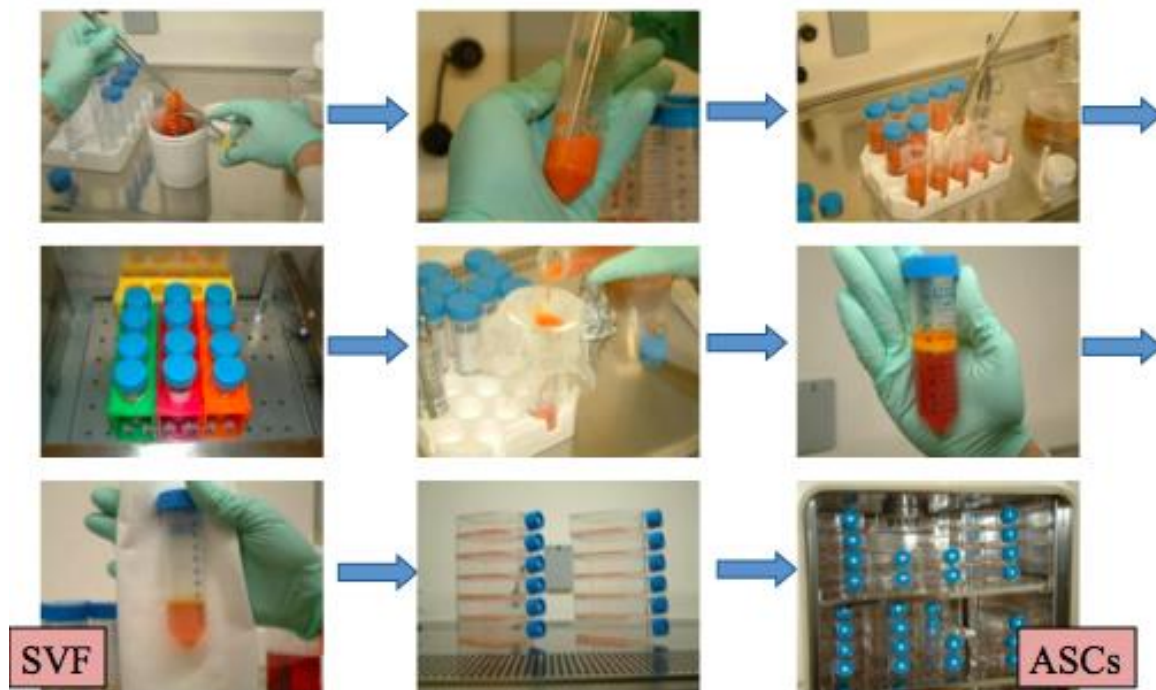
Figure 5. The SVF and ASC isolation process as described by Rubin and Marra [49]. First, whole adipose tissue or lipoaspirate is finely minced and enzyme digested in at 37 °C. Red blood cells are lysed and the suspension is filtered. Following centrifugation, the pellet is considered the stromal vascular fraction. Once plated and cultured on a tissue culture flask at 37 °C and 5% CO_2 for 6-8 hours, the mesenchymal ASCs are obtained. Adapted with permissions from Rubin and Marra [56].

1.2.2 Differentiation Potential of ASCs

"Pre-adipocytes" were first described over 40 years ago, first in rat models [64, 65] and then isolated from human tissues in 1976 by Dardick et al., [66]. Isolated pre-adipocytes were used to study adipocyte biology *in vitro* and different anatomic locations and adipose depots became known to express different biological characteristics such as adipocyte size and lipolytic potential [65]. In 2001, Zuk et al. first published the

11

plasticity of differentiation of pre-adipocytes [30]. The stem cell features of "preadipocytes" became accepted and the term "adipose-derived stem cells" was given to encompass their characteristics of self-renewal, asymmetric division, and multipotency. Over the past decade, several researchers have studied ASCs' ability to differentiate both *in vitro* and *in vivo*. While ASCs typically proliferate quite well in culture, high concentrations of growth factors are necessary to induce lineage specific differentiation. Differentiation of ASCs to other mesenchymal phenotypes has been well established both *in vitro* and *in vivo* [30-43, 53-58, 67-69] while differentiation of ASCs to cell lines of the ectodermal [32, 39, 44-46] and endodermal [47-51] germ layers has been studied, evidence often putative to show successful achievement of the desired phenotype.

It is imperative to note that both the SVF and ASC populations derived from tissues are not pure populations; numerous cell types exist within the SVF and ASC populations, confirmed by cell surface markers identified by flow cytometry [61, 68]. Zimmerlin et al. identified several similar cell surface markers in ASCs compared to bone marrow-derived stem cells and are described in Table 1. Li, et al. described four subpopulations of ASCs within the final stem cell pool cultured *in vitro* [68]. The first subpopulation is a CD31+/34- population classified as "mature endothelial," with the endothelial marker of CD31 but lacking the progenitor marker of CD34. The second subpopulation is classified as "endothelial stem," and both CD31+/34+. A third subpopulation consisted of CD34+/31- and is classified as the "adipose stem cell" group. The final subpopulation, as described by Li, et al., represents a "pericyte group" and isCD146+/90+/31-/34-. These cells reside adjacent to the endothelial cells, as demonstrated by immunostaining [37]. As with bone marrow-derived stem cells, ASCs

do not express MHC-II and do inhibit proliferation of activated peripheral blood mononuclear cells, suggesting a role for modulating the immune system in inflammatory disorders or allogeneic transplantation [67].

The immunomodulatory potential of mesenchymal stem cells (MSCs), particularly, ASCs, make them an attractive tool in cell therapy protocols for the treatment of inflammatory-related diseases such as rheumatoid arthritis or multiple sclerosis [70-72]. Specifically, MSCs possess the ability to suppress T cell responses and modify dendritic cell differentiation, maturation and function; MSCs are not inherently immunogenic and do not induce alloreactivity to T cells and freshly isolated natural kill (NK) cells [73]. A 2014 study further confirmed ASC T helper (Th) type Th1/Th2 cytokine profiles as well as their ability to inhibit lymphocyte proliferation in culture. Sempere et al. found a heterogeneous cytokine production profile, heterogeneous capabilities to produce lymphocytes and NK cells [70].

Studies identifying SVF and ASCs as heterogeneous populations emphasize the importance of defining subpopulation potential. Planat-Bénard, et al. cultured the SVF from human adipose tissue in vitro and determined that a population spontaneously differentiated into cardiomyocytes without the addition of growth factor [31]. Zimmerlin, et al., identified several similar cell surface markers in ASCs (the cultured population) compared to bone marrow-derived stem cells (BMSCs) and are described in Table 1 [4, 62]. Cardiomyocytes were identified by morphology and confirmed by expression of cardiac-specific markers, immunohistochemistry straining, and ultrastructural analysis. The need for cardiomyocyte differentiation without the use of controversial, difficult to culture embryonic stem cells is of high demand in the field of

13

cardiac regeneration. The Planat-Benard et al. group later utilized adipose-derived stem cells in the form of a "cell sheet" in the rat [74] and non-human primate [75] chronic myocardial infarction model. The finding is certainly valuable in the field of cardiac engineering and identifying a source of cardiomyocyte progenitors has been of great interest for therapeutic models targeted towards myocardial infarction.

Table 1. Surface Marker Characterization of ASCs and BMSCs.

Restated from Minteer et al. [4], where ASCs were freshly isolated and examined via flow cytometry [62].

	Adipose-Derived Stem Cells	Bone Marrow Stem Cells
Negative	CD38, CD45, CD106, HLA-DR, DP, DQ (MHC Class II), CD80, CD86, CD40, and CD40L (CD154).	CD34, CD38, CD45 and fox antigens involved in immunological signal transduction such as HLA-DR, DP, DQ (MHC Class II), CD80, CD86, CD40, and CD40L (CD154).
Positive	CD13, CD29, CD34, CD44, CD73, CD90, CD105, CD166, MHC Class I, HLA-ABC.	CD13, CD29, CD44, CD73, CD90, CD105, CD166, MHC Class I, HLA-ABC.

1.2.3 Challenges in ASC Culture

A major challenge of utilizing ASCs derived from human tissue lies in the variation between specimens harvested from different patients and also different subcutaneous depots in the same patient. Schipper et al. studied ASCs from five different subcutaneous adipose depots in 12 female patients (similar BMI), split into three age

ranges: 25-30, 40-45, and 55-60 years [52]. The five subcutaneous depots studied were upper arm, medial thigh, trochanteric, superficial abdominal, and deep abdominal. The goal was to determine a group of cells most suitable for soft tissue reconstruction applications. It was found that ASCs from younger patients proliferated at a faster rate than the ASCs isolated from older patients and apoptosis of ASCs was found to be lowest in younger patients and from the superficial abdominal depot in all age ranges. While lipolysis varied in age and depot, the cells from the patients in the youngest age range had the highest activity in each adipose depot. The functional superiority of ASCs from younger patients and/or the superficial abdominal depot may have implications for tissue engineering applications.

The role of gender and anatomical region on osteogenic differentiation of ASCs has also been studied *in vitro* [69]. ASCs isolated from the superficial and deep adipose layers of male and female patients were exposed to osteogenic differentiation medium for time points of 1, 2, and 4 weeks. Through alkaline phosphatase, alizarin red, and Masson's Trichrome staining, as well as ELISA and Western blot analysis, the group was able to determine that no significant difference in the amount of osteogenic differentiation exists in both fat depots from females, while the superficial depot in the male provided ASCs that differentiated sooner and more efficiently than ASCs from the deep fat depots. Furthermore, it was established that male ASCs differentiated more effectively into osteoblasts than female ASCs from all depots.

For large-scale culture experiments specifically examining adipogenesis, the murine 3T3-L1 cell line can be a useful model when consistency of cells is needed

overtime. These cells can be easily differentiated into adipocytes when stimulated with the proper conditions *in vitro* [67].

1.2.4 Pre-Clinical Models

There are several animal models that are useful for the examination of adipose tissue engineering, and the mouse model has been the most widely examined [43, 44-47, 51]. The effects of species, strain, gender, implant configuration and implant location are all essential parameters when examining mesenchymal stem cells in preclinical studies [62]. When examining stem cell survival and behavior in small animals, there are two logical models for the researcher. One model is to utilize a nude, or athymic, animal, which will not reject human tissue or cells. The athymic nude mouse is maintained as an outbred specific, originated from the NIH. It lacks a thymus, is unable to produce T cells and is, therefore, immunodeficient. Without the thymus, athymic nude mice have a much reduced lymphocyte population composed almost entirely of B-cells and a greatly increased susceptibility to infection [76-79]. Stimuli are still capable of activating the macrophage of thymic deficient mice; mononuclear cells are present and macrophage function is enhanced [80, 81]. This is ideal for those examining the clinically relevant human cell, tumor biology and xenograft research. The second model involves injecting autogenous or syngeneic cells derived from the mouse. For example, this would entail isolating a population of cells from the strain of inbred mice, and injecting those cells into the mouse model. There are advantages and disadvantages of both of these approaches. Either option could result in a shortage of cells, depending on the mesenchymal stem cell

source. A second disadvantage of the nude mouse model is that it will not result in a similar response to that of the human response.

After the animals have been injected with stem cells, it can be challenging to identify and characterize the implanted cells. One method of quantification involves using pre-labeled cells. Cells can be labeled with cell membrane dyes such as PKH26 or using viral technology, such as green fluorescent protein (GFP) labels using lentiviral vectors. The expression of cell membrane dyes decreases with each cell doubling, and the dye could possibly leach into other cells. GFP-labeled cells, however, tend to remain stable throughout the lifetime of the animal. Finally, one can utilize immunostaining to identify the implanted cells. A challenge with immunostaining, however, is the potential for cross-reactivity of antibodies with both human and animal tissue.

1.3 BIOREACTORS

1.3.1 Bioreactor Trends in Tissue Engineering

Traditionally, bioreactors are utilized for various biochemical engineering applications and bioprocesses. For example, a bioreactor to support microbial growth using a vessel to convert nutrients that organisms extract from the culture media into biological compounds. Current topics of investigation include quantifying energy production and monitoring biosynthesis and product formation throughout experimentation.

In 2006, Bilodeau and Mantovani defined bioreactors in tissue engineering and regenerative medicine as "any apparatus that attempts to mimic and reproduce

physiological conditions to maintain and encourage cell culture for tissue regeneration" [82].   Through recent advances within the biomedical arena, bioreactors have been applied to create a cell culture environment more physiologically representative than 2-dimensional cell culture [54, 82-100]. Traditional cell culture typically involves plating the isolated cells on a flat surface, usually a Petri dish or tissue culture treated flasks, and supplementing the cells with a nutrient media. Cells are stored, statically, at37 °C with exposure to 5% carbon dioxide.

Opposed to 2-dimensional static culture, cells can be differentiated into 3-dimensional tissue structures within a bioreactor, making possible several potential applications including microgravity environments [91, 92] and long-term tissue culture [54] attributes that are further described in this thesis and used as a defining characteristics of a "bioreactor." Several classes of bioreactors exist in the biomedical field, and applications vary with bioreactor classification, as bioreactor design influences tissue formation and behavior.   The "E-Cube System" from Corning may allow the culture to be explanted and incorporated into an in vivo model (Fig. 6C).   Dynamic perfusion bioreactors deliver continuous, dynamic perfusion of nutrients and gas exchange to the tissue growing within [87]. The dynamic perfusion bioreactor has been used to culture various tissue types, including cartilage [94] bone [95], adipose [54], and neuronal [83].
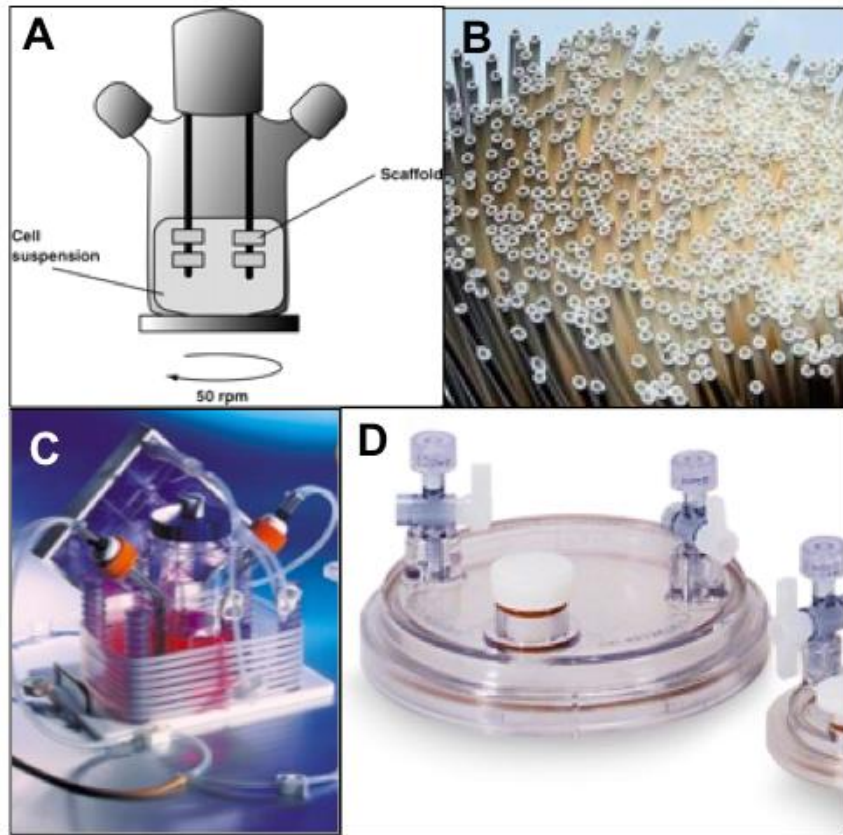
Figure 6. Common bioreactors for tissue engineering. A) Spinner flask diagram [101], B) polyethersulfone hollow fiber membranes [102], C) E-cube system by Corning [103], D) rotating wall vessel [104].

Cells in dynamic perfusion bioreactor cultures grow and attach to an interconnected network of porous, polymeric fibers inside the bioreactor chamber while the nutrient medium is continuously recirculated throughout the system [93]. In addition to cell culture, the dynamic perfusion bioreactor has served as a "bridge to transplant" for patients on the ever-growing transplant lists. Irgang et al developed an extracorpeal bioartificial liver support system in a 3-dimensional, hollow, fiber-based bioreactor to successfully treat patients with porcine liver cells prior to liver transplantation with no known negative immunologic responses or infection [96]. Dynamic perfusion bioreactor

studies in the same German bioreactor laboratory are ongoing with Miki et al. and include differentiating human embryonic stem cells into human hepatocytes within the 3-dimensional culture system, further addressing drug discovery, toxicology studies, and bioartificial liver support systems [97].

In 2008, Brayfield et al. reported application of a hollow fiber scaffold towards directing neurite outgrowth and neuronal cell networking *in vitro* [84]. Polyethersulfone (PES) microporous hollow fibers were albated with krypton fluoride (KrF) excimer laser to generate specifically designed channels for directing neurite outgrowth into the luminal compartments of the fibers. Laser modification to PES membranes resulted in increased hydrophobicity and laminin adsorption on the surface compared with the unmodified PES surface, further correlating to PC12 cell adhesion. PC12 cells differentiated on the laser-created channels, providing a spontaneous cell process growth into the channels of the scaffold wall while preventing entrance of cell bodies. These results suggest the laser-modified PES fibers could be used in combination with perfusion and oxygenation hollow fiber membrane sets to construct a 3D bioreactor for controlling and studying *in vitro* neuronal networking [84].

For other tissue culture models, a more simplistic spinner flask model is commonly used. The spinner flask bioreactor consists of a bottle of culture medium, well mixed by a magnetic stir bar, with the tissue matrix fixed to needles attached to the top lid or floating in the media suspension [93]. Bioreactors with rotating wall vessels involve angular movement of polymeric cylinders within an encasing while the tissue is positioned between the cylinders on biomaterial scaffolds. Alternatively, rotating bioreactors involve movement or rotation of the entire bioreactor system as a whole.

Rotation of the system introduces continuous free fall to the culture, improving nutrient transport to the tissues as well as a more homogenous tissue growth [93].

The requirements for engineering a rotating bioreactor vary based on the tissue to be studied and clinical need to be addressed. Korossis et al stated that, "the overall goal is to have systems that reliably and reproducibly form, store, and deliver functional tissues that can sustain function in vivo." Biomolecularly, variables include metabolic activity of the tissue, biochemical growth factors, and oxygenation to the tissue matrix. Regarding bioprocesses, considerations of a rotating bioreactor include angular velocity, angle of rotation, removal of cellular waste products, time points, and which phase of culture the bioreactor should rotate. Each consideration is a function of the dimensions of the tissue, including concentration of cells at initial inoculation; complexity and, therefore, the physiological environment required of the tissue; and stages of cellular differentiation and maintenance. In addition, the consideration of continuous perfusion to the system contributes complexity to the system, particularly when scale-up is in question [93]. Bioreactors are also commonly utilized in tissue engineering to mechanically precondition tissue and biomedical devices before implanting *in vivo* [98-100].

1.3.2 Bioreactors in Diabetes Mellitus Applications

While exact mechanisms of diabetes mellitus are still under speculation, it is widely accepted that both type I and type II diabetes are characterized by the transport of glucose from blood to cells, a consequence of β-cell failure in the pancreas [105]. Simply, β-cell apoptosis in type I diabetes mellitus is activated, in part, by cytokines produced by invading immune cells. Type I diabetic patients closely monitor insulin

21

levels throughout their entire lifetime and, while an inconvenience, glucose levels in type I diabetic patients are relatively manageable. Alternatively, β-cell death in patients can result with type II diabetes mellitus occurs more gradually. β-cell dysfunction of type II diabetic patients results from elevated levels of glucose and free-fatty acids (FFAs) and, along with other factors, eventually leads to β-cell apoptosis [105].

Patients diagnosed with type II diabetes mellitus are instructed to monitor their blood glucose levels through blood glucose monitoring devices in combination with lifestyle adjustments and management. If the diabetic symptoms progress, oral medication, and possibly insulin, is prescribed. Type II diabetes is often associated with cardiovascular disease risk factors, including elevated blood pressure and cholesterol levels, gall bladder disease, degenerative arthritis, gout, infertility, restrictive lung disease, stroke, and various types of cancers [24-27].

According to the Centers for Disease Control and Prevention, diabetes mellitus affected 29 million, or 9.3% of, United States residents in 2012, a national burden of $245 billion [106]. As diabetic diagnoses and associated symptoms continue to escalate in industrialized countries, further understanding of the disease becomes more significant. One of the first known groups to establish a microgravity environment for cell culturing purposes was a team within the National Aeronautics and Space Administration (NASA) Johnson Space Center in the late 1980's. The NASA team removed almost all shear forces traditionally applied to a cell culture system, forcing the cells to assemble in suspension and form a three-dimensional tissue matrix [107]. VivoRx, a Santa Monica-based pharmaceutical company, licensed the rotating vessel bioreactor technology in the early 1990's for therapeutic and diagnostic commercial applications. Due to short supply

of pancreas cadavers, VivoRx intended to use the device to grow sufficient volumes of human islet cells as an answer to the expanding diabetic market. In 1997, VivoRx reported commencement of FDA-approved Phase I/II clinical trials [108]. The license was later retracted by NASA and Synthecon currently owns licensing rights. The rotating wall vessel (RWV) is commercially available and widely accepted as a three-dimensional culture condition option. In a 2012 update, Barzegari et al., specifically outline microgravity tissue engineering and diabetes applications [109]. The reviewers explain that microgravity has been proven to enhance survival and proliferation of beta islet cells in addition to reducing immunogenicity [110-112].

The RWV system has since provided inspiration to many three-dimensional bioreactor culture models useful in diabetes mellitus applications [112-116]. A horizontally-rotating high aspect ratio vessel is described by Murray et al. to improve structural and functional viability of isolated human islet cells within the microgravity environment [113]. Throughout a ten-day period, structural integrity and glucose-stimulated insulin release were maintained in islets cultured within the system, compared to islets cultured under conventional standards. Islets cultured conventionally were reported to exhibit progressive fragmentation and a rapid loss of secretory function. Furthermore, the authors noted that islets cultured within the microgravity environment were able to re-aggregate and exhibit enhanced secretory capacity [113].

Samuelson and Gerber [114] apply the microgravity concept to a pancreatic progenitor cell population in a three-dimensional culture system. The researchers developed a RWV bioreactor consisting of a pivoting platform to rotate around a fixed point, with motor-controlled rotation power and revolution speed. Cell cultures were

contained in transparent fluoroethylene propylene closed culture bags with Cytodex-3 microcarrier beads along with beta-TC-6 cell lines added in culture media suspensions. Bags were continuously rotated on the bioreactor platform and nutrient media was manually changed two times per week. Cultures were maintained for 5 and 12 days within the RWV bioreactor and the pancreatic cell line proliferated robustly with enhanced transcriptional signaling and improved translation of the insulin gene. The authors propose a future for the novel device in the potential cell-based therapy for treatment of diabetes [114].

Tanaka et al., more recently describe optimization of a cell culture technology using a simulated microgravity generator to induce development of a large amount of pancreatic beta-cell spheroids [115]. Via the described methods, 100 spheroids of 250-micrometer diameters per 1 milliliter of culture media are produced. The spheroids were transplanted *in vivo* into the portal vein of streptozotocin-induced diabetic mice and lowered glycemic levels were observed over 28 days. The spheroids cultured in the microgravity bioreactor expressed several β-cell signature genes at higher levels than the levels found in the cells cultured in a standard 2D culture dish. Transplantation of the spheroids into the portal vein of the streptozotocin-induced diabetic mice amerliorated hyperglycemia, whereas the 2D cultured cells did not have a significant effect [115].

In addition to the RWV bioreactor, hollow fiber bioreactors [117, 118] have been developed to address type I diabetes mellitus therapeutics as well as spinner flask bioreactors with islet cells in suspension [119]. Hoesli et al., developed a mammalian cell immobilization in alginate-filled hollow fiber bioreactors for large-scale batches [117]. The model was successfully applied to primary neonatal pancreatic porcine cell

culture for 10 days. The authors describe potential future study directions that include donor-scale immobilized mammalian cell culture with cell recovery, such as *in vitro* culture of islet-like clusters for use in islet transplantation [117].

Due to the vast mechanical and pathological difference in the cause of type I versus type II diabetes mellitus, it is only logical for therapy and treatment of the two diseases to also vary significantly. Since type II diabetes mellitus is typically tied to other health complications, many tissue engineers have taken to bioreactor technologies to address the diseases' symptoms and characteristics, including diabetic retinopathy [120] and foot wound ulcers [121, 122]. Dutt et al., apply the horizontally rotating bioreactor developed by NASA to establish a co-culture of human retinal cells and bovine endothelial cells incorporated onto laminin-coated Cytodex-3 microcarrier beads over 36 days [120]. The bioreactor was reported to accelerate capillary formation as well as differentiation of retinal precursor cells. With such neovascularization modeling, the bioreactor system could provide an ideal three-dimensional platform to study retinal diseases, including diabetic retinopathy [120].

One common characteristic to diabetes mellitus is the metabolic syndrome, which is influenced by obesity and characterized by abdominal, visceral adipose deposits, causing an "apple shape" [26]. Adipose plays a dominant role in diabetes mellitus as adipocytes contain FFAs and release hormones that even further increase FFAs, high levels of which are toxic to β-cells and lead to dysfunction. As adipocytes increase in size and mass, macrophages accumulate and cause inflammation, increasing a patient's risk to develop diabetes [20]. In muscle and adipose tissues, glucose transporter 4 (GLUT4) is responsible for the transportation of glucose from intracellular stores to the

25

plasma membrane [123]. Therefore, metabolism and blood glucose monitoring are widely studied in applications addressing type II diabetes mellitus [124].

Two particular studies observe the stomach as a bioreactor [123, 124]. Kanner and Lapidot simulated possible reactions that could occur in the acidic pH environment of the stomach that could affect lipid peroxidation [125]. The study hypothesized that prevention of overall lipid peroxidation in the stomach could have an important impact on health and may aid in explaining health benefits of diets rich in polyphenolic antioxidants. Acidic pH of gastric fluid amplified lipid peroxidation and incubation of heated muscle tissue in simulated gastric fluid enhanced hydroperoxide accumulation by 6-fold over 2 hours. The authors suggested that human gastric fluid might be an excellent medium for enhancing the oxidation of lipids and other dietary constituents [125]. Similarly, Gorelik et al., evaluated hydroperoxide and malondialdehyde levels of the stomach during and after digestion in rats [126]. Rats were fed either A) red turkey meat cutlets or B) red turkey meat cutlets and red wine concentrate and stomachs were analyzed 90 minutes after feeding. The study tested the hypothesis that the stomach can act as a bioreactor, in which lipid peroxidation of partially oxidized food (such as red meat and red wine) could occur, resulting in accumulation of lipid peroxidation products. Results indicated that stomach hydroperoxide and malondialdehyde concentrations both dropped substantially 90 minutes after meals and the addition of red wine polyphenols enhanced hydroperoxide reduction by 3-fold. The authors conclude that addition of antioxidants such as red wine polyphenols to meals may reduce potentially harmful effects of oxidized fats in foods [126].

Other additional work has been conducted on lifestyle management factors for patients with diabetes [127, 128]. Sook et al., optimized a stable cell culture condition within a packed-bed bioreactor for production of tagatose, a novel bulk sweetener which tastes similar to sucrose with potential to be used as a low-calorie sweetener in foods, beverages, health foods, and dietary supplements [127]. Ho et al., developed a long-life capillary enzyme bioreactor for highly sensitive determination of blood glucose concentration [128]. While the aforementioned studies focus on lifestyle, the presented thesis addresses adipose behavior and adipose function in culture and how it relates to diseases such as type II diabetes mellitus.

Table 2. Bioreactor Technologies Addressing Diabetes Mellitus [129].

Authors	Bioreactor Type	Application
Chick et al., 1980	Microgravity rotating wall	Pancreatic cell culture
Reach et al., 1990	Hollow fiber membrane	Kinetic modeling, vascular bioartificial pancreas
Todisco et al., 1995	Hollow fiber membrane	Controlled insulin release
John Wong, 1997	NASA microgravity rotating wall	Transplantation of encapsulated islet cells, VivoRx
Naughton et al., 1997	Closed system	Dermagraft characterization; diabetic wound ulcers
Kanner et al., 2001	Stomach model	Dietary lipid peroxidation and effects of plant-derived antioxidants
Kenmerrer and Bagley, 2002	Closed system	Dermagraft scale-up; diabetic wound ulcers
Rutsky et al., 2002	Microgravity	Immunogenicity and functional testing of pancreatic islets
Dutt et al., 2003	NASA horizontal rotating	3D co-culture of human retinal cells with bovine aortic endothelial cells for diabetic retinopathy
Murray et al., 2005	Rotational cell culture system	Glucose responsiveness of human islets
Sook et al., 2005	Packed-bed	Tagatose production
Chawla et al., 2006	Suspension	Production of islet-like structures from neonatal porcine pancreatic tissue
Stepkowski et al., 2006	Microgravity	Tolerance of dendritic cells to pancreatic islet allografts depleted of donor dendritic cells
Ho et al., 2007	Capillary enzyme	Blood glucose determination
Papas et al., 2007	Stirred microchamber	Pancreatic islets, oxygen consumption rate measurements
Gorelik et al., 2008	Stomach model	Food oxidation/antioxidation
Hoeli et al., 2009	Alginate-filled hollow fiber	Large-scale production cellular therapies
Lu et al., 2011	Hollow fiber	3D culture of hepatocytes
Samuelson & Gerber, 2013	Rotating wall vessel	Function and growth testing of a pancreatic cell line
Tanaka et al., 2013	Three-dimensional microgravity culture system	Pancreatic beta-cell spheroid generation

1.4 LIMITATIONS OF PREVIOUS RESEARCH AND SUMMARY

1.4.1 Limitations in Adipocyte Culture Methods

Traditionally, primary ASCs are cultured on flat two-dimensional tissue culture-treated flasks; although, once differentiation into adipocytes is induced, the cells undergo morphological changes and float on top of the medium due to their high lipid content. Adipocytes floating on top of the culture medium leads to the adipocyte clumping together, rendering them unable to reach equal and sufficient access to nutrient medium. As a result, the majority of adipocytes undergo cell lysis within 72 hours. To overcome this challenge, in 1986, Sugihara et al. first laid the groundwork of culturing adipocytes using a ceiling culture method [130]. Sugihara et al. isolated human adipocytes, plated on tissue culture flasks, and filled the flasks entirely with culture medium, ensuring an air-free environment. The culture flasks were turned upside side so that the cells would float to the top and adhere to the top inner surface (ceiling surface) of the flasks. When the cells firmly attached, the flasks were then turned so that the cells were on the bottom inner surface and could be easily observed. After 7-10 days in culture, the cells became multi-ocular (opposed to the uniocular lipid droplet defining mature white adipocytes), indicating de-differentiation [130]. Using the work discovered by Sugihara et al., other teams have studied adipocytes in modified ceiling cultures involving a floating glass surface [131] and adipocyte function [132].

In order to differentiate ASCs to adipocytes and maintain for time periods of days to weeks, a three-dimensional scaffold is necessary. Groups have studied the

differentiation of ASCs into adipocytes in natural [90, 133-135] and synthetic [136-138]

three-dimensional scaffolds, while few have studied the capacity of cell lines to

differentiate into adipocytes in three-dimensional scaffolds [139-142]. Additionally,

several studies have utilized the 3D scaffold culture for successful ASC differentiation

into osteoblast and chondrocyte lineages [143-151]. The studies are described further in

Table 3. While the above work has built the foundations on adipocyte culture, the next

step towards fully understanding adipose tissue's role in diseases such as obesity and type

II diabetes mellitus is to apply the three-dimensional cultures to study adipocyte behavior

and functionality in diabetic environments.

Table 3. Three-dimensional scaffolds for adipose tissue engineering.

Reference	Cell	Differentiation	Scaffold Material
Flynn 2007	Primary ASCs	Adipogenic	Decellularized human placenta and crosslinked hyaluron
Halbleib 2002	Primary ASCs	Adipogenic	Hyaluronic acid
Mauney 2007	Primary ASCs	Adipogenic	Silk fibroin
Masuoka 2006	Primary ASCs	Chondrogenic, Osteogenic, Adipogenic	Atelocollagen honeycomb-shaped
Patrick 1999	Primary ASCs	Adipogenic	Poly (lactic-co-glycolic) acid (PLGA)
Kral 1998	Primary ASCs	Adipogenic	Fluortex-expanded polytetrafluoroethylene
Rubin 2007	Primary ASCs	Adipogenic	Collagenous microbeads
Green 1974	3T3-L1	Adipogenic	Methyl cellulose
Green 1975	3T3-L1	Adipogenic	Methyl cellulose
Kang 2005	3T3-L1	Adipogenic	Polyethylene terephthalate
Kang 2007	Embryonic stem cells	Adipogenic	Polycaprolactone

Utilizing three-dimensional perfusion culture systems surpasses the limitations of two-dimensional culture through the advantages of providing uniform nutrient and gas exchange with more physiological gradients and integral oxygenation. Additionally, bioreactor designs based on interwoven sets of semi-permeable hollow fibers employ a bicarbonate buffer system and CO_2 gas exchange to enable pH regulation to the entire cell compartment volume with negligible shear stresses. Such three-dimensional perfusion culture bioreactors offer a better environment for sustained long-term cultures of cell types without requiring mechanical stimuli [54].

Figure 7 depicts adipose tissue generated within a hollow fiber-based three-dimensional perfusion bioreactor (Fig. 7B and D) compared to ASCs differentiated to the adipocyte lineage in a two-dimensional tissue culture flask (Fig. 7A and C). The Oil Red O in Figure 7A and B represents lipid and is much more noticeable and defined in samples taken from the three-dimensional perfusion bioreactor than from the ASCs differentiated in two-dimensional culture. Similarly, the H&E in Figure 7C and D highlights oil architecture from the two-dimensional differentiated cells but mature adipose tissue from the samples extracted from the bioreactor.
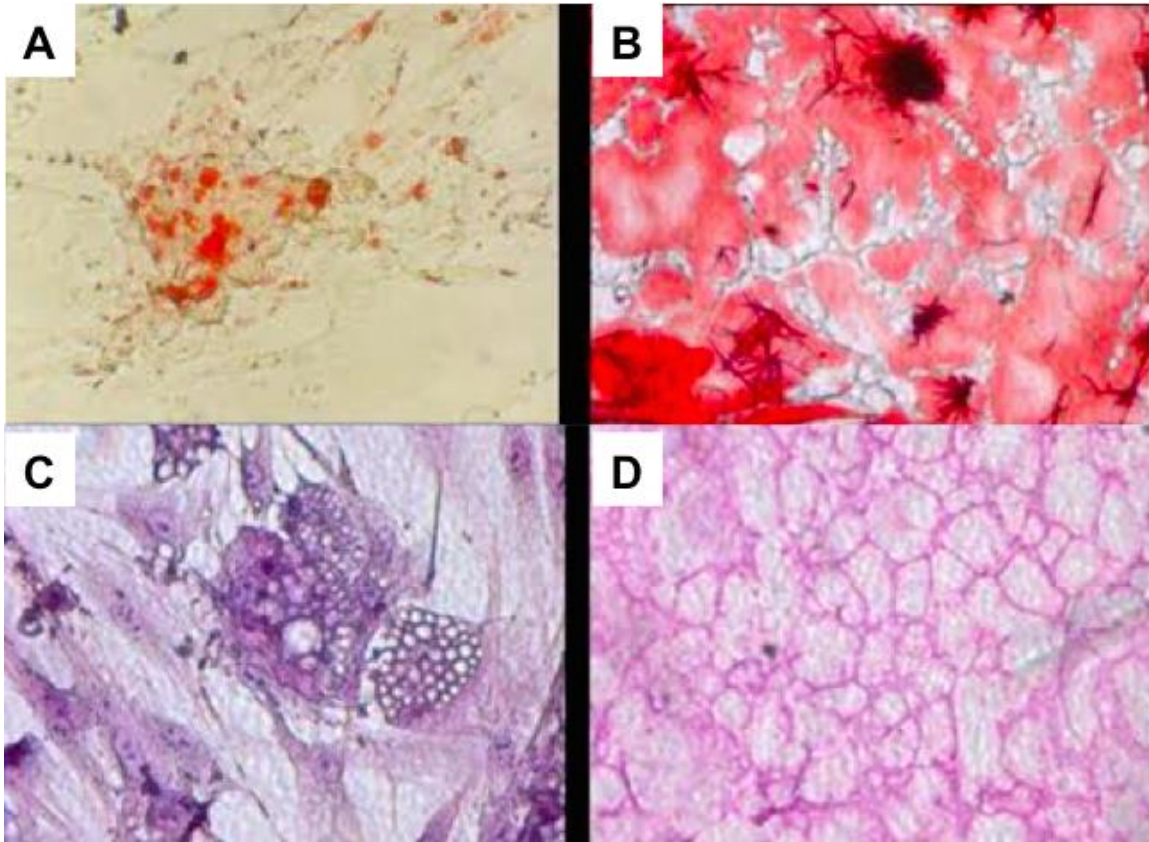
Figure 7. Oil Red O and H&E. A). Oil Red O stain of ASCs cultured in two dimensions on traditional tissue culture flasks, B) Oil Red O stain of extracted adipose tissue cultured within a three-dimensional dynamic perfusion bioreactor; C) H&E of ASCs cultured in two dimensions on traditional tissue culture flasks, D) H&E of extracted adipose tissue cultured within a three-dimensional dynamic perfusion bioreactor.

1.4.2 Challenges in Isolating Tissue from Diabetic Adult Donors

To better understand high impact diseases such as type II diabetes and obesity, the study of adipose tissue, metabolism, and the correlations to whole-body homeostasis and insulin/glucose production are necessary. However, obtaining and culturing adipose tissue from patients with type II diabetes mellitus is a challenge on many accounts.

Obese patients with type II diabetes provide high risks to undergo cosmetic surgery, and other surgical procedures, such as a gastric bypass, do not yield adequate amounts of adipose tissue to harvest and culture ASCs in high numbers.

While our laboratory has previously modeled insulin resistance in the adipose bioreactor over a time period of four hours via introduction of tumor necrosis factor-α (TNF-α) to the system, long-term presence of TNF-α would prove toxic to the tissue. Therefore, an engineered model of type II diabetes mellitus environment *ex vivo* is necessary to study ASC and adipose tissue behavior prior to utilization of such a model towards any anti-diabetic drug discovery study. Additionally, a major limitation of studying adipocyte biology exists in the lack of long-term culture models for monitoring adipocyte behavior. While adipocytes are able to cultured in two dimensions via ceiling culture, time points extending longer than 7-10 days are not possible due to dedifferentiation [130]. In order to address endocrine diseases such as type II diabetes, deeper assessment of adipocyte metabolism and functionality *in vitro* is necessary.

1.4.3 Summary

Adipose tissue, developed from the mesoderm, is vital as insulation and protection to mammalian organisms, but also as an endocrine organ [7, 19, 20]. As the presence of obesity ever increases in developed countries, a continuous learning and understanding of the relationship between adipose tissue, inflammation, and metabolic diseases remains critical. The study of adipose-derived stem cells both *in vitro* and *in vivo* has provided a great deal of information to the behavior and potency of the stem cells, cell culture has been thoroughly established, and has provided several applications

in soft tissue reconstruction. Human ASCs in culture experience differences influenced by regional and anatomic locations, gender, and health; as a result, the murine 3T3-L1 cell line is commonly utilized [52, 152, 153]. The most common pre-clinical model of engineering ASCs involves the mouse model in addition to GFP-labeling the cells as a method of characterization.

Bioreactors pose influential and pivotal roles in tissue engineering and regenerative medicine, providing a longer, more accurate *in vitro* cell culture, shaping drug discovery and tissue explants. Every bioreactor system is unique and several biomolecular and bioprocess parameters must be taken into consideration prior to each tissue engineering application.

With diabetes mellitus on the rise in developed countries, countless studies are being conducted worldwide to address treatments and therapies to both types, I and II. Several pieces of work incorporating bioreactors into type I diabetes mellitus research include pancreatic cell line development and culture within a three-dimensional microgravity environment for long-term maintenance and assembly. Conversely, bioreactor studies addressing type II diabetes mellitus appear to focus on lifestyle management and the side effect diseases associated with type II diabetes.

While the use of bioreactors for pancreatic cell culture dates back to 1980 [154], the field has been validated, modified, and optimized over the past few decades; including kinetic modeling [155], mass transfer of insulin and glucose [156], oxygen consumption rate of islet culture [157], to list only a few. Indeed, much room for advancement continues to exist in the field, fusing alterations on a classic biochemical

engineering tool and the fundamental yet constantly growing biomedical issue of diabetes mellitus.

1.5 SPECIFIC AIMS AND HYPOTHESES

In collaboration with the Bioreactor Laboratory in the McGowan Institute for Regenerative Medicine, our groups have developed an *ex vivo* three-dimensional, dynamic perfusion model to study adipose tissue function, resulting in the long-term culture (e.g. > 70 days) of metabolically active human adipose tissue derived from adult human patients [54]. Within the model, interwoven hollow fiber capillary bundles serve as physically active scaffolds for cell immobilization, where multi-compartment technology allows decentralized but high-performance mass exchange including integral oxygenation.

The specific aims and hypotheses were designed to systematically examine adult human adipocyte function in an established, three-dimensional dynamic perfusion *ex vivo* bioreactor culture model as a potential tool for drug discovery.

Specific Aim1: To analyze metabolic behavior and differentiation of ASCs derived from patients with type II diabetes mellitus within a hollow fiber-based, three-dimensional dynamic perfusion bioreactor. The work performed towards Aim 1 is described in Chapter 2.

Hypothesis: Adipose tissue culture and ASC differentiation is guided by environmental cues and, when exposed to similar culture environments, ASCs isolated from patients

with type II diabetes mellitus will behave similarly to ASCs isolated from patients without type II diabetes mellitus.

Specific Aim 2: To establish a method to develop a physiologically relevant culture environment defined by a hindered insulin-dependent glucose uptake of cultured human adult adipose tissue within the bioreactor system. The work performed towards Aim 2 is presented in Chapters 3.

Hypotheses: ASCs can be differentiated and maintained as adipocytes at a physiological glucose concentration. Stimulation by C2-Ceramide will inhibit insulin-stimulated glucose uptake of the adipocytes within the bioreactor system.

Specific Aim 3: To further enhance the adipose tissue *ex vivo* by optimizing homogeneity within the bioreactor culture. The work performed towards Aim 3 is reported within Chapter 4.

Hypothesis: Inclusion of a decellularized, adipose tissue extracellular matrix (ECM) hydrogel within the *ex vivo* bioreactor culture system will enhance ASC differentiation to the adipocyte lineage and improve adipose tissue homogeneity within the bioreactor.

2.0 METABOLIC BEHAVIOR AND DIFFERENTIATION OF ADIPOSE-DERIVED STEM CELLS FROM PATIENTS WITH TYPE II DIABETES MELLITUS WITHIN A HOLLOW FIBER-BASED, THREE-DIMENSIONAL, DYNAMIC PERFUSION BIOREACTOR.

2.1 INTRODUCTION

2.1.1 Type II Diabetes Mellitus

Type II diabetes and obesity have recently become epidemics in developed countries. According to the Centers for Disease Control and Prevention, diabetes affects 25.8 million people in the United States, or 8.3% of the country's population, and 35.7% of American adults are considered to be obese [158, 159]. As the nation's obesity rate continues to escalate, further understanding on the role of adipose tissue in disease states becomes more significant.

Both types I and II diabetes mellitus are characterized by the lack of insulin-stimulated glucose transport from blood to tissue, a consequence of β-cell failure in the pancreas [105]. Simply, type I diabetes mellitus is a result of β-cell apoptosis activated by cytokines produced by invading immune cells. Type II diabetic patients experience β-cell dysfunction resulting from elevated levels of glucose and free-fatty acids (FFAs), consequences of increased adipocyte size and body mass [20]. Healthy levels of insulin cannot adequately transport the elevated amount of glucose into muscle, fat, and liver to

be broken down into energy. In response, β-cells of the pancreas become exhausted producing more insulin, eventually leading to β-cell apoptosis in addition to the high glucose and insulin levels in the bloodstream [160]. Insulin resistance is a defining characteristic of the pre-diabetic state and typically precedes type II diabetes development unless a drastic lifestyle change is enforced involving extreme weight less and physical activity.

2.1.2 Bioreactor Design

The multi-compartment bioreactor system utilized in the presented thesis involves two interwoven networks of porous hollow-fiber membrane polysulfone bundles intended for medium perfusion and a third interwoven network of oxygenation hollow fibers on which the cells are seeded and cultured, providing a decentralized oxygenation and uniform nutrient and gas exchange with physiological gradients to the tissue (Fig. 8) [54].

The extracapillary space forms a compartment in which cells are inoculated; the total cell compartment inside the three-dimensional hollow fiber-based bioreactor volume is 8 mL. Run via external perfusion systems and pumps, the continuous media perfusion and gas flow through the system can be tailored and have been optimized, based on several previous reports on such bioreactors used for hepatocyte progenitors and embryonic stem cell cultures [161-165]. The bicarbonate buffer system and carbon dioxide gas exchange regulate pH of the entire cell compartment volume with negligible shear stress, creating a permitting environment for sustained, long-term cultures of tens of millions of cells without mechanical stimuli [54]. Previous work further explaining the

38

development of such bioreactor system as applied to adipocyte culture is featured in Gerlach, et al [54].
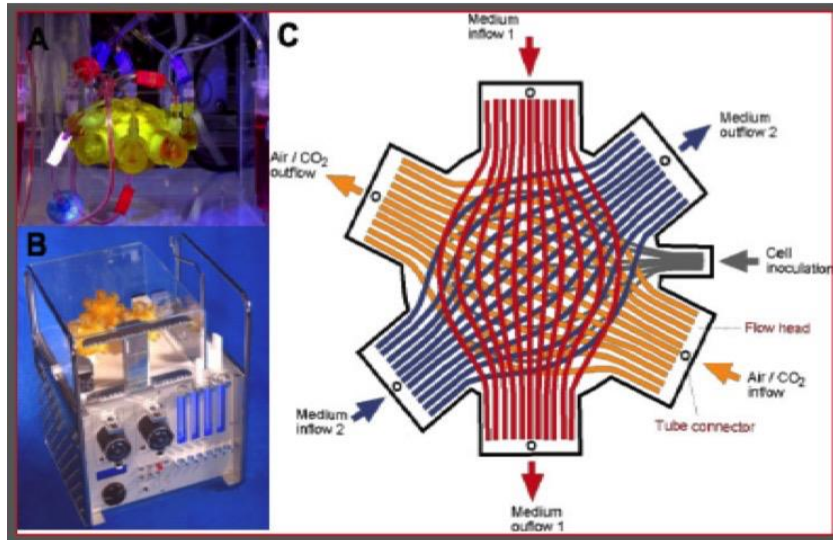
Figure 8. Hollow fiber-based bioreactor setup. A) Photograph of an 8 mL-volume hollow fiber-based bioreactor used; B) Bioreactors incorporated onto the perfusion system and pumps as utilized in the presented work; C) Schematic of nutrient/gas flow in and out of the bioreactor cell compartments through the porous, hollow fiber membranes [54].

2.1.3 Chapter Aims

The work described in this chapter aims to develop a reproducible, *ex vivo* process to study the metabolic activity and adipogenesis of human ASCs within a hollow fiber-based bioreactor for three-dimensional perfusion to function as a potential model for drug discovery, specifically type II diabetes mellitus. The studies in Chapter 2 hypothesize that adipose tissue culture and ASC differentiation is guided by environmental cues and, when exposed to similar culture environments, ASCs isolated from patients with type II diabetes mellitus will behave similarly to ASCs isolated from patients without type II

diabetes mellitus. Presented work includes the analysis and comparison of metabolic behavior and functionality of human ASCs isolated from adult patients with type II diabetes and non-diabetic patients. Such ASCs cultured and differentiated into adipocytes within a three-dimensional, hollow fiber-based bioreactor is presented.

2.2 MATERIALS AND METHODS

2.2.1 ASC Isolation

Adipose tissue was harvested from the abdominal depots of type II diabetic female patients (39 and 62 years old, body mass index (BMI) of 27.4 and 32.0, respectively) and from female patients without diabetes (55 and 25 years old, BMIs of 25.5 and 28.6, respectively), all undergoing elective plastic surgery at the University of Pittsburgh Medical Center in Pittsburgh, PA, USA. Tissue was collected under a human studies exempt protocol approved by the University of Pittsburgh Institutional Review Board (IRB). The University of Pittsburgh waived the need for written informed consent from the participants under an exempt review and approval process. Samples were not pooled between diabetic and non-diabetic patients rather; cells from two separate diabetic samples were combined in one instance to provide sufficient number of cells required for optimal inoculation and cell-to-cell communication within the bioreactor (Table 4, Bioreactor #4). Non-diabetic patients were not pre-diabetic and did not have insulin resistance at time of adipose tissue harvesting.

Abdominal adipose tissue was placed in 50 mL centrifuge tubes at 10 g per tube and soaked in 1 mg·mL^{-1} of freshly prepared collagenase (Type II collagenase,

Worthington Biochemical Product Catalog; Lakewood, NJ, USA). The tissue was finely minced, vortexed, and shaken at 37 °C for 35 minutes until a fatty supernatant layer became apparent. Tubes were again vortexed and filtered through double-layered gauze (J&J Steri-Pad Gauze Pads; New Brunswick, NJ, USA) into sterile 50 mL centrifuge tubes. Digested specimens were then centrifuged at 1000 rpm (6449 x g), 4 °C for 10 minutes, fatty layers aspirated, and resulting pellets suspended in erythrocyte lysing buffer. The solution was once again centrifuged at 1000 rpm (6449 x g), 4 °C for 10 minutes and the pellet, containing the stromal vascular fraction, was resuspended in Dulbecco's Modified Eagle's Medium (DMEM/F12) with 10% v/v fetal bovine serum and 1% v/v penicillin/streptomycin, plated, and stored at 37 °C at 5% CO_2. Cells were expanded in two dimensions using growth medium with low serum (Promocell Preadipocyte Growth Medium, Heidelberg, Germany), passaged at confluency, and characterized as previously described by our laboratory [56].

2.2.2 Bioreactor Inoculation

The bioreactors are prototyped by Stem Cell Systems (Berlin, Germany) and contain three independent hollow fiber membrane systems, interwoven into repetitive subunits, forming a cell compartment that houses 8.0×10^7 cells with a volume of 8 mL (Fig. 7). The capillary network serves three functions: cell oxygenation/carbon dioxide removal, medium inflow, and medium outflow via countercurrent flow operation of two independent membrane systems. As a result of interweaving and high performance mass exchange via counter-current medium flow operation, decentralized gas supply and medium exchange with low gradients is provided to the cultures. The medium fiber

membrane systems are made of polyethersulfone capillary systems (Membrana, Wuppertal, Germany) with a molecular weight cutoff of 400,000 g·mol^{-1} and gas is supplied by hydrophobic multi-laminate hollow fiber membrane systems (MHF; Mitsubishi, Tokyo, Japan).

A total of six bioreactor experiments were performed: three bioreactors cultured with ASCs from females diagnosed with type II diabetes mellitus at time of surgery, and three bioreactors cultured with ASCs from healthy, non-obese, females without type II diabetes. Bioreactor sterilization was performed with ethylene oxide gas and degassed with air. Before cells were introduced into the system, a continuous phosphate buffered solution flush was run within the bioreactor for 72 hours, followed by priming with DMEM/F12 media flush for 24 hours prior to inoculation. Cell suspensions of 8.0×10^{7} total cells per bioreactor were inoculated and cultured throughout a time period of six weeks. The cell compartments were continuously perfused with culture media through the polyethersulfone hollow fiber bundles at a feed rate of 4 mL·hr^{-1} in combination with a recirculation loop at a rate of 20 mL·min^{-1}. Waste medium was removed from the circuit at 4 mL·hr^{-1}. The flows of compressed air and carbon dioxide in the gas compartment were maintained at 20 mL·min^{-1}. Partial pressures of oxygen, carbon dioxide, and acid/base status within the bioreactor were measured daily and the carbon dioxide content was adjusted throughout culture time to maintain the medium pH within the range of 7.35-7.45.

Table 4. Patient age, gender and BMI relative to diabetic state at time of ASC isolation used for bioreactors in Specific Aim 1.

Bioreactor #	Patient Age	Gender	BMI	Diabetic?	Patient #	Cell Passage #
1	35	Female	28.6	No	1	3
2	55	Female	25.5	No	2	3
3	55	Female	25.5	No	2	3
4	62	Female	32.0	Yes	3	5
4	39	Female	27.4	Yes	4	5
5	39	Female	27.4	Yes	4	5
6	39	Female	27.4	Yes	4	5

2.2.3 Cell Culture

Cells were inoculated into the bioreactor cell compartments via a suspension of 8.0×10^7 cells per mL of medium. Cell passages at time of inoculation for each experiment were either passage 3 or 5 and are described in Table 4. Upon completion of a twenty-one day expansion period of the ASCs within the bioreactor cell compartment by perfusion of ASC plating media (DMEM/F12 as described above), to initiate three-dimensional adipogenic differentiation, the feed media was changed for the following fourteen days to adipogenic media containing DMEM/F12, HEPES, biotin, pantothenate, human insulin, dexamethasone, 3-isobutyl-1-methylxanthine (IBMX), PPAR-γ agonist, and antibiotics (ZenBio, Research Triangle Park, NC, USA). Adipocytes were maintained for seven days with feed media containing DMEM/F12, HEPES, fetal bovine serum, biotin, pantothenate, human insulin, dexamethasone, and antibiotics (ZenBio). Cells were not further passaged within the bioreactor; rather, cell fate was influenced by changes in culture medium.

In parallel, ASCs in a two-dimensional control group were cultured in 175 cm^2 tissue culture flasks with ASC plating medium containing 10% v/v fetal bovine serum and 1% v/v penicillin/streptomycin, plated, and stored at 37 °C at 5% CO_2. 2D control ASCs were cultured for three weeks, with static media changes every other day and passaged at 80% confluency. 2D controls were stored for gene and protein assessment.

2.2.4 Metabolic Activity Analysis

Glucose production and consumption of the cells throughout culture within the bioreactors was assessed under a dynamic open-circuit system. A sampling volume of 2 mL was taken daily via a luer-lock sample port; glucose and lactate dehydrogenase levels measured (YSI 2300 STATE Plus Glucose & Lactate Analyzer; YSI Life Sciences, Yellow Springs, OH, USA; Quantichrom Lactate Dehydrogenase Kit; BioAssay Systems, Hayward, CA, USA).

Glucose production/consumption rates of the cells were determined by a previously established protocol considering various parameters including measured glucose concentration within the recirculation sample, total system volume, baseline medium concentrations, flow rate of nutrients through the system, and time points of measurements [161-165, Eqns 2 and 3].

$$R_c = f * \left(\frac{C_a + C_b}{2} - C_f\right) + V * \left(\frac{C_a - C_b}{t_a - t_b}\right) \qquad [2]$$

$$R_p = f * \left(\frac{C_a + C_b}{2}\right) + V * \left(\frac{C_a - C_b}{t_a - t_b}\right) \qquad [3]$$

R_c: Consumption rate at t_a ($t_a > t_b$); mg·min^{-1}
R_p: Production rate at t_a ($t_a > t_b$); mg·min^{-1}
C_a and C_b: Measured concentrations (recirculation at t_a and t_b); mg·dL^{-1}
C_f: Concentration of feed medium; mg·dL^{-1}
f: Feed rate; mL·min^{-1}
V: Volume of system; mL

2.2.5 Tumor-Necrosis Factor-α Functional Testing

After seven days of maintenance, adipocytes within all six bioreactor cultures underwent exposure to 10 ng·mL^{-1} direct injection of tumor necrosis factor (TNF)-α (Roche Applied Sciences, San Francisco, CA, USA) intended to inhibit glucose uptake by the adipocytes. TNF- α exposure lasted for 24 hours and glucose production was measured every 30 minutes. Feed inlet and waste outlet flow rates were set to 10 mL·hr^{-1} to ensure that the entire circuit volume was replaced every hour. Throughout TNF-α exposure, media containing 10 ng·mL^{-1} dosage of TNF-α and no insulin was delivered to the tissue with intention of hindering glucose consumption of the adipocytes.

Once glucose consumption/production had stabilized after 24 hours of TNF-α delivery, all six bioreactors were stimulated with human insulin as a "recovery" (Sigma-Aldrich, St. Louis, MO, USA) by a 5 µM direct injection in addition to delivering feed medium containing insulin to maintain a steady influx of insulin for an 8-hour period.

After the 8-hour stimulation period, feed medium was returned to non-insulin containing medium and glucose consumption measurements were continued for another 20 hours to confirm adipocyte metabolism had returned to baseline before bioreactor disassembly.

2.2.6 Immunohistochemistry and Histology

Upon termination of each bioreactor culture, tissue/fiber samples were extracted from the bioreactors and placed in 10% w/v buffered formalin (Thermo Scientific) and stored at 4 °C in the formalin for fixed histology samples. Samples were stained with AdipoRed Assay Reagent to analyze lipid inclusion (Lonza, Walkersville, MD, USA). Samples were protected from light and incubated at room temperature with AdipoRed staining dilutions according to Lonza protocol for 40 minutes, then exposed to DAPI (0.6 µg/mL, Invitrogen) and AlexaFluor 488 Phalloidin (6.6 µM, Invitrogen) to stain for nuclei and F-actin, respectively, for 10 minutes at room temperature. Immunofluorescence was captured from an Olympus Fluoview 1000 Upright Confocal Microscope (Olympus America, Melville, NY, USA).

Additionally, samples were paraffin embedded, stained with hematoxylin & eosin and Masson's Trichrome, and imaged under bright field microscopy of an Olympus Provis Light Microscope (Olympus America) for architectural assessment and to determine matrix formation.

2.2.7 Scanning Electron Microscopy

Bioreactor explants stored at 4 °C in formalin were air dried and placed onto metal stubs covered in double-sided copper tape. The fibers were then gold-sputtered to a density of 3.5 mm from Cressington 108 auto sputter-coater (Cressington, Watford, UK) and imaged with a JEM-6330f Scanning Electron Microscope (Jeol, Peabody, MA, USA). Scope was operated at 5kV acceleration.

2.2.8 Gene Expression

Tissue samples from all six bioreactor cultures were stored in RNAlater Stabilization Reagent (Qiagen, Valencia, CA, USA) at 4 °C for qPCR. mRNA was collected using Qiagen RNeasy mini Kit and reverse-transcribed into cDNA using First Strand Transcription Kit (Invitrogen, Carlsbad, CA, USA), both according to the manufacturer's protocol. PCR primers were designed using Invitrogen's Vector NTI and synthesized by Invitrogen.

qPCR was performed in triplicate in 96-well optical plates and the primer sequences are as follows: peroxisome proliferator-activated receptor (*PPAR*)-γ forward: 5′-CGAGAAGGAGAAGCTGT TGG-3′; *PPAR-γ* reverse: 5′-TCAGCGGGAAGGACTTTATGTATG-3′; fatty acid binding protein *(FABP)4* forward: 5′-AGCACCATAACCTTAGATGGGG-3′; *FABP4* reverse: 5′-CGTGGAAGTGACGCCTTTCA-3′; glyceraldehyde 3-phosphate dehydrogenase (*GAPHD*) forward: 5'ACAGTCAGCCGCATCTTCT-3'; *GAPDH* reverse: 5'-ACGACCAAATCCGTTCACT-3'; where *GAPDH* was applied as a housekeeping gene.

2.2.9 Protein Expression

Cells were scraped from bioreactor fibers stored in RNAlater at 4 °C using Cell Scrapers from BD Falcon (Franklin Lakes, NJ, USA), centrifuged for 10 minutes at 2,000 rpm (12989 x g), resuspended in sample buffer (NuPAGE LDS Sample Buffer, Invitrogen), and boiled for 5 minutes in water. 10% w/v SDS-based gels were made and loaded with protein marker, 5 µg of positive and negative controls (whole fat sample and two-dimensional ASCs, respectively), and equal samples amounts of cells from diabetic and non-diabetic bioreactors. Gels were run, electrophoretically transferred to membranes (Immobilon Transfer Membranes, Sandwiches, and Blotting Filter Paper; Millipore, Billerica, MA, USA), and blocked with 5% w/v milk (Skim Milk Powder; EMD Chemicals Inc., Darmstadt, Germany) for one hour. Membranes were stored overnight at 4 °C in rabbit polyclonal anti-PPAR-γ (Abcam, Cambridge, MA, USA) at 1:1000 dilution, or mouse polyclonal anti-GAPDH (Abcam) at 1:1000 dilution. After overnight primary antibody incubation, membranes were washed three times with buffer solution (Bio-Rad, Hercules, CA, USA) containing Tween-20 followed by soaking in rabbit or mouse polyclonal secondary antibodies (Jackson Immuno Research, West Grove, PA USA) at 1:50,000 dilution for 60 minutes at room temperature. Membranes were then washed three times with buffer solution containing Tween-20 (Acros Organics, Geel, Belgium) and detected using SuperSignal detection agent (SuperSignal West Femto Maximum Sensitivity Substrate; Thermo Scientific, Pittsburgh, PA, USA). Membranes were taken into a dark room where they were developed onto x-ray film (Blue X-Ray Film; Phenix Research Products, Candler, NC, USA) with a phosphor screen (Storage

Phosphor Screen; Kodak, Rochester, NY, USA) and processed (X-OMAT 2000 Processor; Kodak).

2.2.10 Statistical Methods

Results are presented as mean ± standard deviation. Unpaired, two-tailed *t*-tests were performed to assess differences in metabolic activity between treatment groups. One-way ANOVA followed by Games-Howell post hoc testing was used to determine differences in gene expression between groups. All data were found to be normally distributed and variances were homogenous. Statistical significance is determined at *p*-values less than 0.05.

2.3   RESULTS AND DISCUSSION

2.3.1 Metabolic Activity

Figure 9 represents average glucose production within the bioreactors of the cells and tissue using aforementioned protocol during ASC expansion (days 0-21), ASC differentiation into adipocytes (days 22-36), and adipocyte maintenance (days 37-45) within all six bioreactors, where solid squares signify glucose production/consumption of cells from diabetic patients and empty squares denote cells from non-diabetic patients. Lactate dehydrogenase (LDH) was measured daily to monitor damage to plasma membranes. No increase in LDH concentration within the recirculation media was observed throughout bioreactor culture nor was there any significant difference in LDH concentration between diabetic and non-diabetic ASCs.

Over the entire 45-day culture, glucose production of ASCs from diabetic patients is no different – with the exception of one time point, which had a p-value of 0.0498 – within the bioreactor from glucose production of ASCs from non-diabetic patients, up to a confidence interval of 95% with N-value of 3. Throughout bioreactor culture, average glucose production/consumption of tissue from diabetic samples appeared to remain steady; whereas, tissue from non-diabetic samples exhibited sharply decreased glucose consumption upon differentiation. Such change in glucose uptake could be due to the cells preparing for differentiation, saturation and storing of glucose for lipid accumulation [164-168].
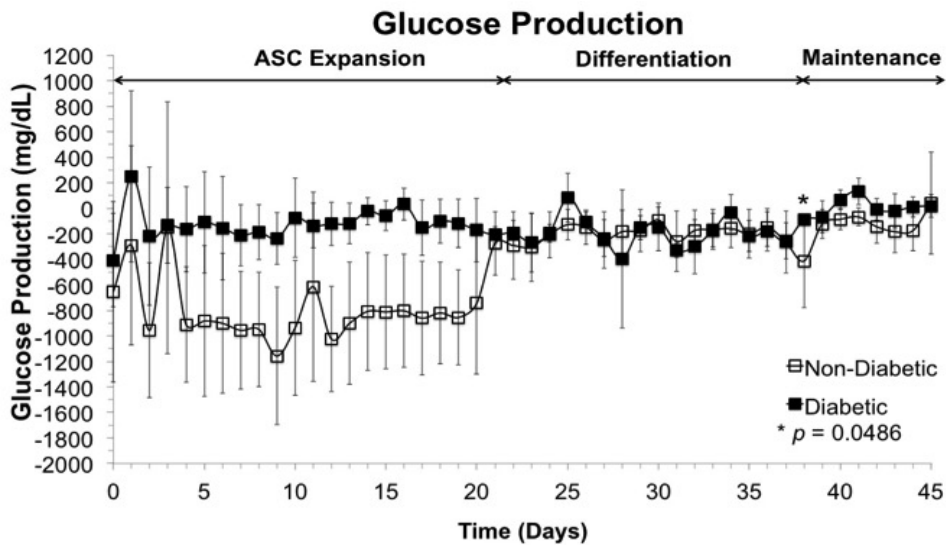
Figure 9. Metabolic activity. Glucose production/consumption trends of three bioreactors seeded with ASCs from non-diabetic patients (empty squares) and three bioreactors seeded with ASCs from type II diabetic patients (filled squares) over 45 days of culture. Days 0-21 represent a time period in which ASCs were allowed to expand within the bioreactor; throughout days 22-36 ASCs were influenced to differentiate into adipocytes by a medium change; adipocytes were maintained from days 37-45. Glucose consumption is predominantly not significantly different (* $p = 0.0498$, $N=3$) within tissue derived from diabetic patients as to tissue derived from patients without diabetes.

2.3.2 TNF-α Functional Testing

Figure 10 depicts the average glucose production of all six bioreactors (three each from diabetic and non-diabetic groups) before, during, and after insulin stimulation of the three-dimensional adipose tissue. Results indicate no significant difference between glucose consumption/production of adipocytes generated from diabetic ASCs and those from non-diabetic ASCs within the hollow fiber-based bioreactor ($p>$ 0.05, N=3) before and after insulin stimulation. During insulin stimulation, bioreactors containing samples from diabetic patients experienced less glucose consumption than those from non-diabetic patients in three of the sixteen time points measured, with a N-value of 3 and p-values of 0.010, 0.043, and 0.023.
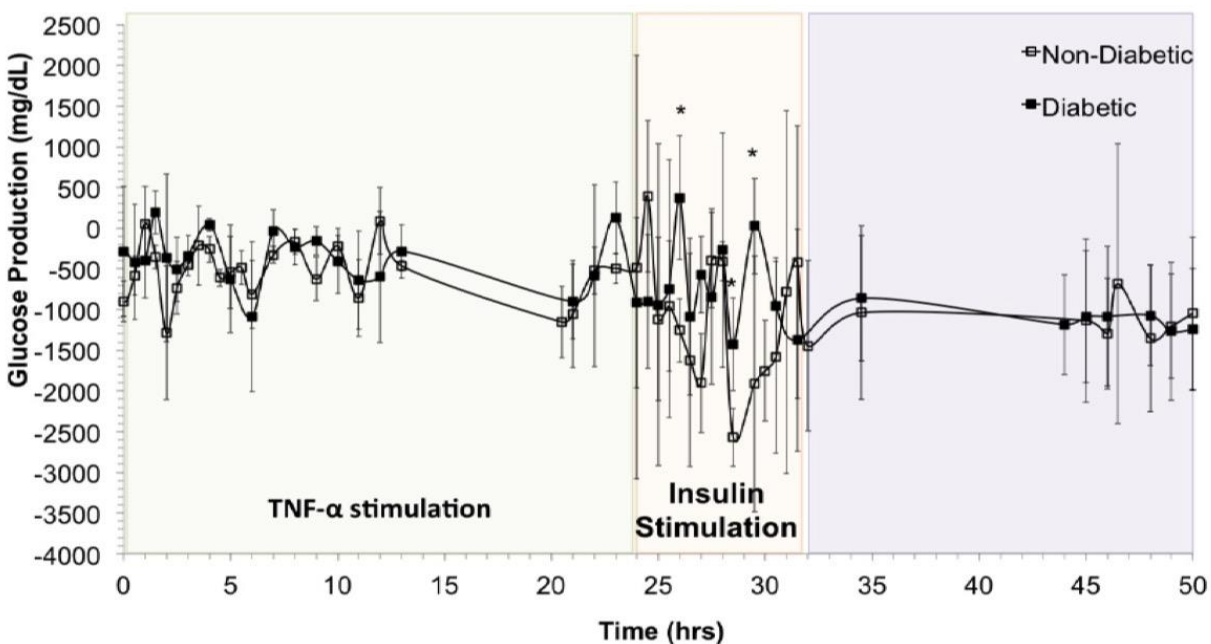
Figure 10. Adipocyte functionality. All six bioreactors were stimulated with TNF-α for twenty-four hours, glucose consumption was measured and noted to be hindered. After reaching a steady glucose consumption rate, insulin was introduced to the system and the functional adipocytes were able to recover from the TNF-α dosage as glucose consumption increased. Tissue from diabetic patients (filled squares) functions with mostly no significant difference (* $p < 0.05$, $N=3$) to tissue from patients without diabetes (empty squares) when stimulated with TNF-a and insulin.

2.3.3 Immunohistochemistry

Imaging results of the tissue generated within the bioreactors are shown in Figures 8-10. Macroscopic tissue formation was observed in and around the hollow fiber membranes upon bioreactor disassembly [Figures 11 and 12]. Regarding both groups of adipose tissue – that differentiated from ASCs obtained from diabetic patients and that

52

from non-diabetic patients – histological analyses revealed closely associated adipocytes throughout all bioreactors and confocal fluorescent imaging identified AdipoRed lipid formation after 45 days of culture within the dynamic perfusion systems, while DAPI and AlexaFluor 488 Phalloidin highlight nuclei and F-actin, respectively
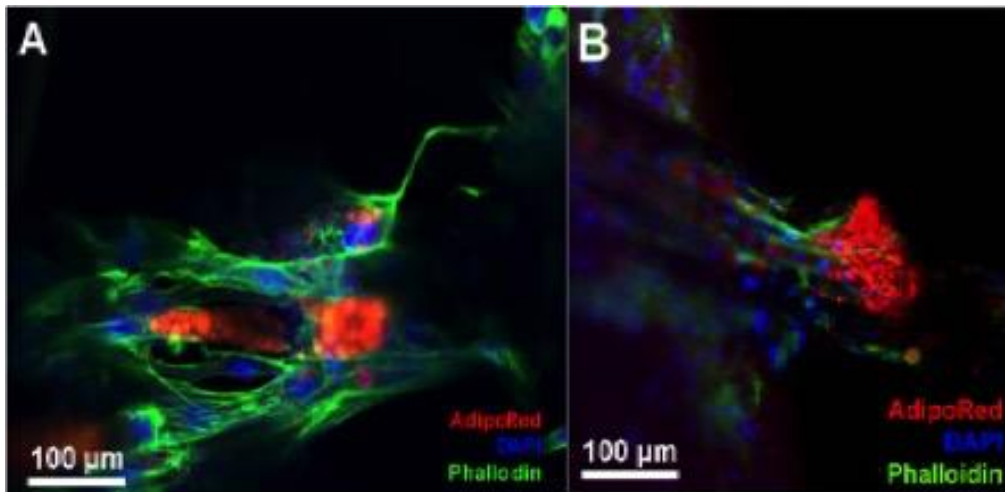
Figure 11. Immunohistochemistry. End-point (45 days) AdipoRed/DAPI/Phalloidin immunohistochemistry from bioreactors containing adipose tissue generated from patients without (A) or with (B) type II diabetes mellitus at 20X, scale bar = 100 μm. Red = AdipoRed, blue = DAPI, green = AlexaFluor 488 Phalloidin.

2.3.4 Histology

Imaging results of the tissue generated within the bioreactors are shown in Figures 11 and 12. Macroscopic tissue formation was observed in and around the hollow fiber membranes upon bioreactor disassembly [Figures 11 and 12]. Regarding both groups of adipose tissue – that differentiated from ASCs obtained from diabetic patients and that from non-diabetic patients – histological analyses revealed closely associated adipocytes throughout all bioreactors.
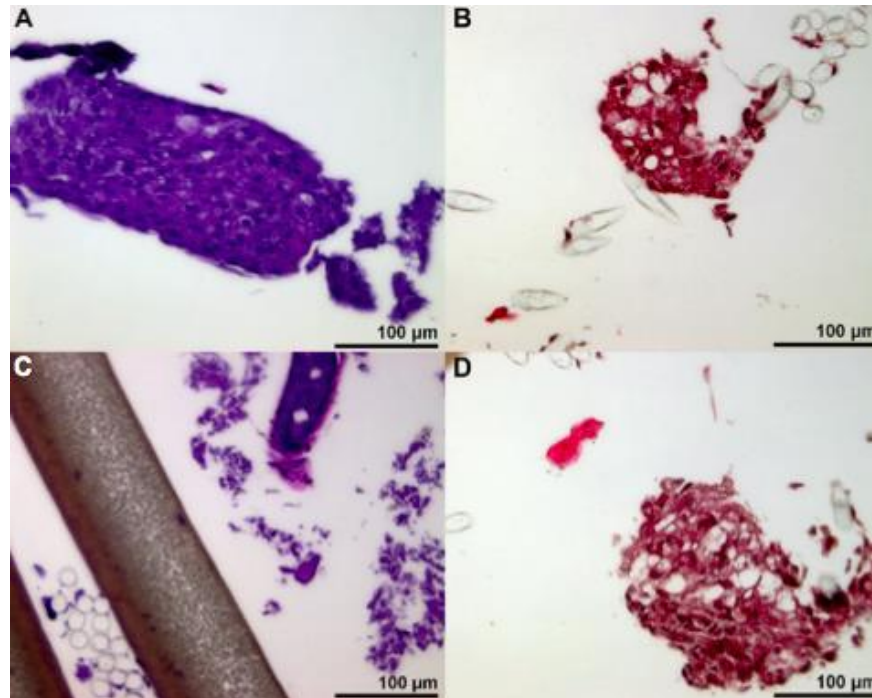
Figure 12. Histology. End-point (45 days) histology from bioreactors containing adipose tissue generated from patients without (A, B) or with (C, D) type II diabetes mellitus; where A and C are H&E, and B and D are Masson's Trichrome, all images captured at 40X magnification, scale bar = 100 μm.

2.3.5 SEM

SEM images of the samples removed from all bioreactors reveal cell growth on and among the hollow fibers [Fig. 13]. White arrows on Figure 10 indicate adipocytes.

.
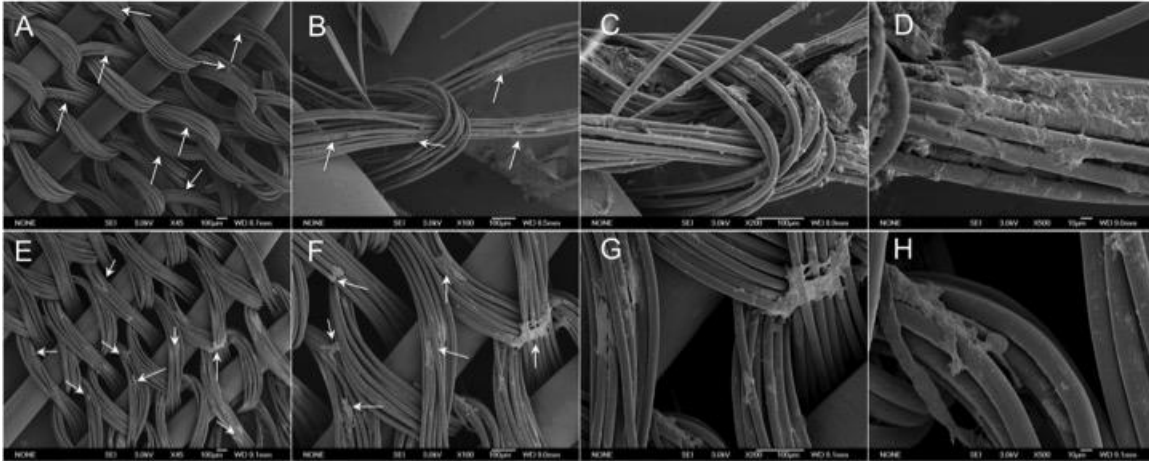
Figure 13. Scanning Electron Micrographs. Scanning Electron Microscopy (SEM) images of adipocytes on fibers extracted from bioreactors after 45 days of culture inoculated with ASCs from (A-D) patients without type II diabetes mellitus and (E-H) patients with type II diabetes mellitus. Adipose tissue is indicated by white arrows at 45X and 100X.

2.3.5 Gene and Protein Expression

Results obtained from qPCR confirm *FABP4* and *PPAR-γ* gene expression of the adipose tissue generated within all six of the bioreactors, with no significant difference in *FABP4* gene expression between adipose differentiated from diabetic and non-diabetic ASCs as determined by one-way ANOVA ($F(4,10)$ $p > 0.05$) [Fig. 14]. A Games-Howell post-hoc test confirmed that *FABP4* gene expression in whole fat was statistically significantly higher than *FABP4* gene expression in ASCs ($p < 0.05$) and was not statistically different from *FABP4* gene expression in samples extracted from both diabetic and non-diabetic bioreactor cultures $p > 0.05$, $N=3$) [Fig. 14]. *PPAR-γ* gene expression was found to be statistically significantly higher in whole fat compared to both 2D ASCs controls and samples extracted from the diabetic bioreactor culture ($p <$

0.05, N=3), whereas, *PPAR-γ* gene expression was not significantly different in samples extracted from the non-diabetic bioreactor culture (*p > 0.05, N=3*) [Figure 14].
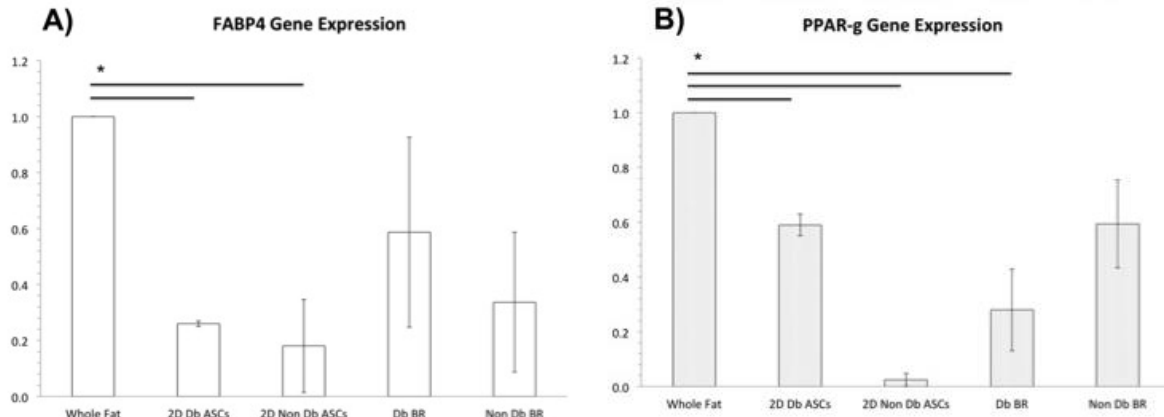
Figure 14. Gene Expression. A) Fatty Acid Binding Protein-4 (*FABP4,* solid white bars) and B) Peroxisome Proliferator-Activated Receptor-γ (*PPAR-γ*, dotted white bars) gene expression is significantly higher (*p< 0.05**,) in native whole adipose tissue than in ASCs grown in 2D culture. *PPAR-γ* gene expression was higher in native whole adipose tissue compared to both 2D ASCs controls and samples extracted from the diabetic bioreactor culture (*p < 0.05, N=3*), whereas, *PPAR-γ* gene expression was not significantly different in samples extracted from the non-diabetic bioreactor culture (*p > 0.05, N=3*) .

PPAR-γ and GAPDH protein expression was exhibited by adipose tissue from bioreactors with diabetic and non-diabetic ASCs as well as whole fat samples [Fig. 15]. While housekeeping protein, GAPDH, confirmed presence of protein in all samples, including two-dimensional ASCs, two-dimensional ASCs did not express PPAR-γ protein, reaffirming the maturity of adipose tissue cultured within the three-dimensional, hollow fiber-based, dynamic perfusion bioreactors.
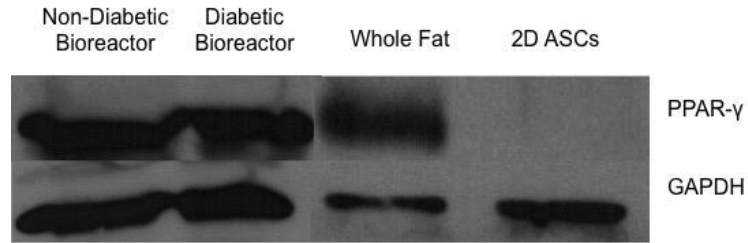
Figure 15. Protein Expression. Images obtained from Western Blots measuring protein expression of PPAR- γ or GAPDH of ASCs cultured in two dimensional tissue culture flasks as a negative control, whole fat sample as a positive control, adipose tissue cultured within the bioreactors over 45 days from diabetic patients, and adipose tissue cultures within the bioreactors from non-diabetic patients.

2.4   CONCLUSIONS

Human adipose-derived stem cells derived from adults with type II diabetes mellitus were cultured within hollow fiber-based membrane, three-dimensional, dynamic perfusion bioreactors for 45 days and metabolic behavior was assessed along with gene and protein expression.   Glucose consumption following TNF-α exposure increased during insulin influence, confirming functionality of the generated adipocytes. Masson's Trichrome, H&E, AdipoRed images in addition to FABP4 and PPAR-γ gene expression and PPAR-γ protein expression of the functional adipocytes show no major difference between adipose tissue generated in three dimensions when isolated from patients with or without type II diabetes mellitus, raising the question of whether the ASCs retain a diseased state when cultured *in vitro*; and how environment affects functionality of human adipose cells in three-dimensional culture.   Following massive weight loss, change in diet and exercise, patients with type II diabetes mellitus experience regression of the insulin-stimulated uptake and lowered blood glucose levels [169].   As type II

diabetes mellitus is clinically reversible, this data supports the hypothesis that human-derived ASCs experience plasticity in culture, dependent on environment. The presented work provides a first step to advance better understanding of adipose tissue as a whole-body endocrine organ and it's key role in metabolic diseases.

3.0 ADIPOCYTE DIFFERENTIATION CULTURE MEDIA OPTIMIZATION OF PHYSIOLOGICALLY RELEVANT GLUCOSE CONCENTRATIONS AND DEVELOPMENT OF A TYPE II DIABETIC ENVIRONMENT *IN VITRO* AND *EX VIVO* CHARACTERIZED BY HINDERED INSULIN-STIMULATED GLUCOSE UPTAKE

3.1   INTRODUCTION

3.1.1 Insulin-Stimulated Glucose Consumption by Adipose Tissue

Adipocytes store lipid in the form of triglycerides, which are presented to the adipocyte in the form of a glycerol molecule and three fatty acid chains. Outlined in Figure 16, once the free fatty acids (FFAs) are transported into the adipocyte, triglycerides are reformed and stored inside the lipid droplet. Hormone sensitive lipase and lipoprotein lipase regulate triglyceride entry, storage, and release in the adipocytes. Additionally featured in Figure 16 is the action of insulin within the adipocyte. Once insulin is accepted by its receptors and brought into the cell, glucose transporter (GLUT) 4 is able to translocate about the membrane and glucose is taken by the adipocyte. An abundance of insulin and glucose in the blood stream – a result of the metabolic syndrome and characteristic of type II diabetes – inhibits and exhausts the insulin receptors and, ultimately, the action of GLUT4.
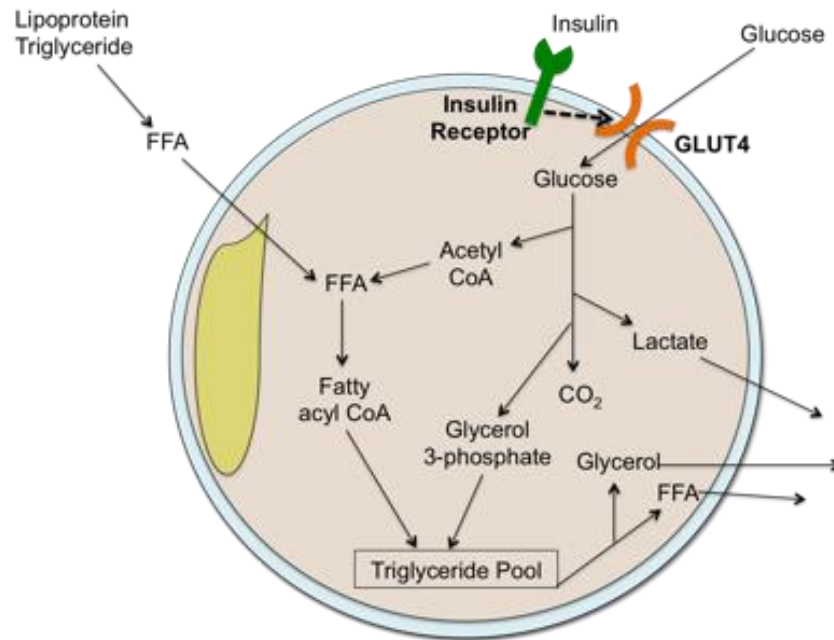
Figure 16. Select molecular mechanisms of an adipocyte. Model of an adipocyte and select molecular mechanisms of the synthesis and degradation of triacylglyercols by adipose tissue in addition to insulin receptor and GLUT4 mechanisms.

When adipocytes increase in size and a person gains weight, several molecular and cellular changes occur and ultimately influence whole-body metabolism [170-179]. Horowitz et al., identified higher free fatty acid and glycerol levels in obese women compared to lean women, suggesting a promotion of insulin resistance – the primary cause of type II diabetes [28, 180]. In addition to FFA, with a strong presence in those with obesity, various other proinflammatory factors are secreted by adipose tissue, including IFNγ, TNF-α, MCP-1, IL-6, IL-1β, and several immune cells [Fig. 16].

Discussed in Chapter 2, ASCs retain no memory of diabetic function when placed in a different culture environment. Because microenvironment is highly influential *ex vivo*, in order to study type II diabetes mellitus, an engineered culture model is necessary. Summers et al., [122, 180] found that C2-ceramide, (a short analog of ceramide, a sphingolipid-fatty acid component of sphingomyelin within the cell membrane lipid bilayer), inhibited glucose transport and GLUT4 translocation in 3T3-L1 adipocytes (a cell line commonly utilized in studying adipose tissue) in two dimensional *in vitro* cell culture.

3.1.2 ASC and Adipocyte Culture Medium Compositions

A widely accepted and used ASC expansion medium consists of a DMEM and DMEM/F12media combination, with 10% fetal bovine serum, some form of antibiotic (typically penicillin/streptomyocin), and typically a miniscule amount of dexamethasone, which prevents any differentiation into another mesenchymal lineage, such as osteoblasts. The glucose concentration of ASC expansion medium is typically around 400 mg/dL, but may vary between batches. Adipocyte differentiation medium produced by ZenBio (item # DM-2) consists of DMEM and Ham's F-12 1:1 v/v combination, with fetal bovine serum, biotin, pantothenate, human insulin, dexamethasone, isobutylmethylzanthine, PPARγ agonist, penicillin, streptomycin, and amphotericin B. ZenBio adipocyte maintenance medium (item # AM-1) consists of DMEM and Ham's F-12 1:1/v/ combination, with fetal bovine serum, biotin, pantothenate, human insulin, dexamethasone, penicillin, streptomycin, and amphotericin B. Untouched, the glucose

concentrations of both differentiation and maintenance medium are around 300 mg/dL. Table 4 further compares notable relevant glucose concentrations.

Because the manufactured ZenBio differentiation and maintenance medium contain glucose levels almost 3 times higher than the normal fasting blood glucose level of an adult human (300 mg/dL in culture medium, compared to 110 mg/dL), a more thorough investigation is necessary to determine if the similarity between metabolic activity of the adipocytes generated from diabetic versus non-diabetic ASCs observed in Chapter 2 is a result of the stem cells not retaining the diseased state, or a consequence of the relatively elevated glucose levels in the culture medium.

3.1.3 Chapter Aims

The work presented in this chapter aims to first establish an *in vitro* method to develop a physiologically relevant culture environment defined by a hindered insulin-dependent glucose uptake of differentiated ASCs in two dimensions. The findings uncovered from this chapter are to be eventually applied towards the cultured human adipose tissue within the hollow fiber-based, three dimensional dynamic perfusion bioreactor system, which is further detailed later in Chapter 3. It is hypothesized that ASCs can be differentiated and maintained as adipocytes at a physiological glucose concentration. Stimulation by C2-Ceramide and free fatty acids will inhibit insulin-stimulated glucose uptake of the differentiated ASCs *in vitro* in two dimensions.

The study described in this chapter aims to apply the results investigated in Chapter 3 to first establish a method to develop a physiologically relevant culture

environment defined by a hindered insulin-dependent glucose uptake of cultured human adult adipose tissue within the hollow fiber-based, three dimensional, dynamic perfusion bioreactor system. It is hypothesized that ASCs can be differentiated and maintained as adipocytes at a physiological glucose concentration within the bioreactor system and that stimulation by C2-Ceramide will inhibit insulin-stimulated glucose uptake of the cultured adipocytes.

3.2   MATERIALS AND METHODS

3.2.1 Human ASC Isolation

Adipose tissue was harvested from the abdominal depots of non-diabetic female patients (66 and 61 years old, body mass index (BMI) of 38.4 and 30.7, respectively) undergoing elective plastic surgery at the University of Pittsburgh Medical Center in Pittsburgh, PA, USA. Tissue was collected under a human studies exempt protocol approved by the University of Pittsburgh Institutional Review Board (IRB). The University of Pittsburgh waived the need for written informed consent from the participants under an exempt review and approval process. Samples were pooled to provide sufficient number of cells required for optimal seeding. Donors were not pre-diabetic and did not have insulin resistance at time of adipose tissue harvesting.

Abdominal adipose tissue was placed in 50 mL centrifuge tubes at 10 g per tube and soaked in 1 mg·mL^{-1} of freshly prepared collagenase (Type II collagenase, Worthington Biochemical Product Catalog; Lakewood, NJ, USA). The tissue was finely minced, vortexed, and shaken at 37 °C for 35 minutes until a fatty supernatant layer

became apparent. Tubes were again vortexed and filtered through double-layered gauze (J&J Steri-Pad Gauze Pads; New Brunswick, NJ, USA) into sterile 50 mL centrifuge tubes. Digested specimens were then centrifuged at 1000 rpm (6449 x g), 4 °C for 10 minutes, fatty layers aspirated, and resulting pellets suspended in erythrocyte lysing buffer. The solution was once again centrifuged at 1000 rpm (6449 x g), 4 °C for 10 minutes and the pellet, containing the stromal vascular fraction, was resuspended in Dulbecco's Modified Eagle's Medium (DMEM/F12) with 10% v/v fetal bovine serum and 1% v/v penicillin/streptomycin, plated, and stored at 37 °C at 5% CO_2. Cells were expanded in two dimensions using growth medium with low serum (Promocell Preadipocyte Growth Medium, Heidelberg, Germany), passaged at confluency, and characterized as previously described by our laboratory [56].

3.2.2 *In Vitro* Cell Culture

ASCs were plated onto 96-well plates at 10,000 cells per well, then differentiated for a period of seven days using the ZenBio differentiation media as a positive control, various dilutions of our laboratory's in-house differentiation medium stepwise from 100, 50, 35, 30, 25, 20% and a negative control of ASC expansion media. Cultures were then maintained using ZenBio maintenance medium for another seven days. In-house differentiation media was diluted with no-glucose DMEM, according to Table 5.

Table 5. Relevant Glucose Concentrations.

Medium	Glucose Level (mg/dL)
100% ZenBio differentiation	352
100% ASC expansion	416
100% In-house differentiation	454
50% Diluted in-house diff	258
35% Diluted in-house diff	164
30% Diluted in-house diff	139
25% Diluted in-house diff	118
20% Diluted in-house diff	96.3
Type II diabetic patient, fasting physiological	> 140
Healthy adult, fasting physiological	70-130

In a separate study to test hindered ASC glucose consumption and to determine an optimal dosage of C2-ceramide as well as appropriate FFA concentrations to be delivered to the tissue within the bioreactor was examined by manipulating human adult ASCs in 96-well plates. Media containing FFA was freshly prepared using a stock solution of FFA ("Ex-cyte") as manufactured by Millipore. ASCs were isolated following the same protocol described above (Chapter 3.2.1.) plated onto 96-well plates at 10,000 cells per well, differentiated for a period of seven days using the optimized, diluted differentiation media at either 35 or 20%, then maintained for seven days in the well plates using the same ZenBio maintenance media. During the seven-day maintenance period, adipocytes in the 96-well plates were exposed to various concentrations of C2-ceramide and FFAs as follows: 150 μM C2-ceramide + FFA, 100μM C2-ceramide + FFA, 25 μM C2-ceramide + FFA, 150 μM C2-ceramide, 100 uM C2-ceramide, 25 μM C2-ceramide, FFA only, maintenance medium only at 35% diluted differentiation, maintenance medium only at 20% diluted differentiation, ASC expansion medium only.

3.2.3 *In Vitro* Metabolic Activity Analysis

Glucose consumption and lactate production was analyzed by removing 100 µL of medium supernatent from each well daily and measured with YSI Glucose & Lactate Analyzer.

3.2.4 Adipogenesis and Nuclei Characterization & Quantification

Upon *in vitro* experiment completion, 96-well plates were fixed by 4% paraformaldehyde for 30 minutes. Samples were stained with AdipoRed Assay Reagent to analyze lipid inclusion (Lonza, Walkersville, MD, USA). Samples were protected from light and incubated at room temperature with AdipoRed staining dilutions according to Lonza protocol for 40 minutes, then exposed to DAPI (0.6 µg/mL, Invitrogen). Plates were read and fluorescence quantified on a Tecan Infinite 200 PROplatereader (Mannedorf, Switzerland), then imaged on an Olympus Provis fluorescence microscope (Olympus America) to gauge lipid inclusion and nuclei assessment. The dilution to yield metabolically functional adipocytes with the highest amount of AdipoRed with the most clinically relevant glucose concentration will be applied to future studies regarding adipose tissue within the bioreactor systems described in Chapter 3.2.5.

3.2.5 Bioreactor Inoculation

The bioreactors are prototyped by Stem Cell Systems (Berlin, Germany) and contain three independent hollow fiber membrane systems, interwoven into repetitive subunits, forming a cell compartment that houses 8.0×10^7 cells with a volume of 8 mL

[Fig. 8]. The capillary network serves three functions: cell oxygenation/carbon dioxide removal, medium inflow, and medium outflow via countercurrent flow operation of two independent membrane systems. As a result of interweaving and high performance mass exchange via counter-current medium flow operation, decentralized gas supply and medium exchange with low gradients is provided to the cultures. The medium fiber membrane systems are comprised of polyethersulfone capillary systems (Membrana, Wuppertal, Germany) with a molecular weight cutoff of 400,000 g·mol^{-1} and gas is supplied by hydrophobic multi-laminate hollow fiber membrane systems (MHF; Mitsubishi, Tokyo, Japan).

A total of four bioreactor experiments were performed: two bioreactors cultured with ASCs in media at a "healthy physiological" condition, and two bioreactors cultured with ASCs in media at a "type II diabetic physiological" condition. Bioreactor sterilization was performed with ethylene oxide gas and degassed with air. Before cells were introduced into the system, a continuous phosphate buffered solution flush was run within the bioreactor for 72 hours, followed by priming with DMEM/F12 media flush for 24 hours prior to inoculation. Cell suspensions of 8.0×10^7 total cells per bioreactor were inoculated and cultured throughout a time period of six weeks. The cell compartments were continuously perfused with culture media through the polyethersulfone hollow fiber bundles at a feed rate of 4 mL·hr^{-1} in combination with a recirculation loop at a rate of 20 mL·min^{-1}. Waste medium was removed from the circuit at 4 mL·hr^{-1}. The flows of compressed air and carbon dioxide in the gas compartment were maintained at 20 mL·min^{-1}. Partial pressures of oxygen, carbon dioxide, and acid/base status within the bioreactor were measured daily and the carbon dioxide content

was adjusted throughout culture time to maintain the medium pH within the range of 7.35-7.45.

3.2.6 *Ex Vivo* Human ASC Culture

Human adult adipose stem cells were inoculated into the bioreactor cell compartments via a suspension of 8.0 x 10^7 cells per mL of medium. Cell passages at time of inoculation for each experiment were either passage 2 or 5 and are described in Table 6. Upon completion of a twenty-two day expansion period of the ASCs within the bioreactor cell compartment by perfusion of ASC plating media (DMEM/F12 as described above), to initiate three-dimensional adipogenic differentiation, the feed media was changed for the following seventeen days to adipogenic media containing DMEM/F12, HEPES, biotin, pantothenate, human insulin, dexamethasone, 3-isobutyl-1-methylxanthine (IBMX), PPAR-γ agonist, and antibiotics (ZenBio, Research Triangle Park, NC, USA). Adipogenic differentiation media was diluted with DMEM containing no glucose to either 20% in two reactors or 35% in two reactors to represent "healthy" or "type II diabetic" environments, respectively. Adipocytes were maintained for seven days with feed media containing DMEM/F12, HEPES, fetal bovine serum, biotin, pantothenate, human insulin, dexamethasone, and antibiotics. Maintenance media was diluted with no-glucose DMEM to either 35% or 50% to represent "healthy" or "type II diabetic" environments, respectively. Next, the "healthy" bioreactor cultures were exposed to 30 μM C2-ceramide stimulation for sixteen days while the "type II diabetic" bioreactors continued the same treatment as during the previous seven-day maintenance period. Finally, as a "recovery" period, all four bioreactor cultures were once again

influenced by the same feed medium experienced in the initial maintenance period (either a 35 or 50% dilution). Cells were not further passaged within the bioreactor; rather, cell fate was influenced by changes in culture medium.

In parallel, ASCs in a two-dimensional control group were cultured in 175 cm^2 tissue culture flasks with ASC plating medium containing 10% v/v fetal bovine serum and 1% v/v penicillin/streptomycin, plated, and stored at 37 °C at 5% CO$_2$. 2D control ASCs were cultured for three weeks, with static media changes every other day and passaged at 80% confluency.

Table 6. Patient age, gender and BMI at time of ASC isolation used for bioreactors in Specific Aim 2.

Bioreactor #	Patient Age	Gender	BMI	C2-cer Treatment?	Patient #	Cell Passage #
1	66	Female	38.4	Yes	5	2
2	66	Female	38.4	No	5	2
3	61	Female	30.7	Yes	6	5
4	61	Female	30.7	No	6	5

3.2.7 *Ex Vivo* Metabolic Activity Analysis

Glucose production and consumption of the cells throughout culture within the bioreactors was assessed under a dynamic open-circuit system. A sampling volume of 2 mL was taken daily via a luer-lock sample port; glucose and lactate dehydrogenase levels measured (YSI 2300 STATE Plus Glucose & Lactate Analyzer; YSI Life Sciences,

Yellow Springs, OH, USA; Quantichrom Lactate Dehydrogenase Kit; BioAssay Systems, Hayward, CA, USA).

Glucose production/consumption rates of the cells were determined by a previously established protocol considering various parameters including measured glucose concentration within the recirculation sample, total system volume, baseline medium concentrations, flow rate of nutrients through the system, and time points of measurements [161-165, equations 2 and 3 Chapter 2.2.4.].

3.2.8 Immunohistochemistry and Histology

Upon termination of each bioreactor culture, tissue/fiber samples were extracted from the bioreactors and placed in 10% w/v buffered formalin (Thermo Scientific) and stored at 4 °C in the formalin for fixed histology samples. Samples were stained with AdipoRed Assay Reagent to analyze lipid inclusion (Lonza, Walkersville, MD, USA). Samples were protected from light and incubated at room temperature with AdipoRed staining dilutions according to Lonza protocol for 40 minutes or with FABP4 antibody (Abcam, San Francisco, CA, USA), then exposed to DAPI (0.6 μg/mL, Invitrogen) and AlexaFluor 488 Phalloidin (6.6 μM, Invitrogen) to stain for nuclei and F-actin, respectively, for 10 minutes at room temperature. Immunofluorescence was captured from an Olympus Fluoview 1000 Upright Confocal Microscope (Olympus America, Melville, NY, USA).

Samples not used for immunofluorescence or SEM were paraffin embedded, stained with haematoxylin & eosin and Masson's Trichrome, and imaged under bright

field microscopy of an Olympus Provis Light Microscope (Olympus America) for architectural assessment and to determine matrix formation.

3.2.9 Scanning Electron Microscopy

Bioreactor explants stored at 4 °C in formalin were air dried and placed onto metal stubs covered in double-sided copper tape. The fibers were then gold-sputtered to a density of 3.5 mm from Cressington 108 auto sputter-coater (Cressington, Watford, UK) and imaged with a JEM-6330f Scanning Electron Microscope (Jeol, Peabody, MA, USA). Scope was operated at 5kV acceleration.

3.2.10 Statistical Methods

Results are presented as mean ± standard deviation. One-way ANOVA was performed to assess differences in metabolic activity, lipid accumulation, and nuclei expression between treatment groups. Tukey HSD or Games-Howell post-hoc testing identified differences between the groups. All data were found to be normally distributed and variances were homogenous. Statistical significance is determined at p-values less than 0.05.

3.3 RESULTS AND DISCUSSION

3.3.1 *In Vitro* Metabolic Activity

The glucose levels found to be most physiologically relevant were established in differentiation media diluted to concentrations of 35% (164 mg/dL) and 20% (96.3 mg/dL) to represent blood glucose levels observed in patients with and without type II diabetes mellitus, respectively [Figure 17]. In the separate study featuring C2-ceramide and FFA exposure, elevated daily glucose measurements confirmed inhibited glucose uptake by the adipocytes exposed to FFAs and C2-ceramide and are exhibited in Figure 15, with 25 μM C2-ceramide without FFAs proving the most optimal for a type II diabetes mellitus glucose concentration [Fig. 18]. While lactate dehydrogenase levels increased slightly after addition of FFA supplement and C2-ceramide, indicating initial cell death, no outstanding presence of LDH was noted subsequently.
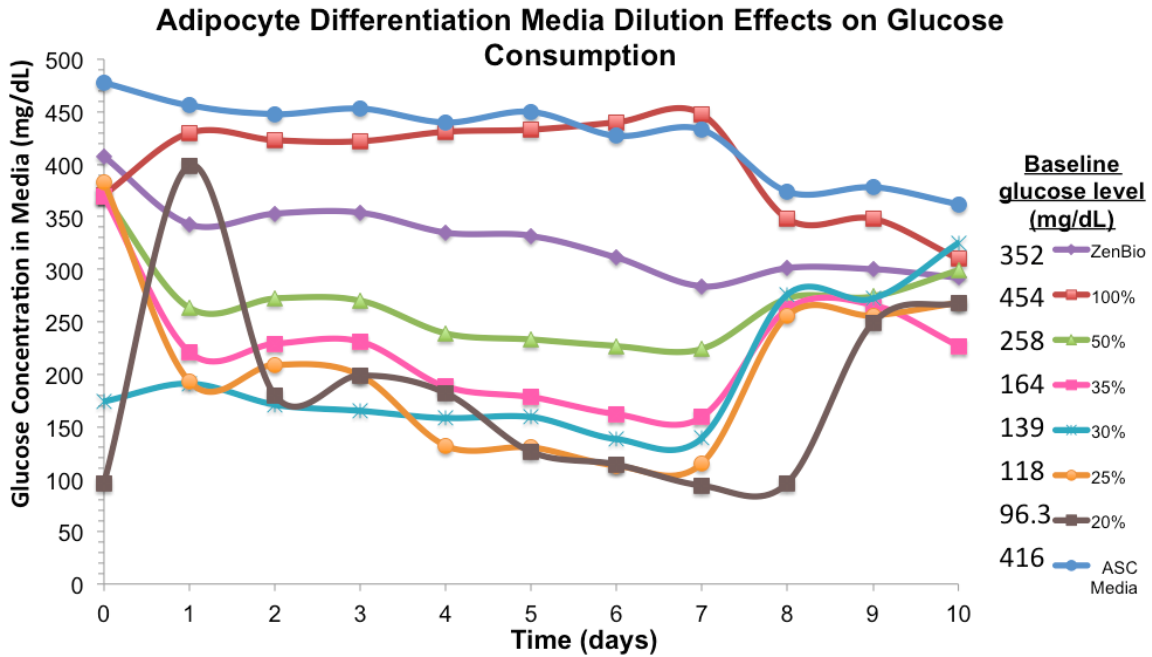
Figure 17. Glucose levels within the culture wells. Differentiation media included biotin, gluatmin, transferrin, pantothenate, insulin, dexamethasone, T3, ciglitazone, IBMX, DMEM, antibiotics, antifungal, and was diluted with glucose-free DMEM. 100 µL samples taken daily and measured via YSI 2300 Stat Plus glucose and lactate analyzer.
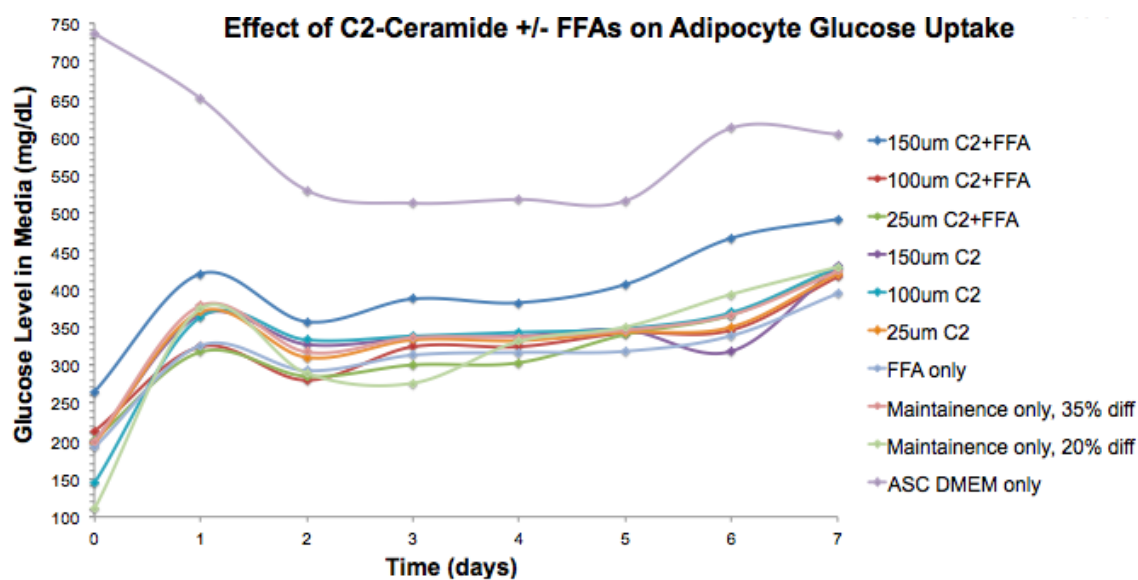
Figure 18. Glucose levels within the culture wells of ASCs differentiated and maintained with stimulation by either C2-ceramide, FFAs, both, or none. C2-ceramide and FFA exposure inhibited glucose uptake as noted by increase in glucose concentration within the culture well samples over time. 100 µL samples taken daily and measured via YSI 2300 Stat Plus glucose and lactate analyzer.

3.3.2 Adipogenesis and Nuclei Characterization & Quantification

AdipoRed quantification was higher in all groups treated with adipocyte differentiation media than in the negative control group, which received ASC plating DMEM-based media only. ASCs receiving differentiation media of pure ZenBio or dilutions of 100%, 50%, and 35% fluoresced higher amounts of AdipoRed, indicating higher adipocyte differentiation over seven days than ASCs exposed to 30%, 25%, and 20%, or ASC plating media only [Fig. 19]. No statistical difference in nuclei

quantification was observed between any groups, indicating dilutions had no effect on cell number after 7 days.
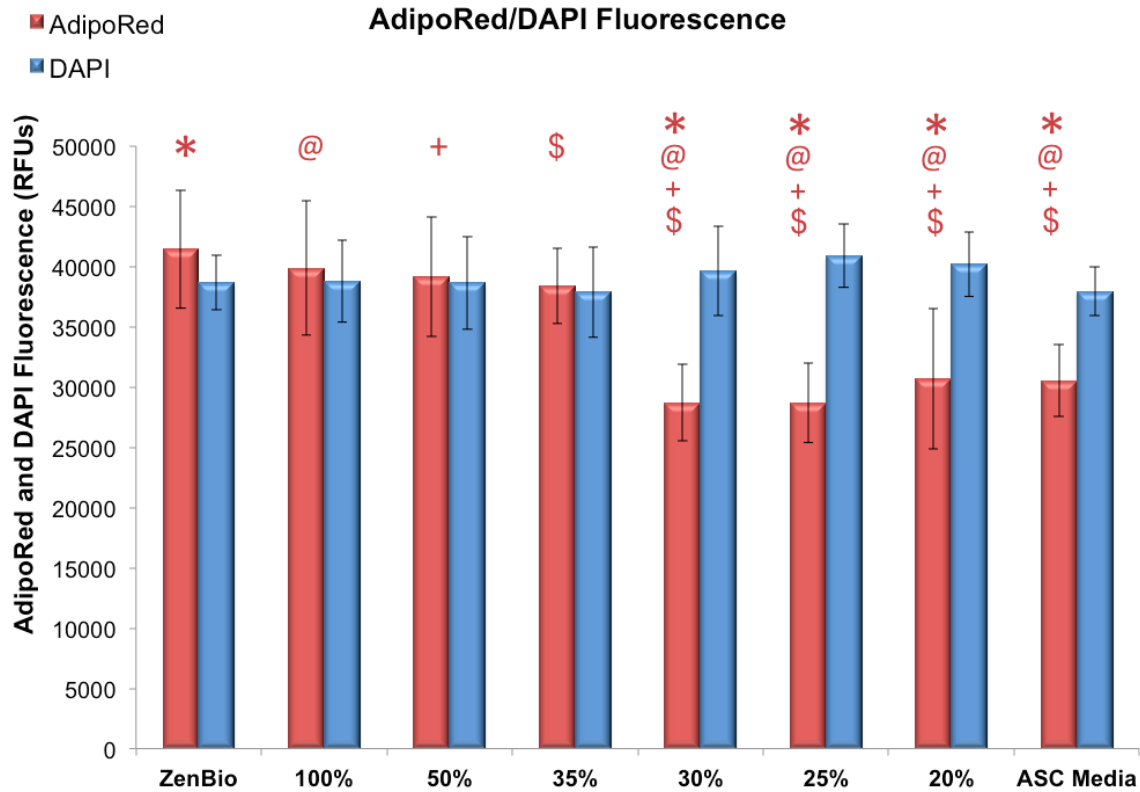
Figure 19. AdipoRed (lipid accumulation) and DAPI (nuclei) fluorescence quantification of ASCs after 7 days of exposure to differentiation medium at physiologically relevant glucose concentrations ranging from healthy to diabetic to plating media controls), established by varying nutrient media dilutions. (*, @, +, $ = $p < 0.05$; N=11; one-way ANOVA, Tukey's post-hoc testing)

AdipoRed quantification was higher in groups treated with both C2-cermide and FFAs than groups treated with C2-ceramide, FFAs alone, or the negative control group, which received ASC plating DMEM-based media only [Fig. 20]. AdipoRed

quantification was indirectly proportionate to C2-ceramide dose when cells were not exposed to both C2-ceramide and FFA.
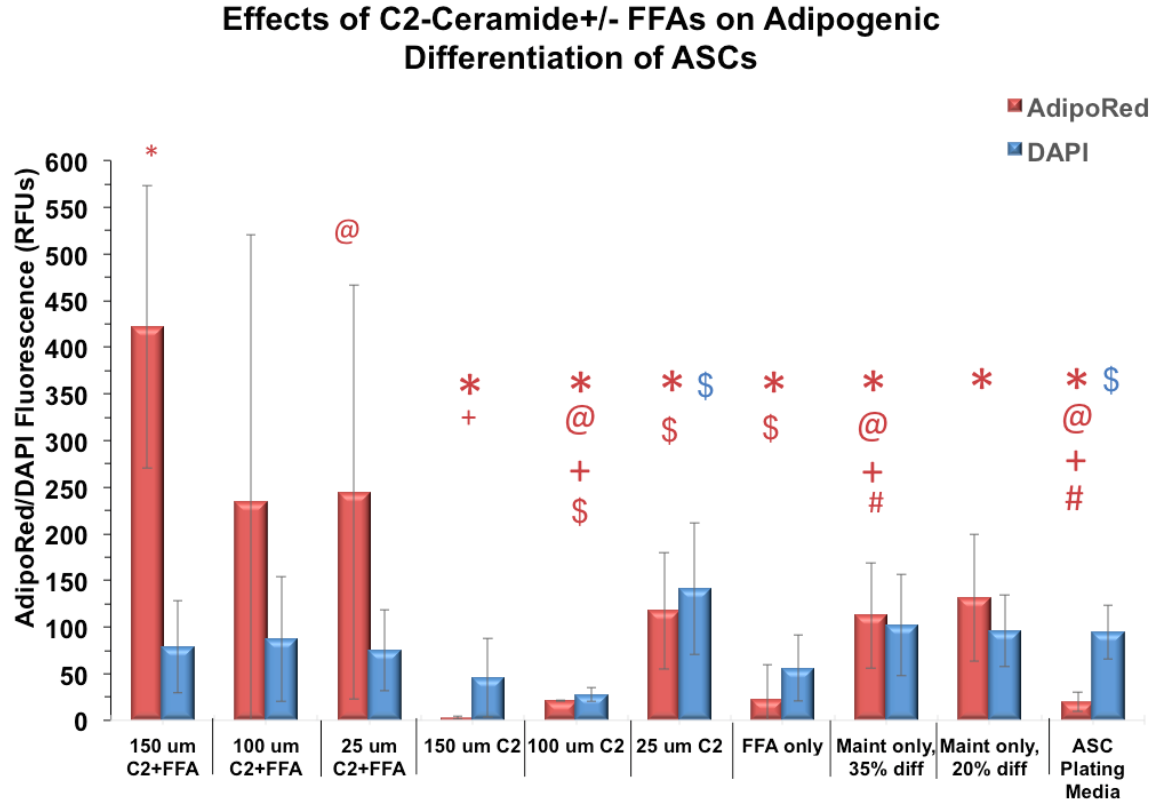
Figure 20. Lipid accumulation and DAPI (nuclei) quantification of ASCs after 7 days of exposure to differentiation medium at physiologically relevant glucose concentrations during exposure to C2-ceramide and free fatty acids. (*, @, +, $, # = $p < 0.05$; N=8; one-way ANOVA, Games-Howell post-hoc testing).

AdipoRed and DAPI fluorescence of ASCs exposed to various differentiation media dilutions were also imaged and are displayed in Figure 21. Correlating with the quantitative representation of differentiation, qualitative differences in differentiation appeared between the 30% and 35% benchmarks [Fig 21].
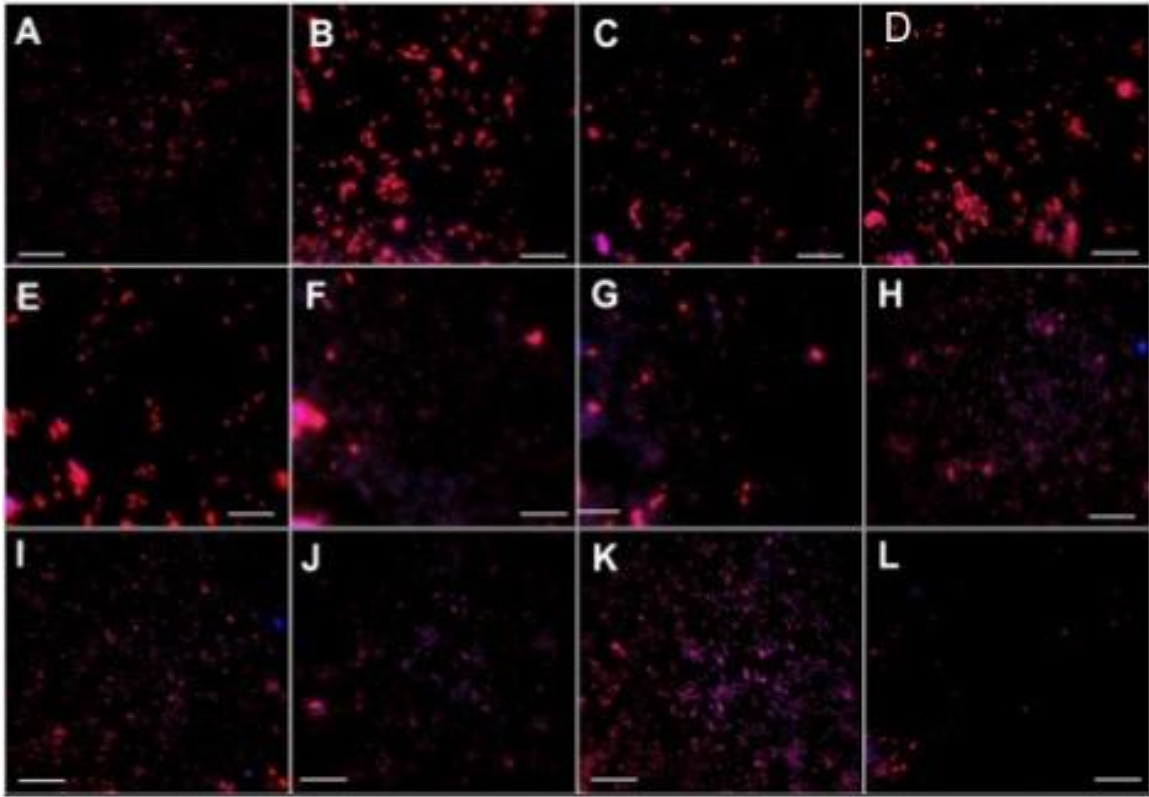
Figure 21. AdipoRed (red) and DAPI (blue) of ASCs exposed to the Adipose Stem Cell Center's in-house differentiation medium at various dilutions over a 7-day period. A) 100% ZenBio differentiation medium, B) 100% in-house differentiation, C) 50% dilution, D) 35% dilution, E) 30% dilution, F) 25% dilution, G) 20% dilution, H) 10% dilution, I) 5% dilution, J) 2.5% dilution, K) 1% dilution, and L) ASC plating medium only. ZenBio serves as positive control differentiation medium, ASC plating medium negative control. Scale bar = 50 μm.

AdipoRed and DAPI fluorescence of ASCs differentiated and metabolically tested with C2-ceramide and/or FFA were also imaged and are shown in Figure 22. Figure 22F confirms positive AdipoRed and DAPI fluorescence of ASCs when differentiated at 35% in-house differentiation media then exposed to 25 μM C2-ceramide.
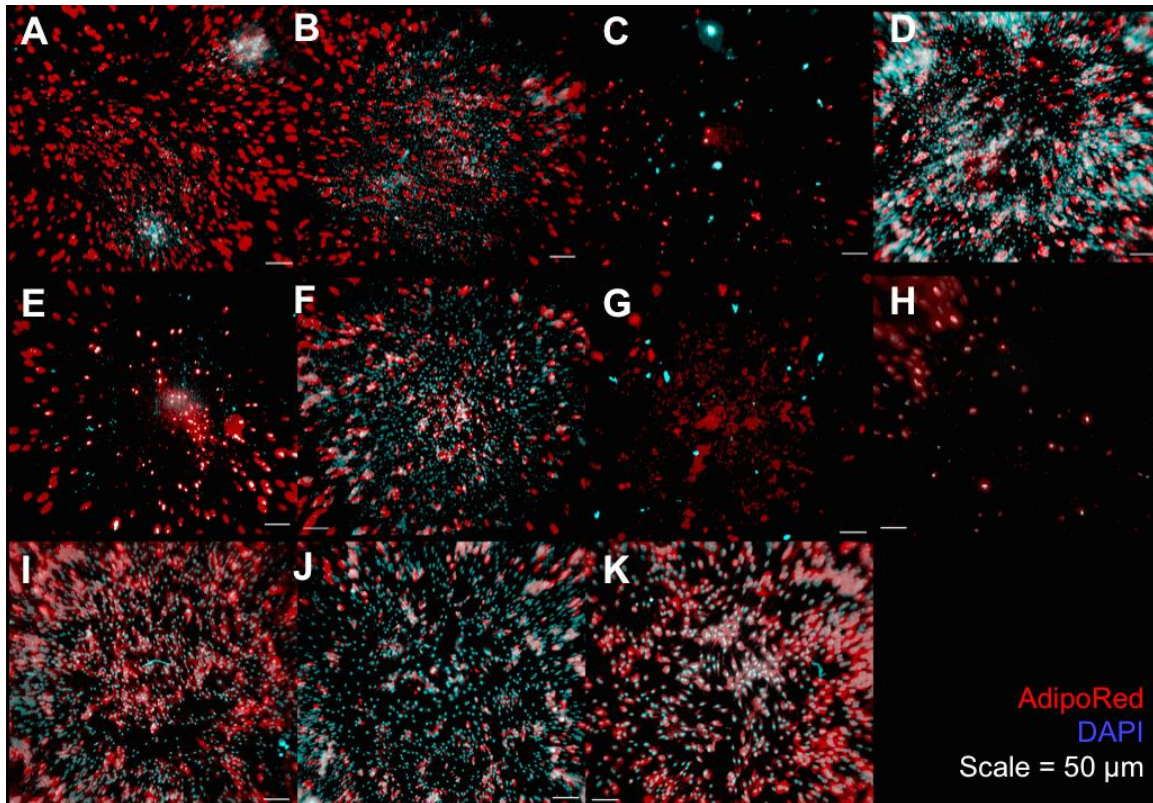
Figure 22. AdipoRed and DAPI of ASCs exposed to C2-ceramide and/or Free Fatty Acids over a 7-day period, differentiated at either 35% or 20% in-house differentiation medium. A) 150µM C2-ceramide + FFA; B) 100µM C2-ceramide + FFA; C) 25 µM C2-ceramide + FFA; D) 150µM C2-ceramide; E) 100µM C2-ceramide; F) 25 µM C2-ceramide; G & H) FFA only; I) Maintenance media only (no C2-ceramide/FFA); J) 20% in-house diff media; K) ASM plating media only. Scale bar = 50 µm. Red = AdipoRed, Blue = DAPI.

3.3.3 *Ex Vivo* Metabolic Activity

Figures 23 and 24 represent average glucose and lactate production within the bioreactors of the cells and tissue using aforementioned protocol during ASC expansion (days 0-22), ASC differentiation into adipocytes (days 23-40), and adipocyte maintenance (days 41-70) within all four bioreactors, where solid squares signify glucose

78

production/consumption of cells receiving a "healthy physiological" treatment and empty squares denote cells receiving the "type II diabetic" treatments. The cultures receiving the media containing the healthy glucose concentration were treated with C2-ceramide at day 48 with the hypothesis that the sphingolipid would inhibit insulin-stimulated glucose uptake by the adipocytes. Days 64-70, the cultures exposed to the C2-ceramide were under a "recovery" period, during which the 35% diluted maintenance medium was re-introduced to the system until experiment termination at day 70.

Throughout bioreactor culture experimentation, average glucose production/consumption of the ASCs in the "healthy physiological" cultures appeared to remain steady, with the exception of two major outliers in the differentiation phase, which were caused by a disruption in the media feeding, a human error. A noticeably large peak at the beginning of the C2-ceramide stimulation was observed; however, an elevated glucose level to indicate a hindered GLUT4 translocation within the adipocyte cell membranes and, thereby, an obstructed insulin-simulated glucose uptake was not continuous throughout the C2-ceraide stimulation phase. Meanwhile, the cultures influenced by feed media containing a glucose concentration comparable to patients with type II diabetes experienced a slightly more dynamic fluctuation in glucose consumption and production [Figure 23].
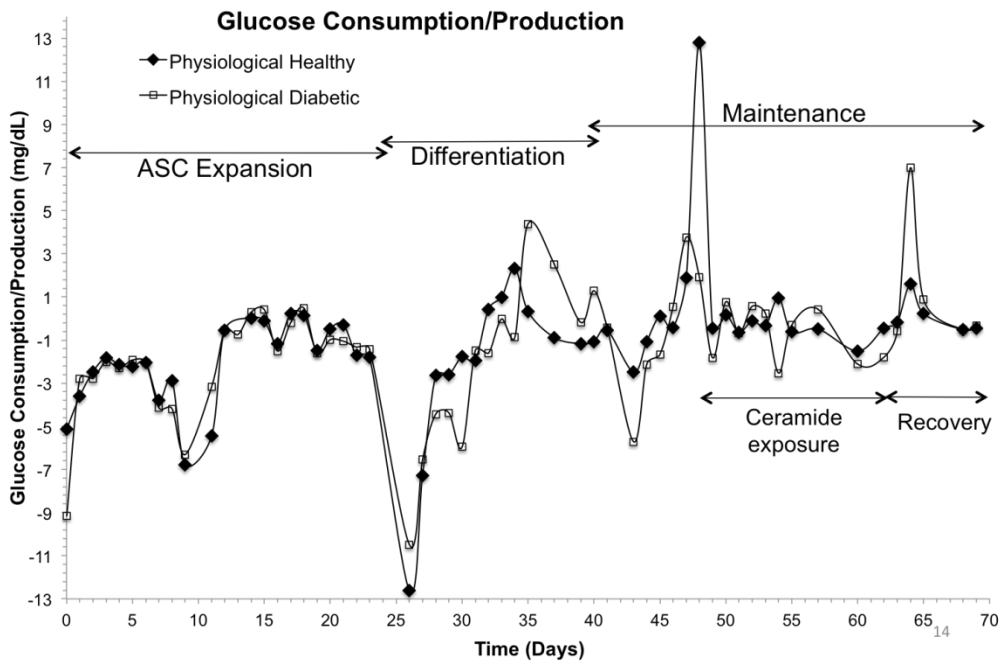
Figure 23. Metabolic activity. Average glucose production/consumption trends of two bioreactors seeded with ASCs, differentiated with treatments of diluted medium to establish a healthy physiological glucose level (solid squares), and two bioreactors seeded with ASCs differentiated with treatments of diluted medium to establish a type II diabetic glucose level (empty squares) over 70 days of culture.

Figure 24 depicts lactate consumption and production throughout the 70-day bioreactor culture of both experimental groups, where solid blocks represent metabolic activity of cultures undergoing a "healthy physiological" level of glucose concentration plus the C2-ceramide exposure period, and empty blocks display cultures fed with media containing glucose concentration at levels similar to those of patients with type II diabetes. No outstanding difference between the two groups was observed throughout culture. However, dynamic lactate production displayed at periods adjacent to medium

period changes may be attributed to ASCs and adipocytes preparing for differentiation or maintenance through storage or release of lactate.
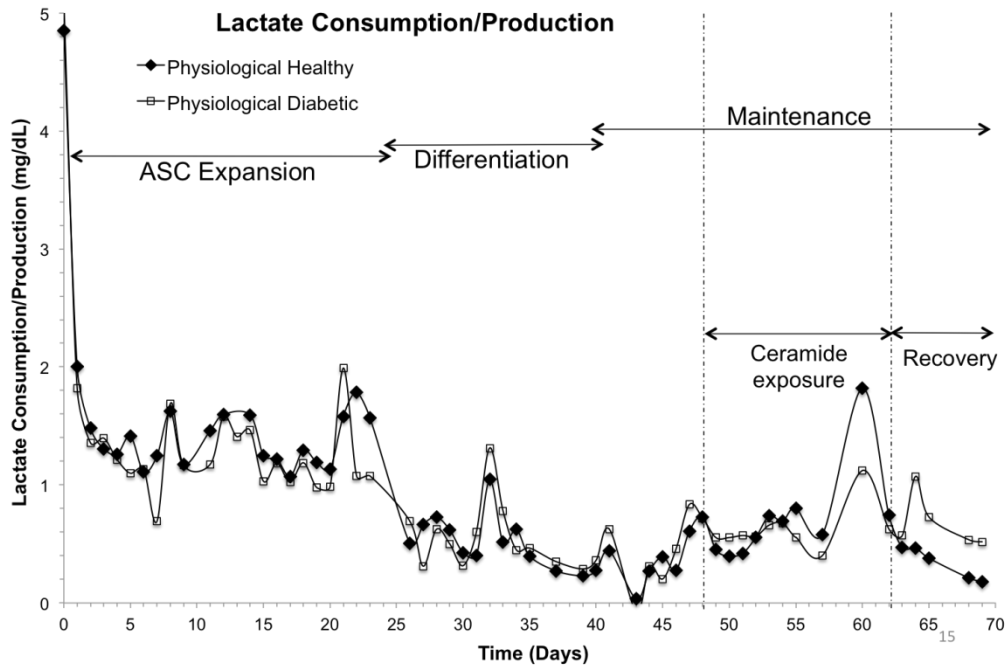
Figure 24. Metabolic activity. Average lactate glucose production/consumption trends of two bioreactors seeded with ASCs, differentiated with treatments of diluted medium to establish a healthy physiological glucose level (solid squares), and two bioreactors seeded with ASCs differentiated with treatments of diluted medium to establish a type II diabetic glucose level (empty squares) over 70 days of culture.

3.3.4 Immunohistochemistry and Histology

Imaging results of the tissue generated within the bioreactors are shown in Figures 25-26. Macroscopic tissue formation was observed in and around the hollow fiber membranes upon bioreactor disassembly [Figures 25 and 26]. Regarding both groups of adipose tissue − that differentiated from ASCs under healthy glucose conditions and that

differentiation from ASCs under conditions similar to glucose conditions of diabetic patients – histological analyses revealed closely associated adipocytes throughout all bioreactors. Confocal fluorescent imaging demonstrated AdipoRed lipid formation and FABP4 expression after 70 days of culture within the dynamic perfusion systems, while DAPI and AlexaFluor 488 Phalloidin highlight nuclei and F-actin, respectively [Fig. 25].
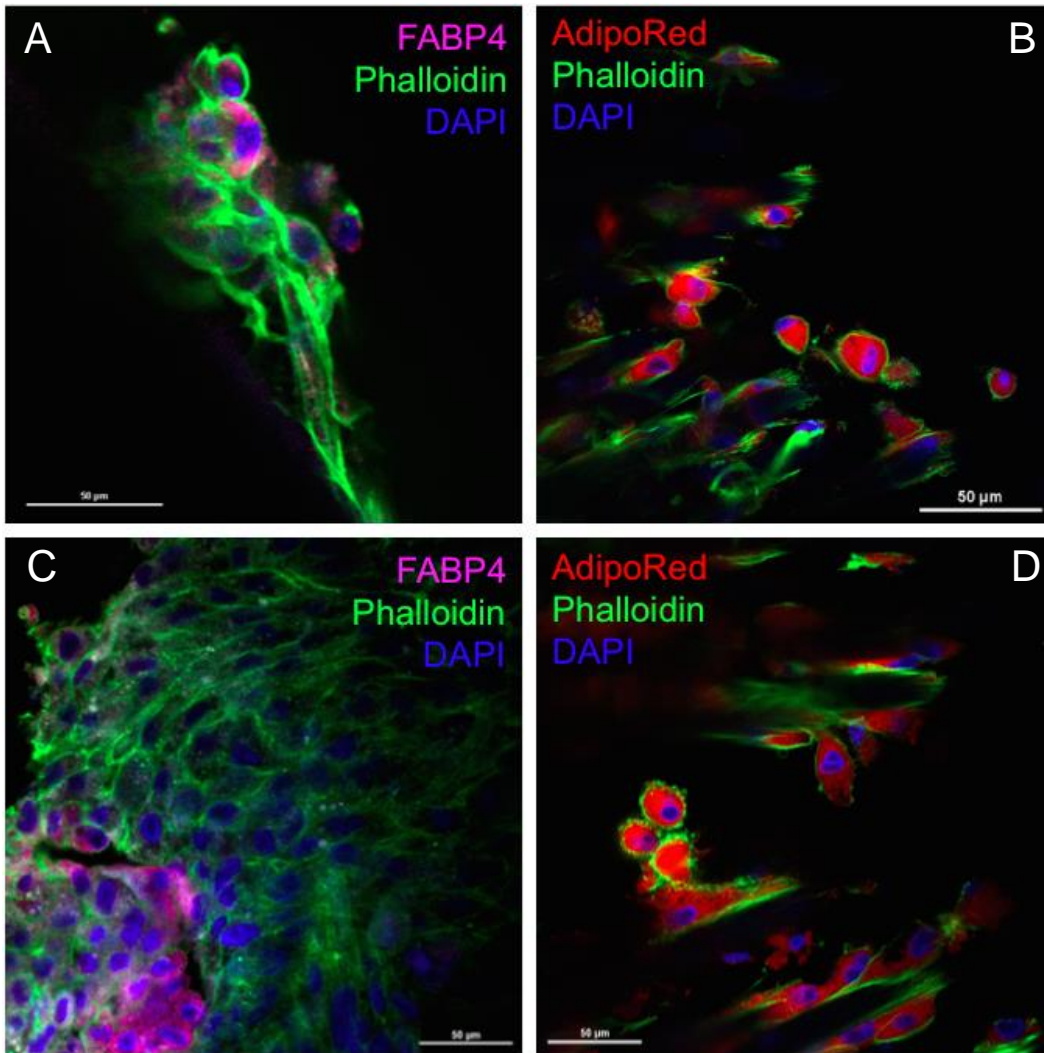
Figure 25. Immunohistochemistry. End-point 70 days, (A, C) FABP4/DAPI/Phalloidin or (B, D) AdipoRed/DAPI/Phalloidin immunohistochemistry from bioreactors containing ASCs differentiated into adipocytes and maintained at (A, B) healthy physiological glucose concentrations followed by C2-ceramide exposure or at (C, D) physiological type II diabetes mellitus glucose concentrations. Scale bar = 50 μm, red = AdipoRed, green = AlexaFluor 488 phalloidin, blue = DAPI.
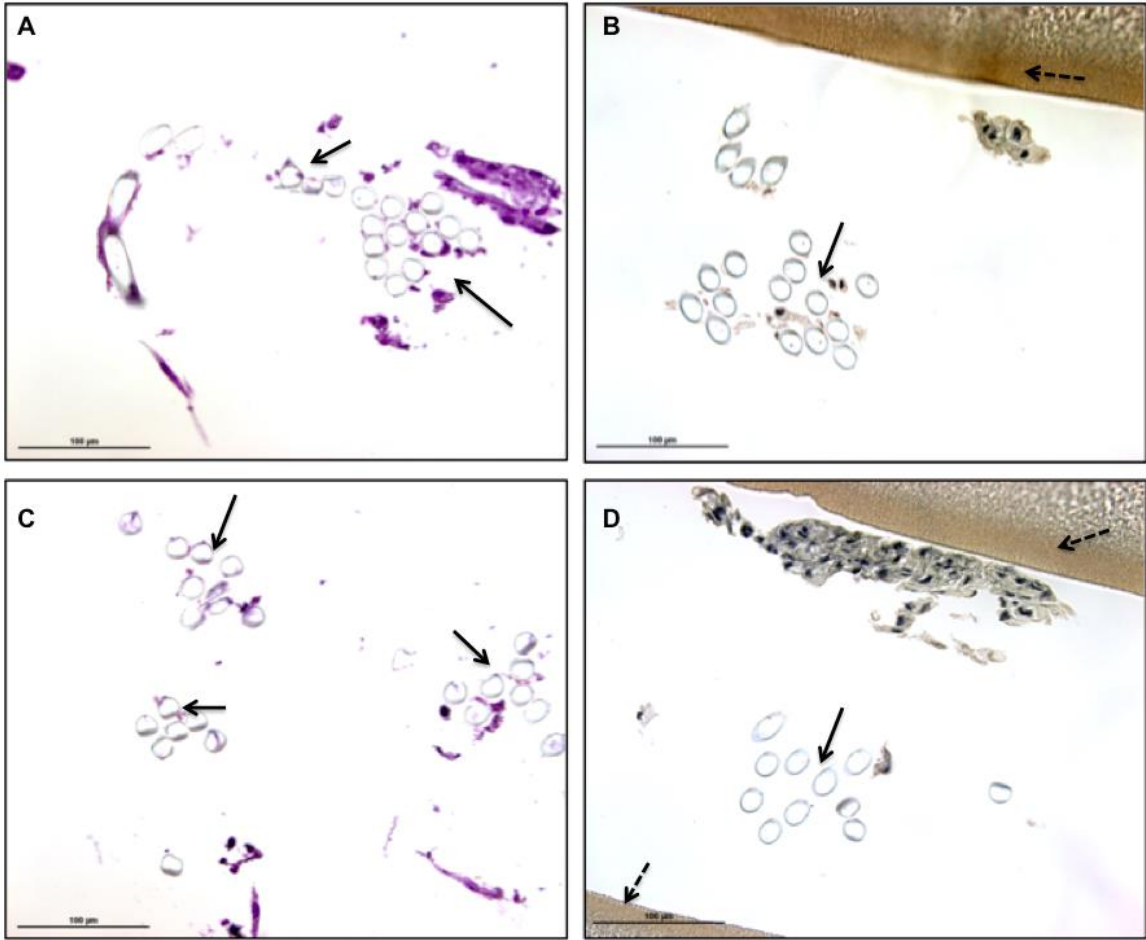
Figure 26. Histology. End-point 70 days, (A, C) H&E or (B, D) Masson's Trichrome from bioreactors containing ASCs differentiated into adipocytes and maintained at (A, B) healthy physiological glucose concentrations followed by C2-ceramide exposure or at (C, D) physiological type II diabetes mellitus glucose concentrations. Solid arrows indicate adipose architecture, dashed arrows indicate bioreactor fiber. Scale bar = 100 μm.

3.3.5 Scanning Electron Microscopy

SEM images of the samples removed from all bioreactors reveal cell growth on and among the hollow fibers with no extreme difference between the two experimental groups [Fig. 27].
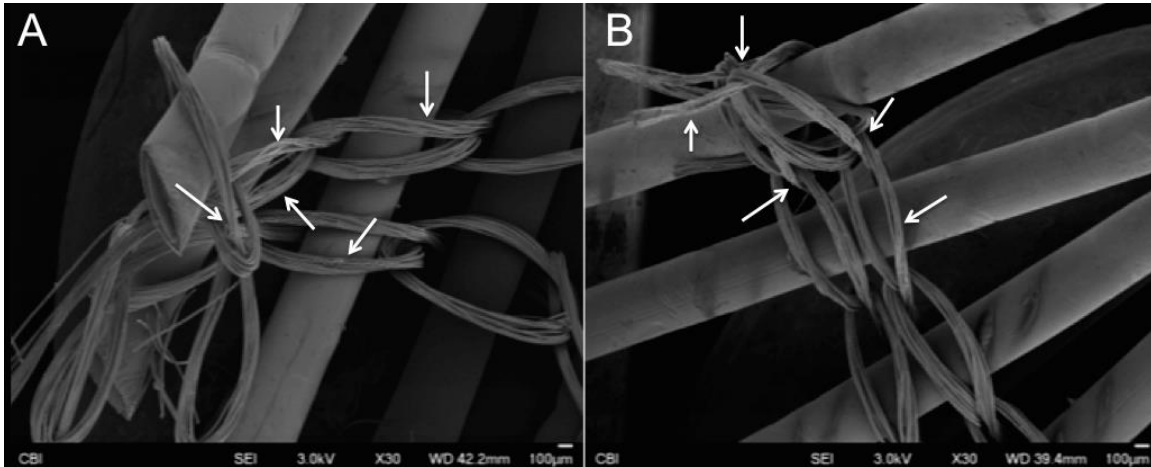
Figure 27. Scanning Electron Micrographs. Scanning Electron Microscopy (SEM) images of adipocytes on fibers extracted from bioreactors after 70 days of culture inoculated with ASCs differentiated and maintained (A) healthy physiological glucose concentrations followed by C2-ceramide exposure or at (B) physiological type II diabetes mellitus glucose concentrations. Scale bar = 100 μm.

3.4   CONCLUSIONS

Adult human ASCs isolated from healthy, non-diabetic patients, were differentiated into adipocytes as treated by culture medium consisting of various levels of glucose and, in a second *in vitro* study, adipocytes were exposed to a culture environment to simulate that of a type II diabetic patient. Once physiologically similar glucose levels

(20% dilution to represent glucose concentration similar to a non-diabetic adult and 35% dilution to represent glucose concentration of an adult with type II diabetes mellitus) were determined within adipocyte differentiation-inducing medium, a type II diabetic environment was created by addition of FFA and C2-Ceramide, inhibiting glucose transport. No major cell death was observed through days 2-7 of adipocyte maintenance, during which FFA and 2-Ceramide were included, indicating low levels of cell toxicity. A concentration of 35 μM C2-ceramide without FFA was found to yield the most optimal hindered glucose uptake by the differentiated ASCs. The presented work lays the groundwork necessary for future application of the developed protocol into a hollow fiber-based bioreactor that allows long-term maintenance of adipose tissue to establish a physiologically relevant, type II diabetic-like environment.

Human adipose-derived stem cells derived from female adults without type II diabetes mellitus were cultured within hollow fiber-based membrane, three-dimensional, dynamic perfusion bioreactors for 70 days and metabolic behaviors were assessed. Masson's Trichrome, H&E, AdipoRed, and FABP4 images of the functional adipocytes show no major difference between adipose tissue generated in cultures with glucose levels at healthy or diabetic concentrations. The lack of elevated glucose levels during C2-ceramide stimulation may be due to a scale-up issue, or a downstream differentiation discrepancy between the study of Summers et al. [123, 181], plus the *in vitro* studies explained in Chapter 3 compared to *ex vivo* scenarios of mature adipocytes exhibited in the bioreactor systems. The presented work provides a first step towards an engineered model necessary to the study of anti-diabetic drug therapy *ex vivo* in addition to a

platform for three-dimensional perfusion and long-term maintenance of functional adipocytes.

4.0 APPLICATION OF A DECELLULARIZED ADIPOSE EXTRACELLULAR MATRIX HYDROGEL TO ENHANCE ADIPOSE TISSUE GROWTH HOMOGENEITY WITHIN A HOLLOW FIBER-BASED, THREE-DIMENSIONAL, DYNAMIC PERFUSION BIOREACTOR

4.1 INTRODUCTION

4.1.1 Decellularized Extracellular Matrix Materials

Decellularization is a process commonly used in tissue engineering and regenerative medicine to isolate the extracellular matrix (ECM) of a tissue by removal of the inhabiting cells to serve as a scaffold for cell growth, differentiation, and tissue development [182-184]. Elimination of the native cells eliminates concerns of organ rejection and lifetimes of immunosuppression medications for patients. Decellularized tissue and organs have offered solutions to several regenerative preclinical applications, including skin grafting, cardiac tissue engineering, lung transplantation, and pancreatic engineering. Numerous methods have been proven to decellularize a variety of tissues, including combinations of mechanical [185-191], chemical [192-201], and enzymatic [202-210] methods. Many studies have concluded that the methods by which the ECM biomaterial is prepared have a significant influence on the biochemical and structural properties of the resulting scaffold.

Biological scaffold materials composed of decellularized ECM have been considered as medicinal devices by regulatory bodies, such as the Food and Drug Administration. With commercialization attempts at injectable and hydrogel forms of ECM products, this form of ECM biomedical products will be classified and regulated as a biologic.

In a 2009 study by Gilbert et al., DNA content and fragment length were determined in both laboratory-produced and commercially available ECM scaffold materials [211]. The team examined six commercially available ECM scaffolds: two from porcine small intestine (Oasis – Cook Biotech, Inc. and Restore – DePuy Orthopaedics), Acell Vet (Acell, Inc.) originating form porcine urinary bladder, Zimmer Collagen Repair Patch (Zimmer, Inc.) originating from porcine dermis, and two from human dermis (Alloderm – Lifecell, corp. and GraftJacket – Wright Medical Technology). The three laboratory-produced ECM scaffolds were derived from porcine small intestine, porcine urinary bladder, and porcine liver. Through DAPI, H&E, DNA quantification through PicoGreen DNA assay, and fragment length analysis, results showed that the majority of DNA is removed from ECM devices, but small amounts remain in most tested materials (with most fragments less than 300 base pairs long) [211]. Despite DNA presence in many of the commercially available ECM products studied, their clinical efficacy has proven successful [212-225]. It is mentioned that complete removal of all cellular contents is likely impossible due to the manner in which cells are embedded within tissue, especially dense tissues such as the dermis, in addition to intracellular cytoplasmic proteins and membrane components being retained in the scaffold materials during the processing steps [211].

89

Host response following surgical implantation of biological surgical ECM devices may vary from poor to excellent [226-230]. The diverse range in outcomes is associated with factors related to device manufacturing methods and the type and intensity of the innate immune response elicited by the final product [230]. Three factors known to influence bioscaffold remodeling include efficacy of decellularization [231-243], use of chemical crosslinking agents [244-252], and age of the source tissue from which the ECM is collected [253-257]. According to Dr. Stephen Badylak, two categories of bioscaffold remodeling include constructive and proinflammatory remodeling. Constructive remodeling of ECM scaffolds involves complete degradation of a degradable biomaterial and gradual replacement by anatomically appropriate and functional tissue. This occurs when an ECM scaffold is prepared by methods through decellularization of the source tissue and avoidance of the use of chemical crosslinking methods for the resultant ECM product [230, 258]. Proinflammatory response to ECM scaffolds can consist of chronic inflammation when the material is used for inappropriate clinical applications and/or when the biomaterial was manufactured via methods that alter the native structure and composition of the matrix [230].

4.1.2 Decellularized Adipose Tissue ECM

Over the past decade, adipose tissue engineering has quickly escalated with attention to the reconstructive properties and advantages innate to adipose tissue [4, 55-63]. While some preclinical research has focused on three-dimensional scaffolds as structural support for promoting adipogenesis and volume retention, an injectable option may prove to be more clinically relevant and would share more similar physical

properties to lipoaspirate than a synthetic or biopolymer scaffold. Most commercially available soft tissue fillers comprise of collagen, hyaluronic acid, hydroxyapatite, or polylactic acid, and many studies are currently investigating injectable synthetic and natural polymers for adipose tissue engineering. A few groups have evaluated ASC proliferation, neovascularization, and adipogenesis under the influence of human adipose tissue either in a lyophilized [259], powder form [260], or as a decellularized, delipidized ECM hydrogel [260, 261].

4.1.3 Chapter Aims

The studies presented in Chapter 4 describe Specific Aim 3 to further enhance the adipose tissue *ex vivo* by optimizing homogeneity within the bioreactor culture. The work is driven by the hypothesis that inclusion of a decellularized adipose tissue extracellular matrix (ECM) hydrogel within the *ex vivo* bioreactor culture system will enhance ASC differentiation to the adipocyte lineage and improve adipose tissue homogeneity within the bioreactor.

4.2 MATERIALS AND METHODS

4.2.1 Decellularization of Adipose ECM

Adipose tissue delipidization, decellularization, and gelation protocols were optimized influenced upon combinations of previous work reported in the literature [261, 263]. Adipose tissue was harvested from the abdominal depot of non-diabetic female

patients undergoing elective plastic surgery at the University of Pittsburgh Medical Center in Pittsburgh, PA, USA. Tissue was collected under a human studies exempt protocol approved by the University of Pittsburgh Institutional Review Board (IRB). De-identified specimens were obtained from discarded surgical tissue under an approved process that did not require subjects to provide written or verbal informed consent.

Whole adipose tissue was run through a meat grinder (Demi 800 HP table top meat grinder) with first a coarse grinding plate then a fine grinding plate, centrifuged at 1000 rpm (6449 x g) and 4 °C for 10 minutes. Once the lipid layer is carefully removed via glass pipetting, the adipose layer was stirred with a 1:1 m/v ratio of 1-propanol for a series of 1.5, 20, 2, 1.5 hours, with a centrifugation, removal of supernatant and lipid, plus replenishing of 1-propanol at each change. Following the 1-propanol washes was a series of EtOH washes of 100% for 30 minutes, 90% for 15 minutes, and 85%, 70%, 70% for 10 minutes, with a centrifugation and removal of supernatant between each step.

For decellularization, adipose tissue was soaked and stirred for thirty hours in a 1M NaCl solution, centrifuged with supernatant removed, then soaked and stirred in 0.1% Triton X-100 for 72 hours. After centrifugation and removal of supernatant, 1-propanol and EtOH washes were repeated. To disinfect, the adipose ECM was washed twice with DI water, centrifuged and supernatant removed, then soaked for no longer than 4 hours in 1% peracetic acid. Solution was centrifuged, supernatant removed, washed with 10X PBS, centrifuged and supernatant removed, then washed with 1X PBS three times. Decellularized adipose ECM was stored at 4 °C in 1X PBS until ready to use.

To form a hydrogel, decellularized adipose ECM was lyophilized (Labconco, Kansas City, MO, USA), grinded via mortar and pestle, then sifted by a Thomas Wiley Mill (Thomas Scientific, Swedesboro, NJ, USA). Decellularized adipose ECM was stored at -20 °C until ready for digestion. To digest the decellularized adipose ECM powder, 1 mg pepsin per 10 mg adipose ECM in 0.1M HCl was stirred for 48 hours. Hydrogel formed at 37 °C within 30 minutes and was sterilized via 20 minutes of UV sterilization.

4.2.2 Characterization of Adipose ECM

4.2.2.1 Histology

Decellularized adipose ECM was fixed in 10% buffered formalin, processed, paraffin embedded, then sectioned at 6 μm-thick slices. Samples were assessed by staining with H&E and imaged on an Olympus Provis Light Microscope (Olympus America, Melville, NY, USA).

Non-paraffin embedded samples were analyzed via Scanning Electron Microscopy (SEM), samples were air dried and placed onto metal stubs covered in double-sided copper tape. The samples were then gold-sputtered to a density of 3.5 mm from Cressington 108 auto sputter-coater (Cressington, Watford, UK) and imaged with a JEM-6330f Scanning Electron Microscope (Jeol, Peabody, MA, USA). Scope was operated at 5kV acceleration.

To evaluate nuclei presence, a sample of decellularized adipose ECM and a native adipose sample were stained with DAPI and imaged on an Olympus Provis Light Microscope.

4.2.2.2 Immunohistochemistry

To test antibody specificity of the decellularized adipose ECM, paraffin embedded samples were rehydrated, antigens unmasked via a 10 mM sodium citrate buffer pH 6.0 for 40 minutes at 97.0 ±1 °C.   Slides were blocked for engodgenous peroxidase activity with 3% H_2O_2 for 20 minutes, then blocked with an Avidin/Biotin solution (Vector Laboratories, Burlingame, CA, USA) plus an antibody diluent containing SuperBlock T20 (Thermo Fisher), goat serum, and BSA in addition to the primary antibody of choice overnight at 4 °C.   Biotin-conjugated secondary antibody were incubated on samples for 30 minutes and exposed via DAB chromagen.   Slides were counterstained with hematoxylin, dehydrated, and coverslipped with permount then imagined on an Olympus Provis Light Microscope.

4.2.2.3 *In vitro* cell viability

Before inoculating valuable bioreactor systems with a novel biological hydrogel, cell viability must be evaluated. ASCs were seeded at 10,000 cells per well within a 96-well plate either with or without the decellularized adipose ECM gel, and were either stimulated by differentiation media or maintained with ASC plating media at studied at 1 or 7 days. Cell feed medium was changed every other day and cells stored at 37 °C at 5%

CO_2. At 1 and 7 days, ASCs were fixed with 4% paraformaldehyde for 30 minutes, washed with 1X PBS and quantitatively examined via Live/Dead staining.

4.2.3 ASC Isolation

Adipose tissue was harvested from the abdominal depot of a non-diabetic female patient (58 years old, body mass index (BMI) of 36.0) undergoing elective plastic surgery at the University of Pittsburgh Medical Center in Pittsburgh, PA, USA. Tissue was collected under a human studies exempt protocol approved by the University of Pittsburgh Institutional Review Board (IRB). De-identified specimens were obtained from discarded surgical tissue under an approved process that did not require subjects to provide written or verbal informed consent. Donors were not pre-diabetic and did not have insulin resistance at time of adipose tissue harvesting.

Abdominal adipose tissue was placed in 50 mL centrifuge tubes at 10 g per tube and soaked in 1 mg·mL^{-1} of freshly prepared collagenase (Type II collagenase, Worthington Biochemical Product Catalog; Lakewood, NJ, USA). The tissue was finely minced, vortexed, and shaken at 37 °C for 35 minutes until a fatty supernatant layer became apparent. Tubes were again vortexed and filtered through double-layered gauze (J&J Steri-Pad Gauze Pads; New Brunswick, NJ, USA) into sterile 50 mL centrifuge tubes. Digested specimens were then centrifuged at 1000 rpm (6449 x g), 4 °C for 10 minutes, fatty layers aspirated, and resulting pellets suspended in erythrocyte lysing buffer. The solution was once again centrifuged at 1000 rpm (6449 x g), 4 °C for 10 minutes and the pellet, containing the stromal vascular fraction, was resuspended in Dulbecco's Modified Eagle's Medium (DMEM/F12) with 10% v/v fetal bovine serum

and 1% v/v penicillin/streptomycin, plated, and stored at 37 °C at 5% CO_2. Cells were expanded in two dimensions using growth medium with low serum (Promocell Preadipocyte Growth Medium, Heidelberg, Germany), passaged at confluency, and characterized as previously described by our laboratory [56].

4.2.4 Bioreactor Inoculation

The bioreactors are prototyped by Stem Cell Systems (Berlin, Germany) and contain three independent hollow fiber membrane systems, interwoven into repetitive subunits, forming a cell compartment that houses 8.0×10^7 cells with a volume of 8 mL [Fig. 8]. The capillary network serves three functions: cell oxygenation/carbon dioxide removal, medium inflow, and medium outflow via countercurrent flow operation of two independent membrane systems. As a result of interweaving and high performance mass exchange via counter-current medium flow operation, decentralized gas supply and medium exchange with low gradients is provided to the cultures. The medium fiber membrane systems are made of polyethersulfone capillary systems (Membrana, Wuppertal, Germany) with a molecular weight cutoff of 400,000 g·mol^{-1} and gas is supplied by hydrophobic multi-laminate hollow fiber membrane systems (MHF; Mitsubishi, Tokyo, Japan).

Table 7 describes the experimental design of Specific Aim 3. A total of six bioreactor experiments were performed: three bioreactors received ASCs in combination with the decellularized adipose ECM at inoculation, and three bioreactors received ASCs in media suspension, with no ECM addition at inoculation. Bioreactor sterilization was performed with ethylene oxide gas and degassed with air. Before cells were introduced

into the system, a continuous phosphate buffered solution flush was run within the bioreactor for 72 hours, followed by priming with DMEM/F12 media flush for 24 hours prior to inoculation. Cell suspensions of 4.5×10^7 total cells per bioreactor were inoculated and cultured throughout a time period of five weeks. The cell compartments were continuously perfused with culture media through the polyethersulfone hollow fiber bundles at a feed rate of 4 mL·hr^{-1} in combination with a recirculation loop at a rate of 20 mL·min^{-1}. Waste medium was removed from the circuit at 4 mL·hr^{-1}. The flows of compressed air and carbon dioxide in the gas compartment were maintained at 20 mL·min^{-1}. Partial pressures of oxygen, carbon dioxide, and acid/base status within the bioreactor were measured daily and the carbon dioxide content was adjusted throughout culture time to maintain the medium pH within the range of 7.35-7.45.

Table 7. Experimental design of Specific Aim 3.

Bioreactor #	Decellularized Hydrogel?
1	**Yes**
2	**No**
3	**Yes**
4	**No**
5	**Yes**
6	**No**

4.2.5 Cell Culture

Cells were inoculated into the bioreactor cell compartments via a suspension of 4.5×10^7 cells per mL of medium and/or adipose ECM [Fig. 27]. Cell passage at time of inoculation was at passage 4. Upon completion of a twenty-one day expansion period of the ASCs within the bioreactor cell compartment by perfusion of ASC plating media

(DMEM/F12 as described above), to initiate three-dimensional adipogenic differentiation, the feed media was changed for the following fourteen days to adipogenic media containing DMEM/F12, HEPES, biotin, pantothenate, human insulin, dexamethasone, 3-isobutyl-1-methylxanthine (IBMX), PPAR-γ agonist, and antibiotics (ZenBio, Research Triangle Park, NC, USA). Adipocytes were maintained for seven days with feed media containing DMEM/F12, HEPES, fetal bovine serum, biotin, pantothenate, human insulin, dexamethasone, and antibiotics.Cells were not further passaged within the bioreactor, rather, cell fate was influenced by changes in culture medium.

In parallel, ASCs in a two-dimensional control group were cultured in 175 cm^2 tissue culture flasks with ASC plating medium containing 10% v/v fetal bovine serum and 1% v/v penicillin/streptomycin, plated, and stored at 37 °C at 5% CO_2. 2D control ASCs were cultured for forty-four days with static media changes every other day and passaged at 80% confluency.
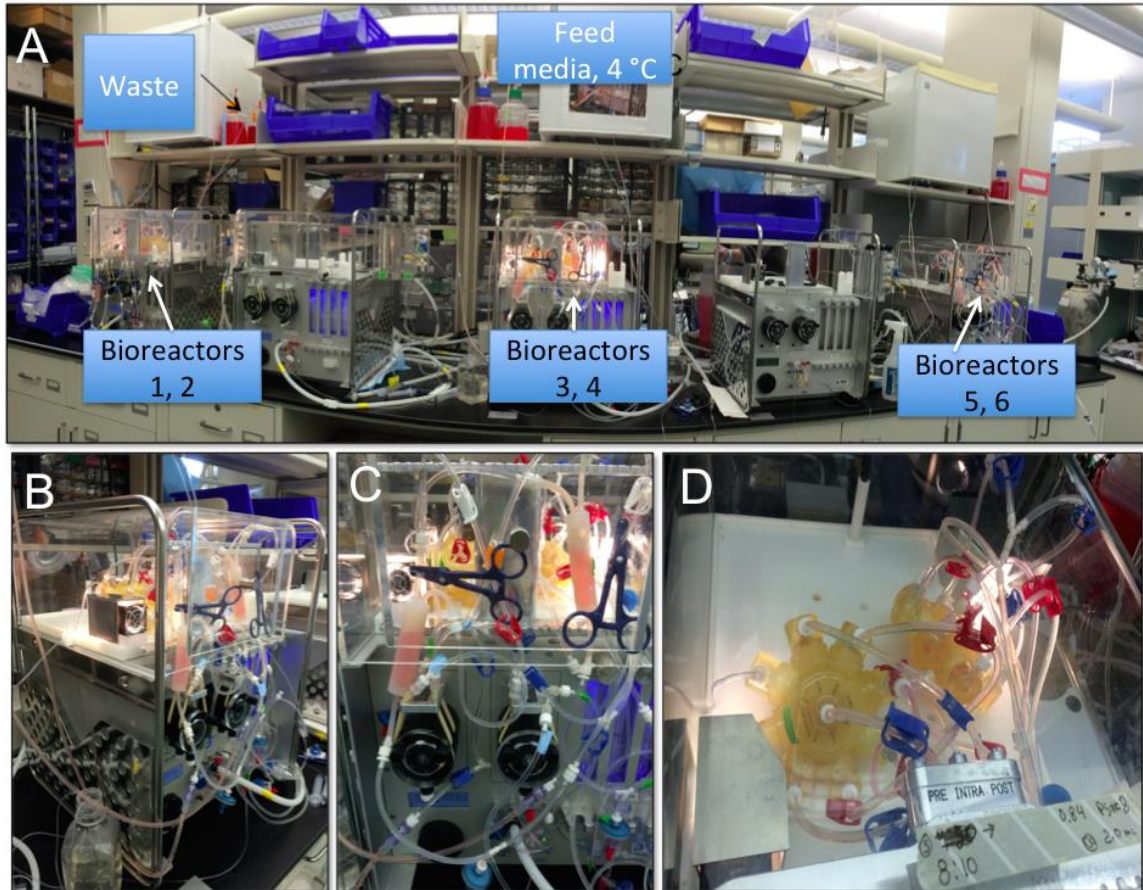
Figure 28. Bioreactor setup for Specific Aim 3. Six bioreactors connected to three perfusion pumps set to circulate feed media at a 4.5 mL/hr rate. Feed media is stored at 4 °C and is highlighted in the schematic along with the waste buckets, which are discarded when full. Bioreactors 1, 3, and 5 received a decellularized adipose ECM hydrogel upon bioreactor inoculation with ASCs, while bioreactors 2, 4, and 6 were inoculated with ASCs only.

4.2.6 Metabolic Activity Analysis

Glucose production rate throughout culture was assessed under a dynamic open-circuit system. A sampling volume of 2 mL was taken daily via a luer-lock sample port; glucose and lactate dehydrogenase levels measured (YSI 2300 STATE Plus Glucose & Lactate Analyzer; YSI Life Sciences, Yellow Springs, OH, USA; Quantichrom Lactate Dehydrogenase Kit; BioAssay Systems, Hayward, CA, USA).

Glucose production/consumption rates of the cells were determined by a previously established protocol considering various parameters including measured glucose concentration within the recirculation sample, total system volume, baseline medium concentrations, flow rate of nutrients through the system, and time points of measurements [161-165, Eqns 2 and 3 Chapter 2.2.4.].

4.2.7 Tumor-Necrosis Factor-a Functional Testing

After seven days of maintenance, adipocytes within all six bioreactor cultures underwent exposure to 10 ng·mL^{-1} direct injection of tumor necrosis factor (TNF)-α (Roche Applied Sciences, San Francisco, CA, USA) intended to inhibit glucose uptake by the adipocytes. TNF-α exposure lasted for 24 hours and glucose production was measured every 30 minutes. Feed inlet and waste outlet flow rates were set to 10 mL·hr^{-1} to ensure that the entire circuit volume was replaced every hour. Throughout TNF-α exposure, media containing 10 ng·mL^{-1} dosage of TNF-α and no insulin was delivered to the tissue with intention of hindering glucose consumption of the adipocytes.

Once glucose consumption/production had stabilized after 24 hours of TNF-α delivery, all six bioreactors were stimulated with human insulin as a "recovery" (Sigma-Aldrich, St. Louis, MO, USA) by a 5 µM direct injection in addition to delivering feed medium containing insulin to maintain a steady influx of insulin for an 8-hour period. After the 8-hour stimulation period, feed medium was returned to non-insulin containing medium and glucose consumption measurements were continued for another 20 hours to confirm adipocyte metabolism had returned to baseline before bioreactor disassembly.

4.2.8 Immunohistochemistry and Histology

Upon termination of each bioreactor culture, tissue/fiber samples were extracted from the bioreactors and placed in 10% w/v buffered formalin (Thermo Scientific) and stored at 4 °C in the formalin for fixed histology samples. Samples were stained with AdipoRed Assay Reagent to analyze lipid inclusion (Lonza, Walkersville, MD, USA). Samples were protected from light and incubated at room temperature with AdipoRed staining dilutions according to Lonza protocol for 40 minutes, then exposed to DAPI (0.6 µg/mL, Invitrogen) and AlexaFluor 488 Phalloidin (6.6 µM, Invitrogen) to stain for nuclei and F-actin, respectively, for 10 minutes at room temperature. Immunofluorescence was captured from an Olympus Fluoview 1000 Upright Confocal Microscope (Olympus America, Melville, NY, USA).

Additionally, samples were paraffin embedded, stained with Masson's Trichromeand imaged under bright field microscopy of an Olympus Provis Light Microscope (Olympus America) for architectural assessment, to determine matrix formation, and to verify human tissue growth.

To test antibody specificity within the bioreactor culture samples, paraffin embedded samples were rehydrated, antigens unmasked via a 10 mM sodium citrate buffer pH 6.0 for 40 minutes at 97.0 ±1 °C.   Slides were blocked for endogenous peroxidase activity with 3% H_2O_2 for 20 minutes, then blocked with an Avidin/Biotin solution (Vector Laboratories, Burlingame, CA, USA) plus an antibody diluent containing SuperBlock T20 (Thermo Fisher), goat serum, and BSA in addition to the primary antibody of choice overnight at 4 °C.   Biotin-conjugated secondary antibody were incubated on samples for 30 minutes and exposed via DAB chromagen.   Slides were counterstained with haematoxylin, dehydrated, and coverslipped with permount.

4.2.9 Statistical Methods

Results are presented as mean ± standard deviation.   Unpaired, two-tailed *t*-tests were performed to assess differences in metabolic activity between treatment groups. All data were found to be normally distributed and variances were homogenous.   Statistical significance is determined at *p*-values less than 0.05.

4.3 RESULTS AND DISCUSSION

4.3.1 Decellularized Adipose ECM Characterization

4.3.1.1 Histology

When stained with H&E, the architectural properties of the adipose ECM appeared vastly different from that of native whole adipose tissue [Fig. 29].

Qualitatively, adipocyte architecture was not observed in the decellularized adipose ECM, indicating delipidization. Furthermore, nuclei visible in the native whole adpose tissue were not apparent in the decellularized sample, suggesting successful decellularization.
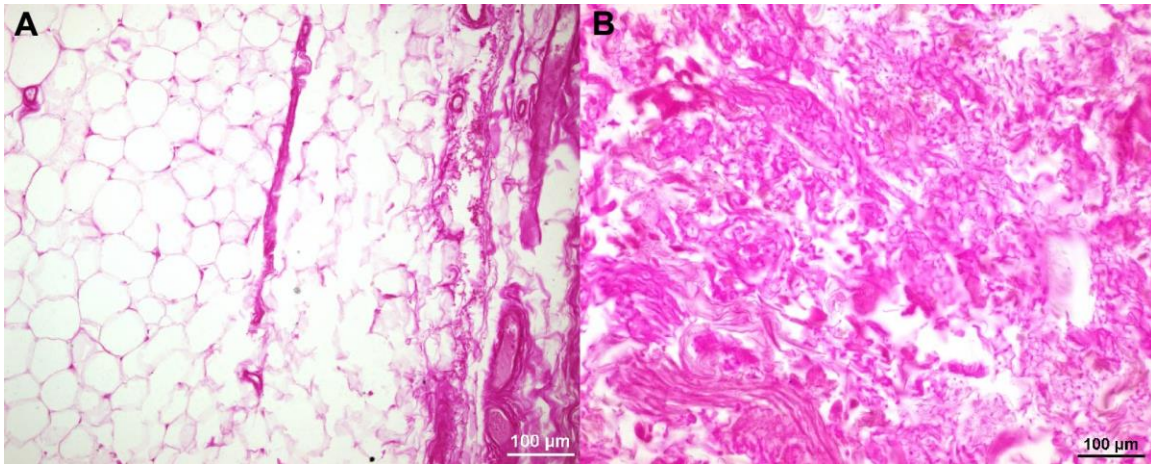
Figure 29. H&E staining of A) native adult human whole fat tissue and B) decellularized adipose ECM. Scale bar = 100 μm.

Observation via scanning electron microscopy reveals the decellularized adipose ECM displayed the architecture of apparent vacuoles, approximately 100 μm in which adipocytes may have existed before delipidization [Fig. 30]. The porous nature of the remaining matrix encourages the underlying hypothesis of Specific Aim 3 that incorporation into the bioreactor system will enhance adipogenesis and proliferation of tissue *ex vivo.*
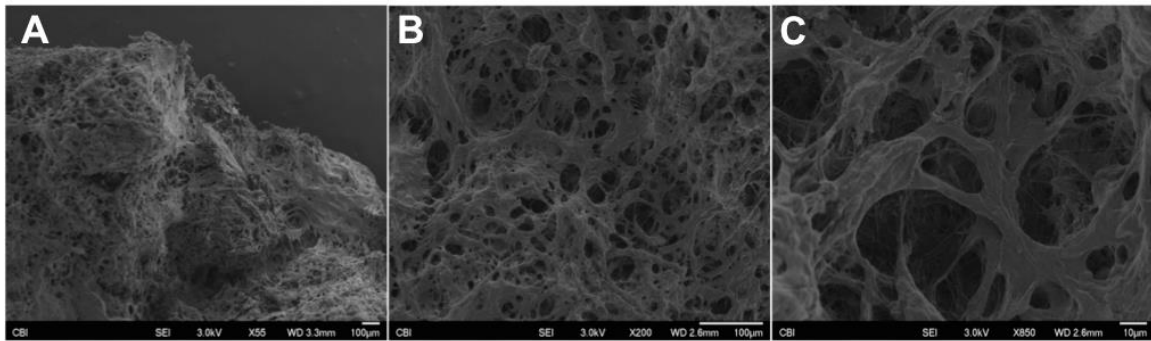
Figure 30. Scanning electron microscopy of decellularized adipose ECM at increasing magnifications: A) 55X, scale = 100 μm; B) 200X, scale = 100 μm; C) 850X, scale = 10 μm.

Assessing the decellularization of the adipose tissue with DAPI fluorescence, it is noted that, compared to native whole adipose tissue (Fig. 31B), the decellularized adipose ECM exhibited in Figure 31A has comparatively less nuclei; however, some nuclei still remain.
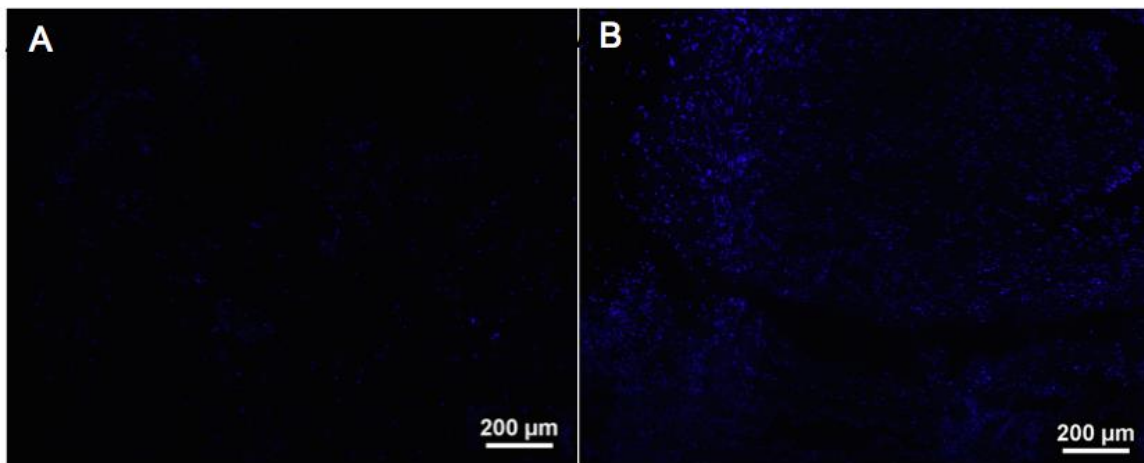
Figure 31. Nucleic assessment of A) decellularized adipose ECM and B) human whole fat tissue. Scale bar = 200 μm.

4.3.1.2 Immunohistochemistry

Collagens I, III, IV, and VI in addition to heparan sulfate proteoglycan (HSPG) and nidogen expression within the decellularized adipose ECM were studied and compared to native whole adipose tissue. While Collagens I, III, and VI were highly expressed in the decellularized adipose ECM, collagen IV, HSPG and nidogen were expressed at a lower level; however, still expressed [Figs. 32 and 33, Table 8].

Collagens I, III, and VI are typically found alongside one another and were both expressed in the decellularized adipose ECM. Collagen IV forms the basal lamina and the epithelium-secreted layer of the basement membrane. HSPG are the proteoglycan of heparan sulfate, attaching in close proximity to the cell surface or extracellular matrix proteins, and nidogen is a glycoprotein belonging to the basement membrane, connecting together networks formed by collagens and laminins.

Expression of collagens I, III, IV, and VI in addition to HSPG and nidogen, it can be concluded that the ECM remains intact after the mechanical and chemical decellularization of the whole adipose tissue.
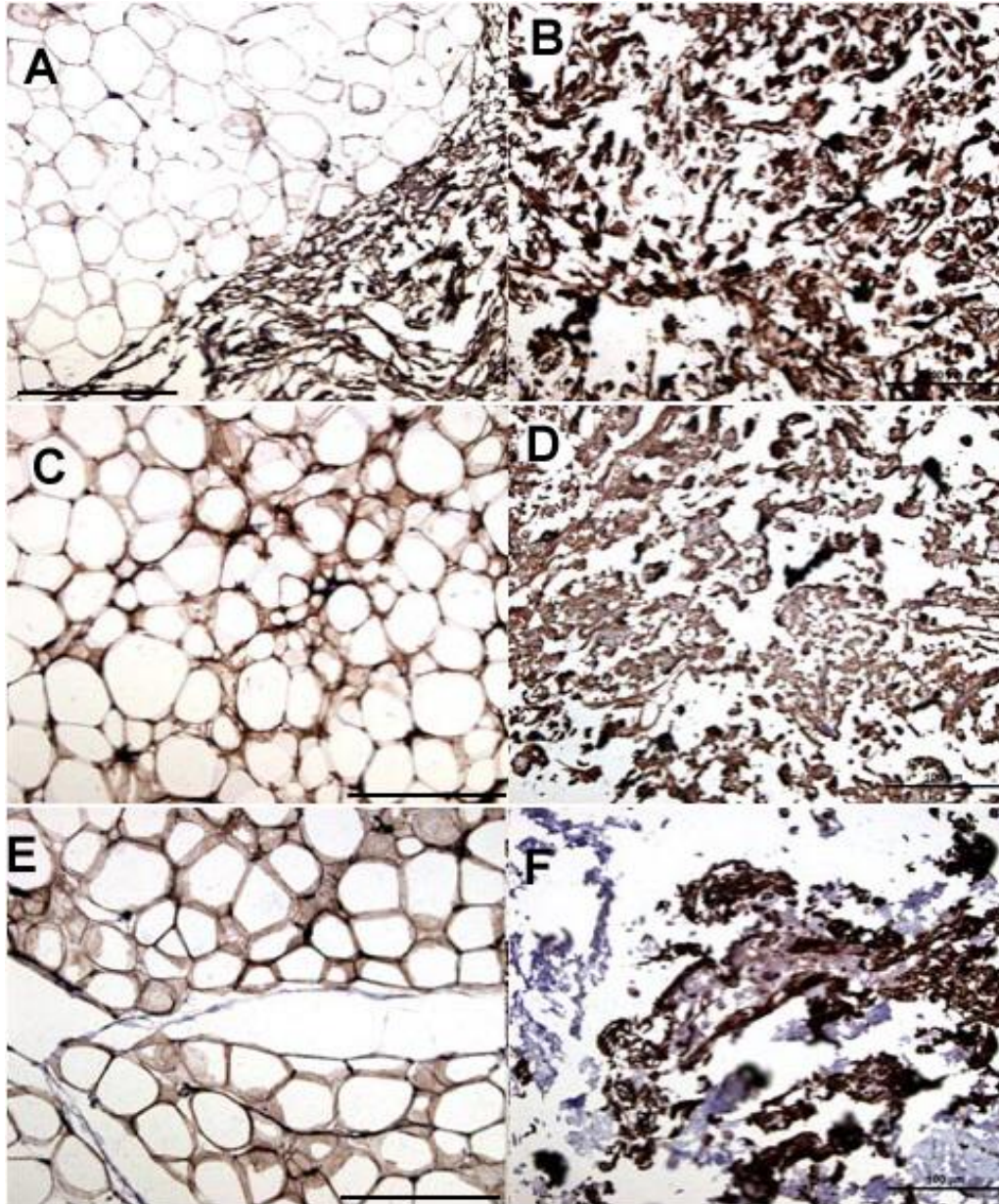
Figure 32. Immunohistochemical expression of A, B) collagen I; C, D) collagen III; and E, F) collagen IV, where the left column (A, C, E) is native human whole adipose tissue and the right column (B, D, F) is decellularized adipose ECM. Scale bar = 100 μm.
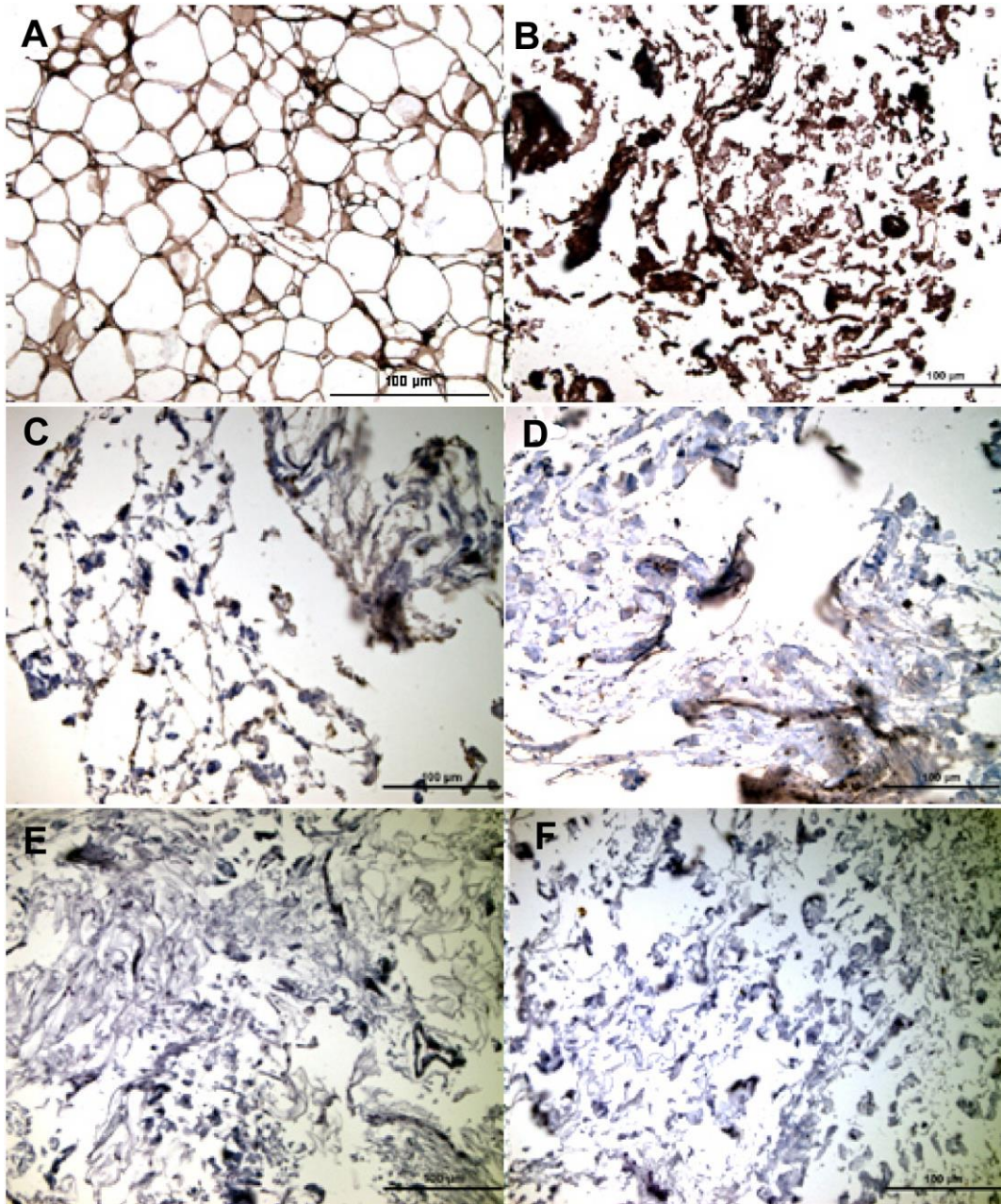
Figure 33. Immunohistochemical expression of collagen VI, HSPG, and nidogen, where the left column of is images of native human whole fat tissue and the right column is images of decellularized adipose ECM. Scale bar = 100 μm.

Table 8. Components in Native Human Whole Adipose Tissue and Decellularized ECM Biomaterial

Components	Physiological Function	Native Human Adipose Tissue	Decellularized Adipose
Collagens			
Type I	Cell guidance and migration, structure, and support	☐	☐
Type III		☐	☐
Type IV		☐	☐
Type VI		☐	☐
Proteoglycans			
HSPG	Binds growth factors	☐	☐
Glycoproteins			
Nidogen	Cell proliferation, migration, and attachment	☐	☐

4.3.1.3 *In vitro* cell viability

ASCs were cultured in 96 well plates either containing 100 μL of the decellularized adipose ECM hydrogel or no hydrogel. The experiment was ended 24 hours [Fig. 34] or 7 days after seeding [Fig. 35] and either exposed to adipocyte differentiation medium or simply ASC plating medium, which would not initiate differentiation. At experiment termination, cell viability was quantified via Live/Dead staining which exposes live cells retaining the dye calcein fluorescing green, or dead cells allowing ethidium homodimer-1 (EthD1) through the damaged membranes and fluorescing red.

At 24 hours, no significant difference was observed in cell death between groups. However, the groups without the adipose ECM hydrogel had a significantly higher number of live cells than the groups without adipose ECM hydrogel ($p < 0.05$, $N=8$, Fig. 34).

At 7 days, no statistically significant difference in live cells was observed between any treatment groups, while there were differences in cell death between all groups ($p < 0.05$, $N=8$, Fig. 35). Such a dramatic difference may be due to an effect of the adipose ECM hydrogel on the fluorescence quantification.
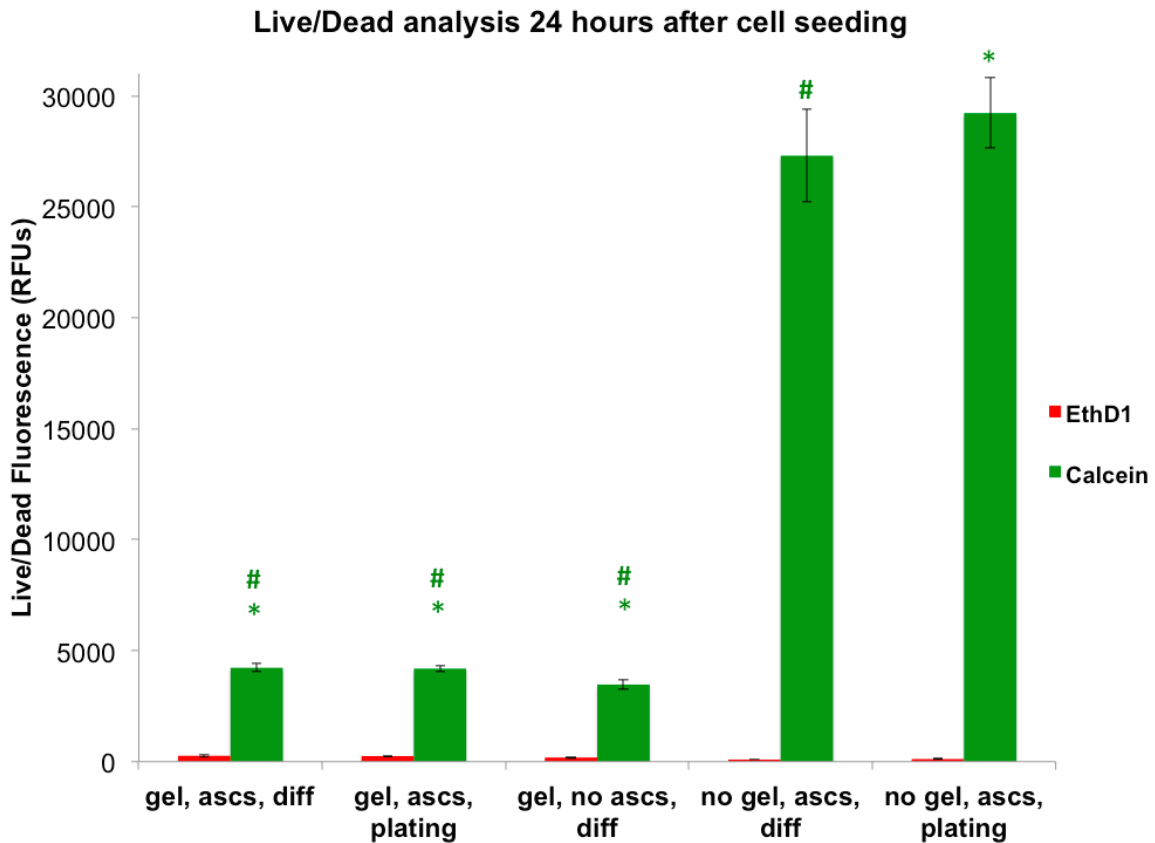
Figure 34. Cell viability after 24 hours of ASCs either cultured on adipose ECM hydrogel or directly on surface of 96 well plates. *, # $p < 0.05$, $N=8$, mean ± standard deviation.
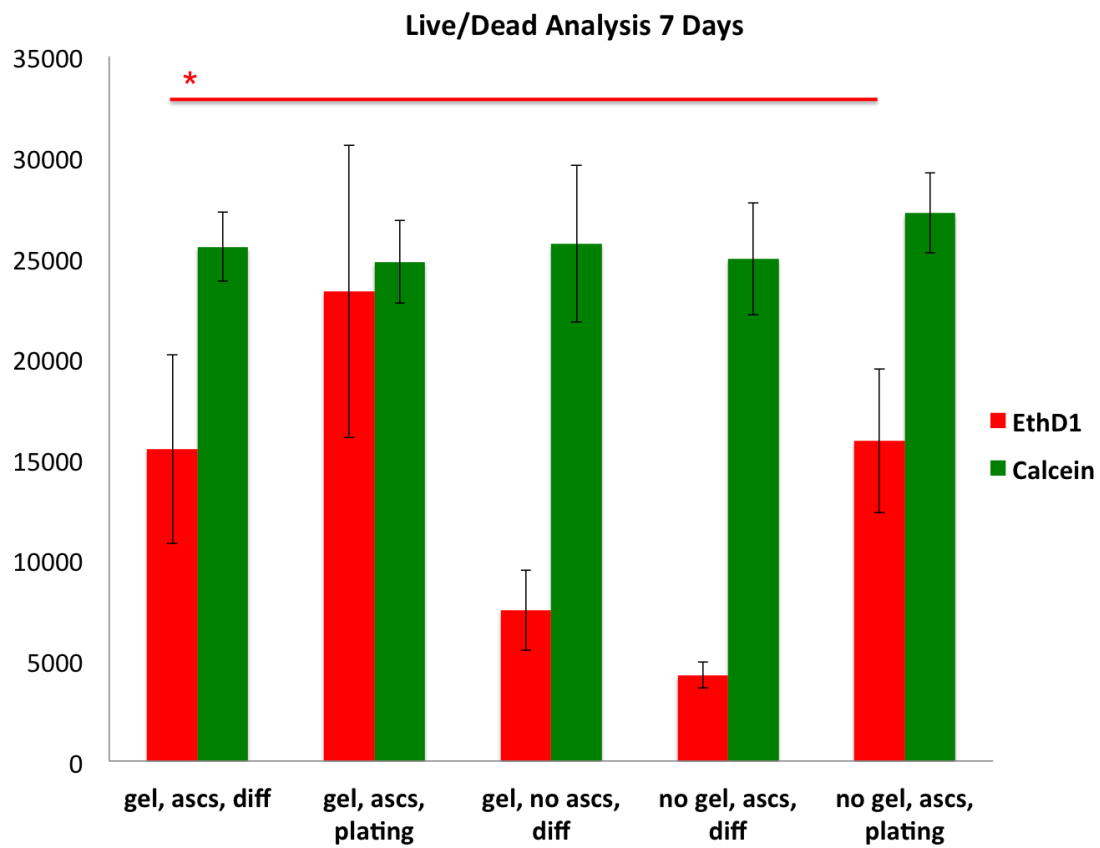
Figure 35. Cell viability after 7 days of ASCs either cultured on adipose ECM hydrogel or directly on surface of 96 well plates. * $p < 0.05$, N=8, mean ± standard deviation.

4.3.2 Metabolic Activity

Figure 36 represents average glucose production and Figure 36 represents average lactate production within the bioreactors of the cells and tissue using aforementioned protocol during ASC expansion (days 0-21), ASC differentiation into adipocytes (days 21-35), and adipocyte maintenance (days 35-43). Solid squares signify glucose production/consumption of cells that were inoculated with decellularized adipose hydrogel and empty squares denote cells that were inoculated with feed medium only, no decellularized adipose hydrogel.

Over the entire 43-day culture, glucose and lactate production of ASCs inoculated with decellularized adipose tissue hydrogel is no different within the bioreactor from glucose and lactate production of ASCs inoculated without decellularized adipose tissue hydrogel, up to a confidence interval of 95% with a *N*-value of 3. However, as indicated in Figure 36, lactate production rate dropped to zero at day 3 of culture, indicating low cell proliferation rates. The low lactate production continued throughout culture.
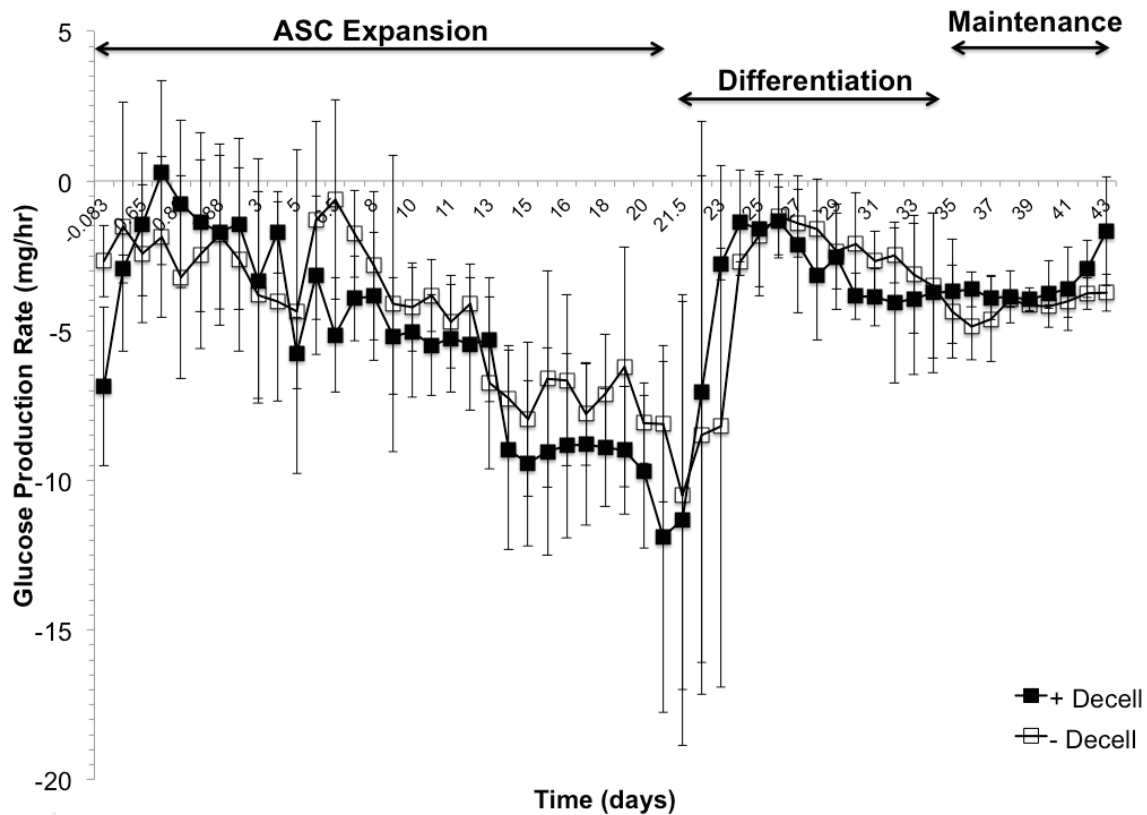
Figure 36. Metabolic activity. Glucose production/consumption (mg/hr) trends of three bioreactors seeded with ASCs supplemented with a decellularized adipose ECM hydrogel (filled squares) and three bioreactors seeded with ASCs only (empty squares) over 43 days of culture. Days 0-21 represent a time period in which ASCs were allowed to expand within the bioreactor; throughout days 21-35 ASCs were influenced to differentiate into adipocytes by a medium change; adipocytes were maintained from days 35-43. Glucose consumption is not significantly different ($p > 0.05$, $N=3$) between groups.
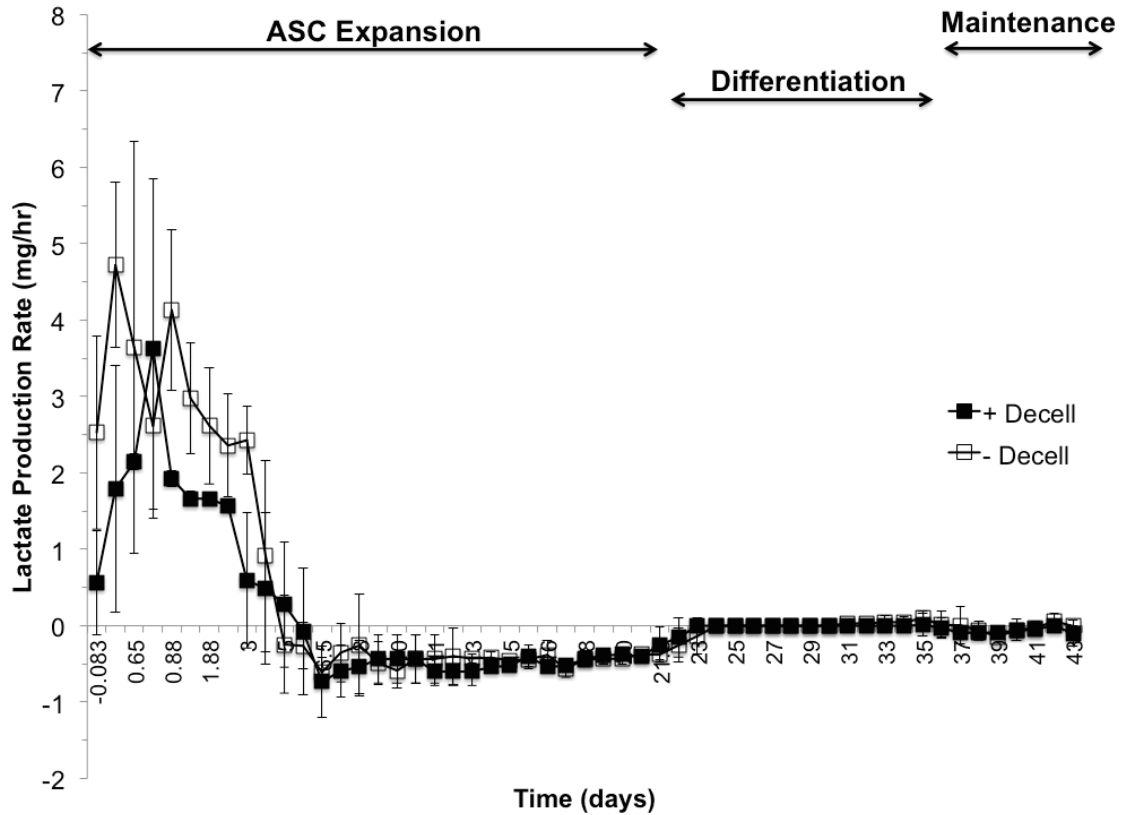
Figure 37. Metabolic activity. Lactate production/consumption (mg/hr) trends of three bioreactors seeded with ASCs supplemented with a decellularized adipose ECM hydrogel (filled squares) and three bioreactors seeded with ASCs only (empty squares) over 43 days of culture. Days 0-21 represent a time period in which ASCs were allowed to expand within the bioreactor; throughout days 21-35 ASCs were influenced to differentiate into adipocytes by a medium change; adipocytes were maintained from days 35-43. Lactate consumption is mostly not significantly different (* $p > 0.05$, N=3) between groups.

4.3.3 TNF- α Functional Testing

Figure 38 depicts the average glucose production of all six bioreactors – three each received a decellularized adipose ECM hydrogel upon inoculation (filled squares) and three inoculated with ASCs only (empty squares) – before, during, and after insulin

stimulation.   Results   indicate   no   significant   difference   between   glucose

consumption/production of between the groups (*p*> 0.05, *N*=3) before, during, and after

insulin stimulation.   While glucose consumption did slightly decrease during TNF-α

stimulation, an initial spike in glucose consumption was observed at the beginning of

insulin stimulation but cells did not seem to recover or return to baseline once stimulated

with feed medium containing TNF-α and no insulin.   Such results question whether

mature, functional adipocytes were present within the bioreactor cultures.
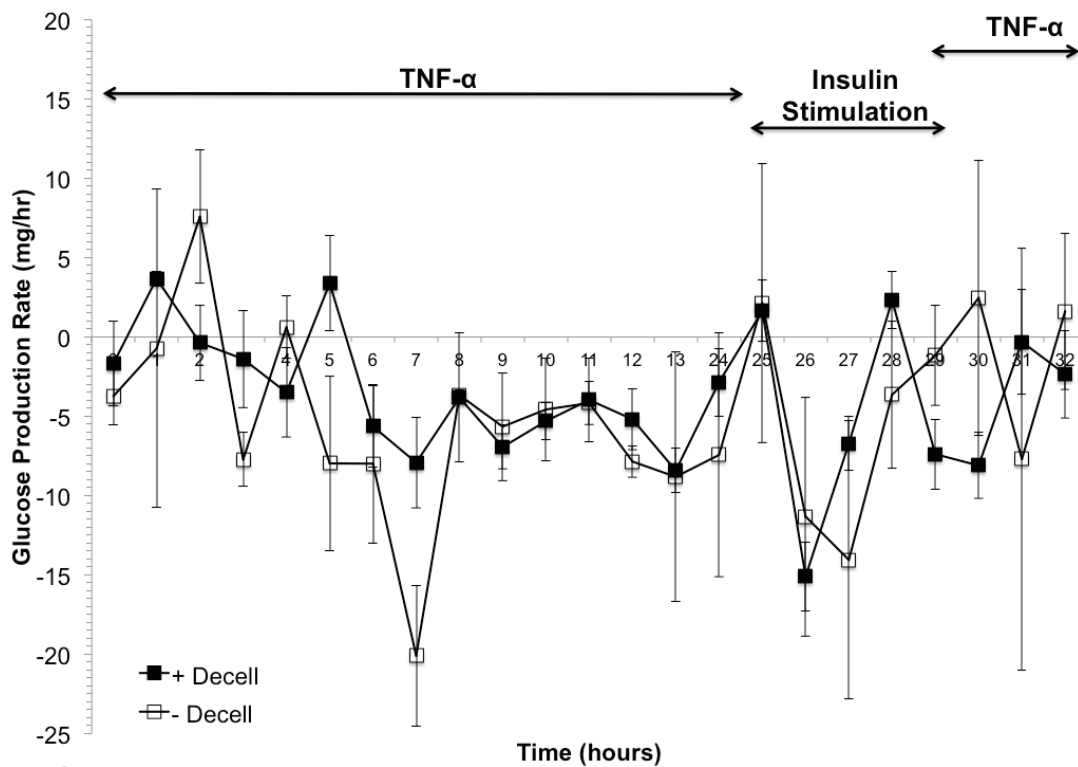
Figure 38. Adipocyte functionality. All six bioreactors were stimulated with TNF-α for twenty-

four hours, glucose consumption was measured and noted to be slightly hindered. After reaching

a steady glucose consumption rate, insulin was introduced to the system. Cells inoculated with a

decellularized adipose ECM hydrogel (filled squares) functions with no significant difference (* *p*

< 0.05, *N*=3) to cells inoculated without a hydrogel (empty squares) when stimulated with TNF-a

and insulin.

4.3.4 Histology and Immunohistochemistry

Imaging results of the tissue generated within the bioreactors are shown in Figures 39-41. Macroscopic tissue formation was observed in and around the hollow fiber membranes upon bioreactor disassembly [Figs. 38-40]. Regarding both groups of tissue – that differentiated from ASCs inoculated in combination with a decellularized adipose ECM hydrogel and that differentiated from ASCs inoculated with plating medium only – histological analyses with Masson's Trichrome reveal collagen-dense tissue formation, with some adipocyte architecture formed (indicated by black arrows in Figure 39). Lack of adipocyte architecture conflicted by observation of metabolic activity from the cultures prompted evaluation of a human-specific antibody. Figure 40 examines the human leukocyte antigen (HLA), which should positively stain for human cells only. While some positive stain was observed, the architecture of the samples extracted from the bioreactor cultures cannot be identified as similar to that of native human adipose tissue (Figure 40A).

Confocal fluorescent imaging of AdipoRed was conducted to demonstrate lipid formation after 43 days of culture within the dynamic perfusion systems, while DAPI and AlexaFluor 488 Phalloidin are meant to highlight nuclei and F-actin, respectively. Figure 40 shows some lipid accumulation from the bioreactors inoculated with ASCs and decellularized adipose ECM (Fig. 41 A and C) but the only fluorescence from the bioreactors withheld from the decellularized adipose ECM (Fig. 41 B and D) is a result from potential autofluorescence. Furthermore, no phalloidin is apparent in any sample, indicating no filamentous actin from the tissues grown within the bioreactor cultures.
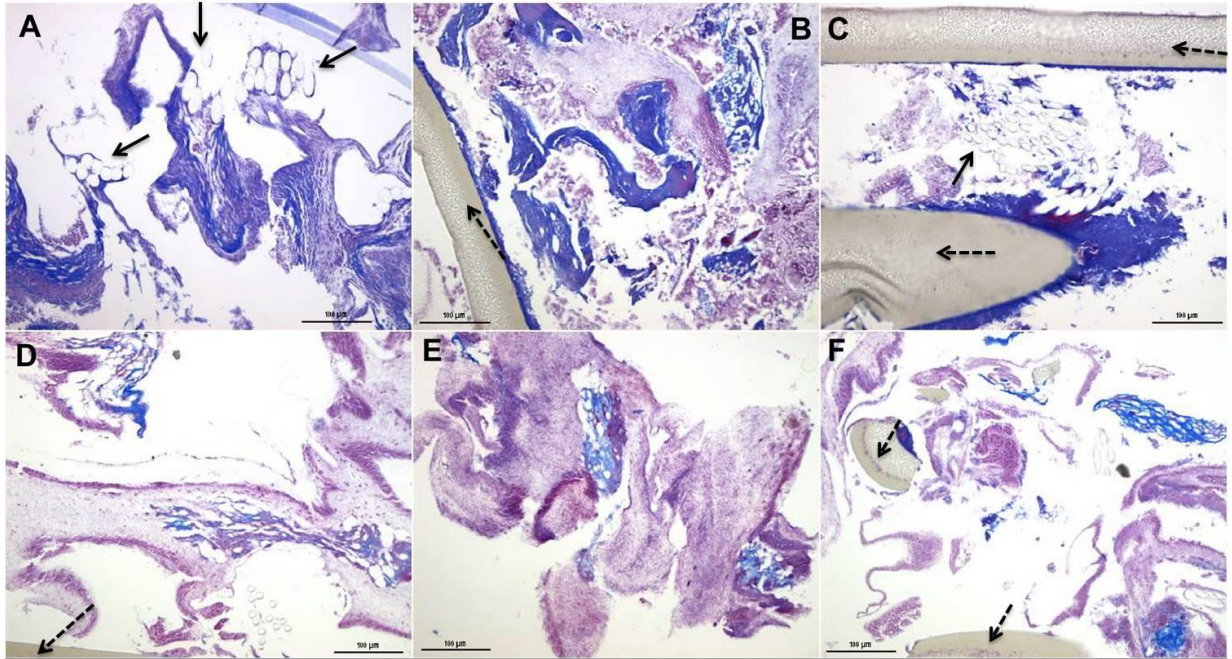
Figure 39. Histology. End-point (43 days) histology stained with Masson's Trichrome from bioreactors inoculated with ASCs and decellularized adipose ECM (A-C) or with ASCs only (D-F). Solid arrows indicate adipose architecture, dashed arrows indicate bioreactor fibers. Scale bar = 100 μm.
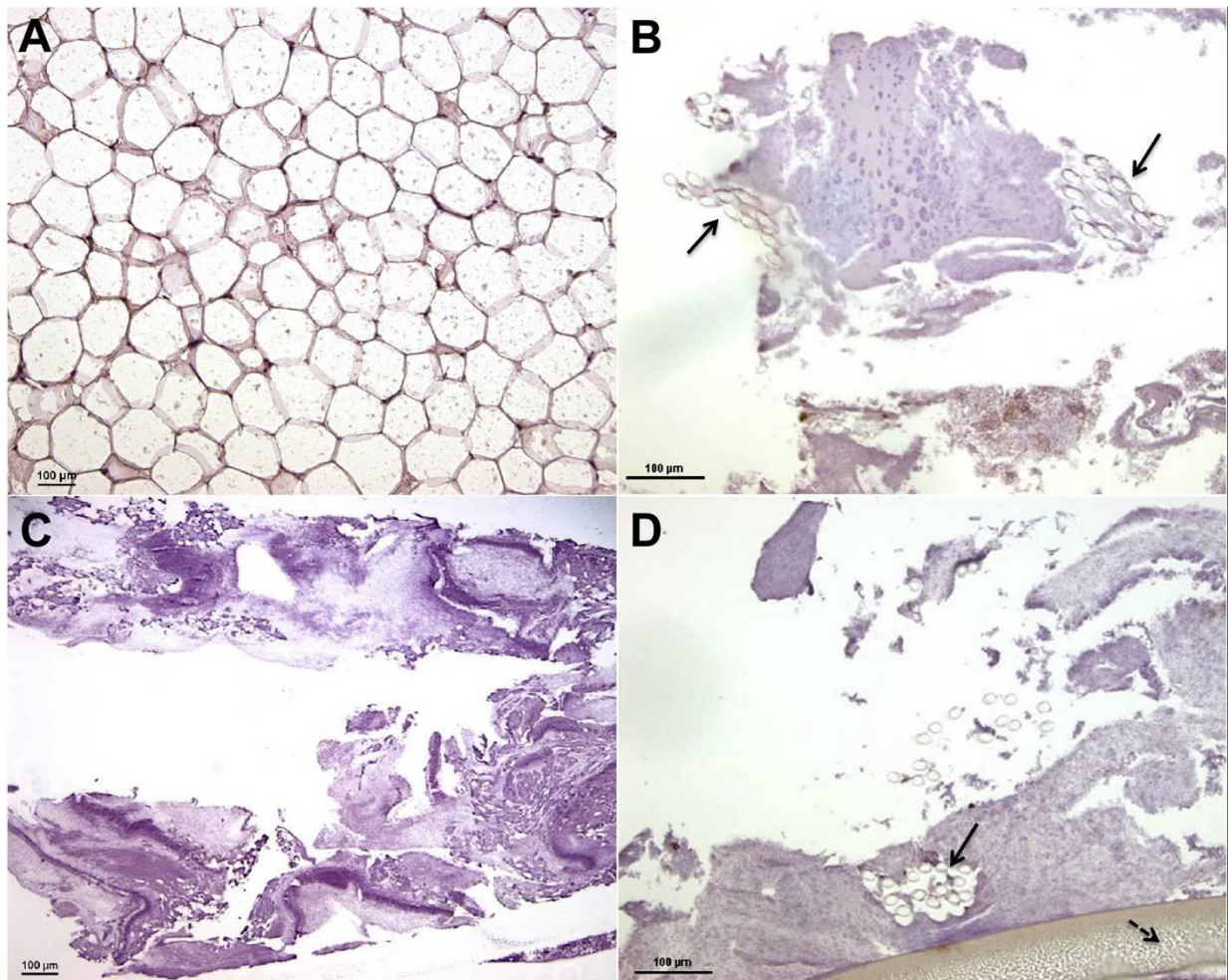
Figure 40. HLA Staining. A) Whole fat from adult human tissue samples, B) sample extracted from a bioreactor receiving ASCs + decellularized adipose ECM, C) negative control – sample extracted from a bioreactor culture but no primary antibody added to staining procedure, D) sample extracted from a bioreactor receiving ASCs and no decellularized adipose ECM. Solid arrows indicate adipose architecture, dashed arrows indicate bioreactor fiber. Scale bar = 100 μm.
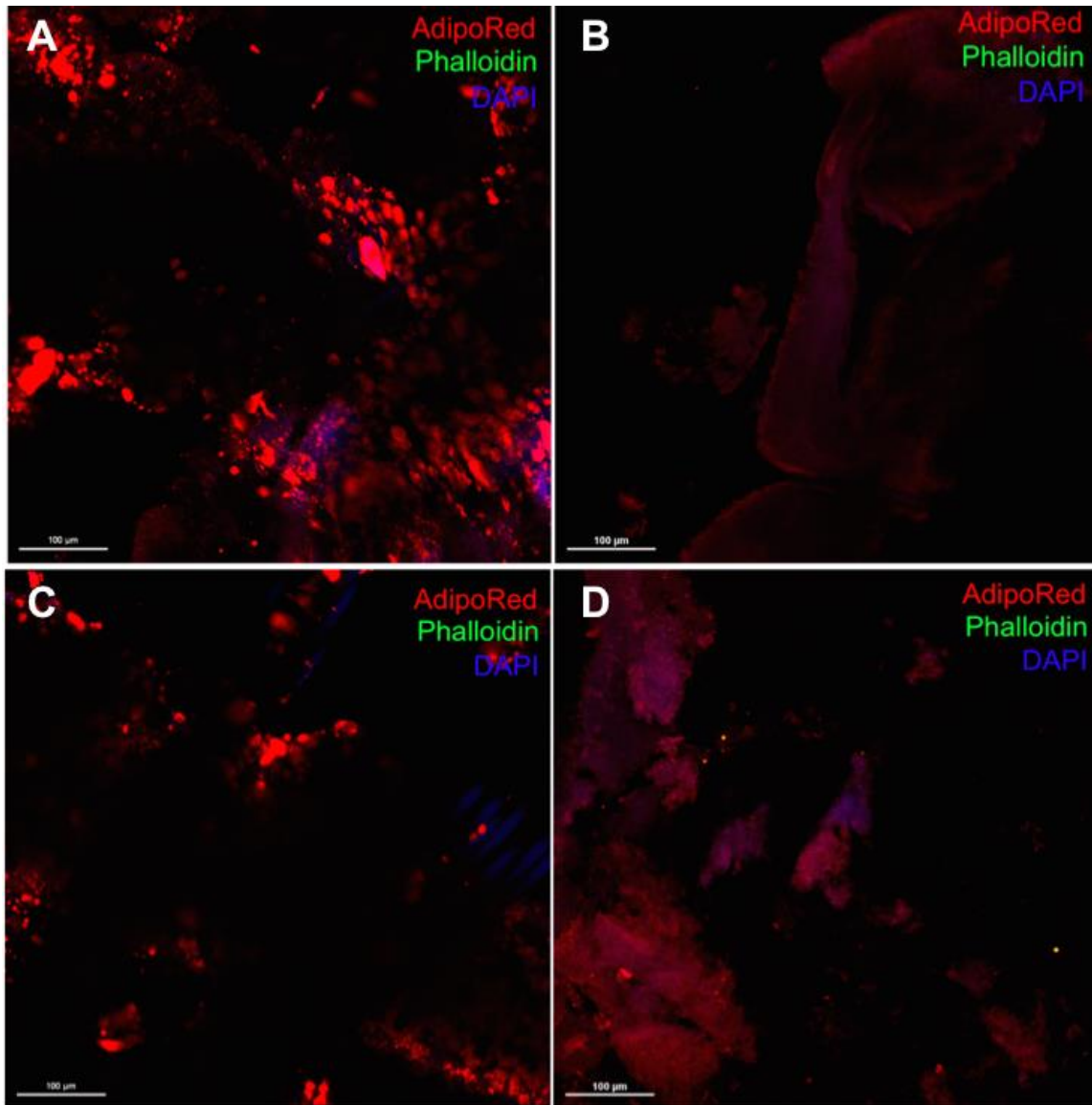
Figure 41. Immunofluorescence. End-point (43 days) AdipoRed/DAPI/Phalloidin immunofluorescence from bioreactors containing A and C) ASCs + decellularized adipose ECM or B and D) ASCs only. Scale bar = 100 μm.

4.4 CONCLUSIONS

A decellularized adipose ECM biological material was developed, characterized, and applied to the hollow fiber-based, three dimensional, dynamic perfusion bioreactor culture system described in earlier chapters with the hypothesis that the ECM material

would enhance adipogenesis and tissue homogeneity within the bioreactor culture. Before bioreactor application, the ECM material was characterized architecturally by H&E and SEM, nucleic content was assessed by DAPI staining, and ECM content was determined by immunohistochemistry. Cell viability at 1 and 7 days was evaluated prior to bioreactor inoculation.

Six hollow fiber-based, three dimensional, dynamic perfusion bioreactors were inoculated with human adult adipose stem cells, and three were in combination with the developed decellularized adipose ECM, three were with ASCs alone. Cells were allowed to expand within the bioreactor cultures for 21 days, then influenced by adipocyte differentiation medium for 14 days, then maintained for 7 days. At the end of the 7-day maintenance period, all bioreactors were exposed to TNF-α under the hypothesis that mature adipocytes would experience hindered glucose consumption, then recover when stimulated with insulin, and return to the baseline glucose levels when the TNF-α is re-introduced. Daily glucose and lactate levels in the cultures were measured and, when analyzed, consumption rates were averaged, no difference was found between groups in the glucose or lactate consumption rates. Results from the bioreactor experiments presented in Specific Aim 3 should be taken with caution as technical difficulties ensued throughout experimentation. Such difficulties are further detailed in section 5.2.

The TNF-α and insulin exposure had little effect on any culture system, questioning whether mature adipocytes were achieved in the cultures. Further supporting this assessment is the lack of lactate production within the bioreactor culture systems, uniocular adipocytes, lipid accumulation, and F-actin revealed in the AdipoRed immunofluorescence.

5.0   DISCUSSION

5.1 SUMMARY OF RESULTS

ASCs derived from discarded adipose tissue of patients with type II diabetes at time of isolation were found to behave metabolically and appear architecturally similar to those derived from patients without type II diabetes mellitus when differentiated and maintained as adipocytes in the bioreactor system. When cultured at a physiologically relevant glucose level matching that of patients with type II diabetes or without, ASCs are able to proliferate, differentiate into adipocytes, and be maintained within the bioreactor system. A decellularized adipose ECM hydrogel was developed and applied to the bioreactor cultures; however, based upon the ambiguous results obtained from the bioreactor extracted cultures, no conclusion regarding adipocyte differentiation or metabolic activity between groups can be made.

5.1.1   Specific Aim 1

With obesity rapidly approaching epidemic-status in developed countries, followed by type II diabetes mellitus, the need to further understand cellular and molecular mechanisms underlying such diseases becomes more apparent. A key influence in these diseases, but still often overlooked as an endocrine-functioning organ, is adipose tissue. Attractive characteristics of adipose tissue make it an appealing source of human stem cells for regenerative medicine applications. Furthermore, purity of ASCs

and variance between patients are both well characterized [52, 56, 68]; however, traditional, two-dimensional culture of adipose-derived stem cells does not allow long-term lipid accumulation and, therefore, maintenance of adipocytes [264].

Previously, our laboratory has established a three-dimensional perfusion bioreactor culture system, providing an environment suitable for long-term maintenance of adipocytes within a hollow fiber-based, dynamic mass exchange bioreactor that provides decentralized oxygenation [54]. With the intention of serving as a potential tool for anti-diabetic drug discovery, Specific Aim 1discusses, to the best of our knowledge – for the first time – differentiation of ASCs isolated from diabetic tissue into functional adipocytes within a hollow fiber-based, dynamic, three-dimensional perfusion bioreactor.

The similar metabolic trends observed between diabetic and non-diabetic tissues led us to hypothesize that adipose-derived stem cells, once removed from elevated glucose and insulin-leveled environments of type II diabetic patients, retain no "memory" of the diseased state, confirming insulin/insulin-receptor binding to be environment-dependent. While ASCs from diabetic patients consumed less glucose than ASCs from non-diabetic patients during the first three weeks of bioreactor culture, results were not significantly different ($p > 0.05$, N=3). After the "ASC Expansion" period, ASCs were exposed to a change in feed media – to induce differentiation into adipocytes – during this phase and the "adipocyte maintenance" phase, glucose consumption was expected to not increase, indicating differentiation and maintenance rather than ASC proliferation. To evaluate adipocyte functionality within the bioreactor of both tissue types (diabetic and non-diabetic), after exposure to TNF-α, insulin was introduced to all bioreactors and glucose uptake was observed to increase over an eight-hour period and eventually return

to the inhibited TNF-α level. Throughout insulin stimulation, three statistically significant time points were observed between the diabetic and non-diabetic groups ($p < 0.05$, N=3), indicating that adipocytes from diabetic patients may not recover with insulin as functionally as adipocytes from non-diabetic patients. While the dissimilarity is small, the disparity in glucose consumption may reflect the ability of tissue from diabetic ASCs to recover after 24 hours of inhibited glucose uptake [169, 264]. However, after the 8 hours of insulin stimulation, glucose consumption was inhibited to the same degree between the two groups ($p > 0.05$, N=3).

While the cells studied within this report are derived from different patients within the two experimental groups, previous work in our laboratory has been conducted establishing ASCs obtained from different patients within certain age and BMI ranges hold inconsequential differences between proliferation and differentiation capabilities [52]. No prominent, qualitative difference was noted between architecture or formation, of adipocytes differentiated from diabetic versus non-diabetic ASCs when cultured and differentiated in the hollow fiber bioreactors for 45 days. When stained with AdipoRed, DAPI and Phalloidin AlexaFluor 488, lipid-loaded vacuoles indicate mature adipose tissue upon the extracted hollow membrane fibers from all bioreactors, including those inoculated with cells from diabetic patients [Figs. 9 and 10]. In Figure 10, the Phalloidin indicates a less organized lipid-storing tissue from the bioreactors seeded with ASCs from diabetic patients. No quantitative variance was detected of adipocyte gene marker, FABP4, expressed between adipocytes differentiated from diabetic patients, non-diabetic patients, and whole adipose tissue samples [Fig. 12]. PPAR-γ protein expression exhibited through Western Blotting was confirmed from diabetic and non-diabetic

bioreactor samples and whole adipose samples.Protein band strength in the Western Blotting is not equal between groups and samples extracted for Western Blotting were taken at random from the bioreactors.

It can be concluded from Specific Aim 1 that ASC proliferation, differentiation and maintenance is dependent on microenvironment and, when placed at the same culture conditions, ASCs from patients with type II diabetes mellitus will behave similarly to ASCs from patients without type II diabetes long-term in three dimensions *ex vivo*. These conclusions hold promise for future clinical applications such as ASC therapy addressing diabetic wounds.

5.1.2   Specific Aim 2

Based on the conclusions formed in Specific Aim 1, it is clear that, in order to study type II diabetes long-term *ex vivo*, a physiologically relevant culture condition must be engineered. Since the traditional culture medium used in ASC culture contains a glucose concentration 3-4 times greater than that observed in healthy fasting adults and 2-3 times higher than that observed in patients with type II diabetes mellitus, further investigation of ASC behavior under the influence of feed medium containing physiological glucose levels is essential.

In 96 well plates, ASCs were seeded and cultured by feed medium at various glucose concentrations. Differentiation and cell viability was assessed in addition to cell behavior once exposed to various environments similar to that of a patient with type II diabetes mellitus. A 20% and 35% dilution of adipocyte differentiation medium were

found to be the most physiologically relevant to glucose concentrations of patients without and with type II diabetes mellitus, respectively. Free fatty acids (FFAs) and the sphingolipid, C2-ceramide, were added to adipocyte culture media and glucose consumptions was hindered the most ideally at a concentration of 10 μM C2-ceramide without FFAs.

The established culture conditions were applied to the hollow fiber-based, three-dimensional dynamic perfusion bioreactor system. ASCs were able to proliferate, differentiate, and be maintained in both culture conditions. However, when C2-ceramide was added to the healthy glucose concentration cultures, no major change in glucose consumption was experienced. A potential rationale for this observation may be due to a scale-up issue; two-dimensional experiments in the 96 well plates were applied to 10,000 cells per well, whereas ASCs are inoculated into the bioreactors at 80,000,000 cells per reactor. Another possibility may lie within the maturity level of the adipocytes; the glucose consumption hindered by C2-ceramide in the 96 well plate experiments were of adipocytes immediately post-differentiation, and the C2-ceramide was included in the bioreactor studies after a week of maintenance to mature adipocytes in three dimensions.

5.1.3 Specific Aim 3

To further enhance adipogenesis and to promote adipose tissue homogeneity within the bioreactor cultures, a decellularized adipose ECM hydrogel was developed using modified methods of previous literature [261, 263]. The adipose ECM was characterized by H&E, SEM, DAPI, immunohistochemistry, and cell viability through Live/Dead. The developed adipose ECM was found to have no lipid architecture, no

124

notable nuclei, a porous surface, and retained several important ECM components such as collagens I, III, IV, VI, heparan sulfate proteoglycans (HSPG), and nidogen.

When ASCs were seeded onto the adipose ECM, at 24 hours, a significant increase was observed in live cells from groups without the adipose ECM compared to the groups of cells seeded onto the adipose ECM. However, after a week of culture, no difference in live cells was found. The decellularized adipose ECM was able to form a hydrogel following pepsin digestion and at 37 °C. The hydrogel was combined with ASCs and inoculated into three of the six bioreactors; the other three bioreactors received ASCs only. All cultures were expanded for 21 days, then exposed to adipocyte differentiation feed medium for 14 days, and maintained for 7 days. Following maintenance, TNF-α followed by insulin were introduced to the system to test the functionality of the tissue within the bioreactors.

Addition of the decellularized adipose ECM did not have a statistically significant effect on glucose or lactate production rates of the ASCs and, while AdipoRed indicated slight lipid inclusion, the adipose ECM incorporation did not enhance adipogenesis and mature adipocytes were not found within any of the six bioreactor cultures. However, this final experiment was fraught with technical difficulties as indicated by the lack of lactate production within the bioreactor culture systems, uniocular adipocytes, lipid accumulation, and F-actin revealed in the AdipoRed immunofluorescence.

5.2 TECHNICAL CONSIDERATIONS

Three-dimensional perfusion technology, such as that described throughout this dissertation is more technical than traditional Petri dish or two-dimensional tissue culture flask culture. The three-dimensional bioreactors used in this dissertation involved pumps and continuous media exchange through a dynamic system, which is constantly under perfusion where pressure problems may occur. Opposed to traditional two-dimensional cell culture that involves daily pipetting, three-dimensional perfusion utilizes an input of constant nutrient medium with continuous output of waste. If a bottle of nutrient medium becomes empty, or the liquid volume falls below the reach of the straw drawing the medium into the bioreactors, air bubbles will occur in the system. Air bubbles within the system could cause membrane fouling, premature closing of the capillaries and pressure buildup. If not monitored closely, this would lead to an automatic shut down of the pump system.

During the experiments described in Specific Aim 3, a phenomenon such as this occurred more than once, including automatic shut down of the pump system. The pumps were restarted and, if necessary, the bioreactor systems were transferred to a different set of pumps. Nutrient media run empty if fresh media bottles are not delivered or replaced in time, or if the system pumps at a faster rate. The system may pump too quickly if the pressure on the tubing is lowered caused by an incorrect setup of race sizing on the pumps.

Furthermore, at the time of cell inoculation into the bioreactors, all stopcocks must be in proper position, otherwise air would occur in the system. Another consequence of air in the system is that cells could dry out. While oxygenation keeps the cells alive within the compartment, but automatic shut down of the pumps would result in no CO_2, leading to acidic buildup in the system. All of the mentioned technical challenges could be avoided by a careful setup and by potential implementation of a camera system to allow constant monitoring of the systems after hours.

Another classification of technical challenges that may have potentially occurred in Specific Aim 3 would be a bacterial infection. The bioreactor systems are highly sensitive and extremely vulnerable to infection throughout all experimentation. Bacterial infection would continue to consume glucose, as observed in Specific Aim 3. Throughout experimentation, white, flaky debris were found in the bubble traps and waste containers of all bioreactors, including those not inoculated with a decellularized hydrogel. Unfortunately, the debris was unable to be analyzed as the texture would adhere to the inside of the bubble trap and disintegrated during processing.

5.3 FUTURE DIRECTIONS

Diabetes mellitus and obesity exist as rapidly increasing issues in developed countries, a deeper understanding of adipose tissue as an endocrine organ is necessary. The application of autologous adipose stem cell therapy to patients with type II diabetes before, during, and after the disease is a pressing issue that holds serious potential to

many fields including regenerative medicine, plastic surgery and reconstruction, endocrinology, and diabetic wound healing. Future directions include optimizing medium components, clinical application of the decellularized adipose hydrogel to soft tissue reconstruction and graft volume retention, engineering a long-term diabetic model of adipocytes in a bioreactor, and utilizing the model as a drug discovery tool for various factors addressing diabetes, obesity, and adipose graft volume retention.

Due to the limitations of the presented studies and technical difficulties encountered, further studies must be completed before the aforementioned future directions may be obtained. For such studies, considering the experience in the described current work, the following suggestions are given.

Specific Aim 1. To continue development of a long-term culture environment that mimics II diabetes mellitus *ex vivo*.

Hypothesis: Addition of macrophages M1 and M2 into the culture will create insulin resistance of adipocytes within a hollow fiber-based, three-dimensional dynamic perfusion bioreactor.

Rationale: The studies described in Specific Aim 2 were designed to create an environment representative of type II diabetes mellitus via glucose uptake hindrance influenced by exposure to FFAs and C2-ceramide in the culture medium. However, no notable difference was observed within the adipocyte cultures *ex vivo*. Obesity and type II diabetes are both characterized by adipose tissue macrophages (ATMs) and ATMs are accepted correlations to adipose tissue insulin resistance [264, 265].

Specific Aim 2. To further discover adipose-derived stem cells from patients with type II diabetes mellitus within a diabetic environment *ex vivo*.

Hypothesis: ASCs isolated from tissue of patients with type II diabetes mellitus influenced by a decellularized adipose extracellular matrix isolated from patients with type II diabetes mellitus will exhibit less glucose uptake, proliferation, and differentiation capabilities than ASCs isolated from tissue of healthy patients influenced by a decellularized adipose ECM from healthy patients.

Rationale. Specific Aim 1 within the presented thesis supports adipose tissue behavior within a three-dimensional dynamic perfusion bioreactor relying upon the surrounding microenvironment. While the cellular components of the incorporated matrix will have been removed, the ECM is expected to contain less structural proteins such as collagen I, III, IV, VI, nidogen, or HSPG that contribute to cellular organization, migration, and proliferation.

Specific Aim 3. To enhance adipogenesis and encourage neovascularization within a hollow fiber-based, three-dimensional dynamic perfusion bioreactor.

Hypothesis: Exposure of platelet-rich plasma (PRP) to healthy ASCs will enhance adipogenesis and encourage clinical usage for wound healing application.

Rationale. Clinical evidence has supported the addition of PRP to autologous fat graft transplantations to improve fat-graft survival by influencing differentiation of pre-adipocyte cells contained the graft tissue [264-275].

BIBLIOGRAPHY

1. Cinti S. *The Adipose Organ.* Editrice Kurtis: Milano, 1999.

2. Nedergaard J, Bengtsson T, Cannon B. "Unexpected evidence for active brown adipose tissue in adult humans" *Am J Physiol Endocrinol Metab.* Aug 2007; 293(2):E444-452.

3. "Brown adipose tissue − when it pays to be inefficient" Celi FS. *N Engl J Med.* Apr 9, 2009;360:1553.

4. Minteer, Danielle, Kacey G. Marra, and J. Peter Rubin. "Adipose-derived mesenchymal stem cells: biology and potential applications." *Mesenchymal Stem Cells-Basics and Clinical Application I.* Springer Berlin Heidelberg, 2013. 59-71.

5. Freedman MR, Horwitz BA, Stern JS. "Effect of adrenalectomy and glucocorticoid replacement on development of obesity" *Am J Physiol.* 1986; 250: R595-R607.

6. Picon L and Levacher C. "Thyroid hormones and adipose tissue development" *J Physiol.* 1979; 75:539-543.

7. Hausman GJ, Wright JT, Dean R, Richardson RL. "Cellular and molecular aspects of the regulation of adipogenesis" *J Anim Sci.* 1993; 71:33-55.

8. Hausman GJ and Hausman DB. "Endocrine regulation of porcine adipose tissue development: cellular and metabolic aspects" In: Hollis GR (eds). *Growth of the Pig.* CAB International: London, 1993, pp 49-73.

9. Hausman GJ, Wright JT, Jewell DJ, Ramsay TG. "Fetal adipose tissue development." *Int J Obesity.* 1990; 14: 177-185.

10. Kelmendi-Doko, A, Marra KG, Tan H, Rakers A, Rubin JP. "Adipogenic Factors Effect in Adipose Tissue Retention." International Federation of Adipose Therapeutics and Science. Eden Roc Renaissance Hotel, Miami, Florida. 5 Nov. 2011.

11. Nougues J, Reyne Y, Barenton B, Chery T, Garandel B, Soriano J. "Differentiation of adipocyte precursors in a serum-free medium is influenced by glucocorticoids and endogenously produced insulin-like growth factor-I." Int J Obes Res 1993; 17:159–167.

12. Richardson RL, Hausman GJ, Wright JT. "In situ binding and immunocytochemistry of insulin-like growth factor I receptors in primary cultures of porcine adipose tissue stromal vascular cells treated with indomethacin." J Anim Sci 1994; 72:969–975.

13. Wright JT, Hausman GJ. "Insulin like growth factor-I (IGF-I)- induced stimulation of porcine preadipocyte replication." In Vitro Cell Dev Biol 1995; 31: 404–408.

14. Blake WL, SD.Clarke. "Induction of adipose fatty acid binding protein (a-FABP) by insulin-like growth factor-1 (IGF-1) in 3T3-L1 preadipocytes." Biochem Biophys Res Commun 1990; 30:87–91.

15. Boney CM, Moats-Staats BM, Stiles AD, D'Ercole AJ. "Expression of insulin-like growth factor-I (IGF-I) and IGF-binding proteins during adipogenesis." Endocrinology 1994; 135: 1863–1868.

16. Smith PJ, Wise LS, Berkowitz R, Wan C, Rubin CS. "Insulin like growth factor-I is an essential regulator of the differentiation of 3T3-L1 adipocytes." J Biol Chem 1988; 263: 9402–9408.

17. Richardson RL, Hausman GJ, Wright JT. "Growth factor regulation of insulin-like growth factor (IGF) binding proteins (IGFBP) and preadipocyte differentiation in porcine stromalvascular cell cultures". Growth Dev Aging 1998; 62: 3–12.

18. "Adipocyte Function" Laboratory of Translational Nutritional Biology, Swiss Federal Institute of Technology Zurich; 11 Aug 2011. *<http://www.ifnh.ethz.ch/ftn/research/AdipFunct>*. Accessed 6 February 2012.

19. Kershaw EE and Flier JS. "Adipose Tissue as an Endocrine Organ" *J Clin Endocrinol &Metabol.* June 2004; 89(6): 2548-2566.

20. Greenberg AS and Obin MS. "Obesity and the role of adipose tissue in inflammation and metabolism" *Am J of Clin Nutrit*. 2006; 83(suppl): 461S-465S

21. "U.S. Obesity Trends" Centers for Disease Control and Prevention; 21 July 2011. <http://www.cdc.gov/obesity/data/trends.HTML>. Accessed 12 February 2012.

22. Anderson KM and Kannel WB. "Obesity and disease" In: Bjorntorp P, Brodoff BN (eds). *Obesity*. J.B. Lippincott Co: Philadelphia, 1992, pp 465-473.

23. Matsuzawa Y, Fujioka S, Tokunaga K, Seichiro T. "Classification of obesity with respect to morbidity" *Proc Soc Exp Biol Med.*1992; 200: 197-201.

24. Montague CT and O-Rahilly S. "The perils of portliness" *Diabetes*. 2000; 49: 883-888.

25. Pi-Sunyer FX. "Health Hazards of Obesity" *Ann Intern Med.* 1993; 119: 655-660.

26. Mokdad AH, Ford ES, Bowman BA, Dietz WH, Vinicor F, Bales VS, Marks JS. "Prevalence of Obesity, Diabetes, and Obesity-related Health Risk Factors" *J Amer Med Assoc*. 2001; 289: 76-79.

27. Horowitz JF and Klein S. "Whole body and abdominal lipolytic sensitivity to epinephrine is suppressed in upper body obese women" *Am J Physiol Endocrinol Metab*. 2000; 278: E1144-1152.

28. Horowitz JF, Coppack SW, Paramore D, Cryer PE, Zhao G, Klein S. "Effect of short-term fasting on lipid kinetics in lean and obese women" *Am J Physiol*. 1999; 276: E278-284.

29. Catalán, Victoria, et al. "Adipose tissue immunity and cancer." *Frontiers in physiology* 4 (2013).

30. Zuk PA, Zhu M, Mizuno H, Huang J, Futrell JW, Katz AJ, Benhaim P, Lorenz HP, Hedrick MH. "Multilineage Cells from Human Aipose Tissue: Implications for Cell-Based Therapies" *Tissue Engin*. 2001; 7(2): 211-228.

31. Planat-Bénard V, Menard C, André C, Puceat P, Perez A, Garcia-Verdugo JM, Pénicaud L, Casteilla L. "Spontaneous Cardiomyocyte Differentiation from Adipose Tissue Stroma Cells" *Circulat Res*. 2004; 94: 223-229.

32. Zuk PA, Zhu M, Ashjian P, De Ugarte DA, Huang JI, Mizuno H, Alfonso ZC, Fraser JK, Benhaim P, Hedrick MH. "Human Adipose Tissue Is a Source of Multipotent Stem Cells" *Mol Biol Cell*. Dec 2002; 13(12): 4279–4295.

33. Lee, JH and Kemp DM. "Human adipose-derived stem cells display myogenic potential and perturbed function in hypoxic conditions" *Biochem Biophys Res Comm*. 2006; 341(3): 882-888.

34. Rodriguez LV, Alfonso ZC, Zhang R, Leung J, Wu B, Ignarro LJ. "Clonogenic Multipotent Stem Cells in Human Adipose Tissue Differentiate in Muscle Cells" *PNAS*. 2006; 103(32); 12167-12172.

35. Gaustad, KG, Boquest AC, Anderson BE, Gerdes AM, Collas P. "Differentiation of human adipose tissue stem cells using extracts of rat cardiomyocytes" *Biochem Biophys Res Comm*. 2004; 314(2); 420-427.

36. Miranville A, Heeschen C, Sengenés C, Curat CA, Busse R, Bouloumié A. "Development of Postnatal Neovascularization by Human Adipose Tissue-Derived Stem Cells" *Circul*. 2004; 110: 349-355.

37. Choi YS, Cha SM, Lee YY, Kwon SW, Park CJ, Kim M. "Adipogenic differentiation of adipose tissue derived adult stem cells in nude mouse" *Biochem Biophys Red Comm*. 2006; 345(2); 631-637.

38. Lin Y, Chen X, Yan Z, Liu L, Tang W, Zheng X, Zhiyong L, Qiao J, Li S, Tian W. "Multilineage differentiation of adipose-derived stromal cells from GFP transgenic mice" *Molec and Cellul Biochem.* 2006; 285(1-2): 69-78.

39. Ning H, Lin G, Lue TF, Lin CS. "Neuron-like differentiation of adipose tissue-derived stromal cells and vascular smooth muscle cells" *Differentiation*. 2006; 74(9-10): 510-518.

40. Cowan CM, Aalami OO, Shi YY, Chou YF, Mari C, Thomas R, Quarto N, Nacamuli RP, Contag CH, Wu B, Longaker MT. "Bone Morphogenetic Protein 2 and Retinoic Acid Accelerate *in Vivo* Bone Formation, Osteoclast Recruitment, and Bone Turnover" *Tissue Engin*. March/April 2005; 11(3-4): 645-658.

41. DiRocoo G, Iachininoto MG, Tritarelli A, Straino S, Zacheo A, Germani A, Crea F, Capogrossi MC. "Myogenic potential of adipose-tissue-derived cells" *J Cell Sci.* 2006; 119(4): 2945-2952.

42. Miyahara Y, Nagaya N, Kataoka K, Yanagawa B, Tanaka K, Hao H, Ishino K, Ishida H, Shimizu T, Kangawa K, Sano S, Okano T, Kitamura S, Mori H. "Monolayered mesenchymal stem cells repair scarred myocardium after myocardial infarction" *Nature: Medici.* April 2006; 12(4): 459-465.

43. Strem BM, Hicok KC, Zhu M, Wulur I, Alfonso ZC, Schreiber RE, Fraser JK, Hedrick MH. "Multipotential differentiation of adipose tissue-derived stem cells" *Keio J Medici.* 2005; 54(3); 132-141.

44. Ando H, Yanagihara H, Hayashi Y, Obi Y, Tsuruoka S, Takamura T, Kaneko S, Fujimura A. "Rhythmic Messenger Ribonucleic Acid Expression of Clock Genes and Adipocytokines in Mouse Visceral Adipose Tissue" *Endocrinol.* Dec 2005; 146(12): 5631-5636.

45. Kang SK, Lee DH, Bae YC, Kim HK, Baik SY Jung JS. "Improvement of neurological deficits by intracerebral transplantation of human adipose tissue-derived stromal cells after cerebral ischemia in rats" *Experim Neurol.* Oct 2003; 183(2): 355-366.

46. Constantin G, Marcon S, Rossi B, Angiari S, Calderan L, Anghileri E, Gini B, Bach SD, Martinello M, Bifari F, Galie M, Turano E, Budui S, Sbarbati A, Krampera M, Bonetti B. "Adipose-derived mesenchymal stem cells ameliorate chronic experimental autoimmune encephalomyelitis" *Stem Cells.* 2009; 27(10): 2624-2635.

47. Brzoska M, Geiger H, Gauer S, Baer P. "Epithelial differentiation of human adipose tissue-derived adult stem cells" *Biochem Biophys Res Comm*. 2005; 330(1): 142-150.

48. Visconti RT, Bonora A, Jover R, Mirabet V, Carbonell F, Castell JV, Gomez-Lechon MJ. "Hepatogenic differentiation of human mesenchymal stem cells from adipose tissue in comparison with bone marrow mesenchymal stem cells". *World J Gastroenterol. 2006;* 12(036): 5834-5845.

49. Seo MJ, Suh SY, Bae YC, Jung JS. "Differentiation of human adipose stromal cells into hepatic lineage in vitro and in vivo" *Biochem Biophys Res Comm.* Mar 2005; 328(1): 258-264.

50. Chandra V, Swetha G, Phadnis S, Nair PD, Bhonde RR. "Generation of Pancreatic Hormone-Expressing Islet-Like Cell Aggregates from Murine Adipose Tissue-Derived Stem Cells" *Stem Cells*. 2009; 27(8): 1941-1953.

51. Kajiyama H. "Pdx1-transfected adipose tissue-derived stem cells differentiate into insulin-producing cells in vivo and reduce hyperglycemia in diabetic mice" *Internat J Develop Biol. 2010;* 54(4): 699-705.

52. Schipper BM, Marra KG, Zhang W, Donnenberg AD, Rubin JP. "Regional Anatomic and Age Effects on Cell Function of Human Adipose-Derived Stem Cells" *Ann Plast Surg*. May 2008; 60(5): 538-544.

53. Frye CA, Patrick CW. "Three-Dimensional Adipose Tissue Model Using Low Shear Bioreactor" *In vit Cellul & Develop Biol*. 2006; 42(5): 109-114.

54. Gerlach JC, Lin YC, Brayfield CA, Minteer DM, Li H, Rubin JP, Marra KG. "Adipogenesis of Human Adipose-Derived Stem Cells Within Three-Dimensional Hollow Fiber-based Bioreactors" *Tissue Engr: C*. 2012; 18(1):54-61.

55. Brayfield C, Marra K, Rubin JP. "Adipose Stem Cells for Soft Tissue Regeneration" *Plast Chir*. 2010; 42:124-128.

56. Rubin JP, Marra KG. "Soft Tissue Reconstruction" *Methods Mol Bio.* 2011; 702: 395-400.

57. Brayfield CA, Marra KG, Rubin JP. "Adipose Stem Cells for Soft Tissue Regeneration" *Handchir Mikrochir Plast Chir*. 2010; 42: 124-128.

58. Philips BJ, Marra KG, Rubin JP. "Adipose stem cell-based soft tissue regeneration" *Expert Opin Biol Ther.* 2012 Feb; 12(2): 155-163.

59. Smith DM, Cooper GM, Afifi AM, Mooney MP, Cray J, Rubin JP, Marra KG, Losee JE. "Regenerative surgery in cranioplasty revisited: the role of adipose-derived stem cells and BMP-2" *Plast Reconstr Surg.* Nov 2011; 128(5): 1053-1060.

60. Cherubino M, Rubin JP, Miljkovic N, Kelmendi-Doko A, Marra KG. "Adipose-derived stem cells for wound healing applications" Ann Plast Surg. Feb 2011; 66(2): 210-215. Review.

61. Tan H, Rubin JP, Marra KG. "Injectable in situ forming biodegradable chitosan-hyaluronic acid based hydrogels for adipose tissue regeneration" *Organogen.* Jul-Sep 2010; 6(3): 173-180.

62. Zimmerlin L, Donnenberg AD, Rubin JP, Basse P, Landreneau RJ, Donnenberg VS. "Regenerative therapy and cancer: in vitro and in vivo studies of the interaction between adipose-derived stem cells and breast cancer cells from clinical isolates" *Tiss Eng Part A*. Jan 2011; 17(1-2): 93-106.

63. Stumvoll, Michael, Barry J. Goldstein, and Timon W. van Haeften. "Type 2 diabetes: principles of pathogenesis and therapy." *The Lancet* 365.9467 (2005): 1333-1346.

64. Hollenberg CH and Vost A. "Regulation of DNA Synthesis in Fat Cells and Stromal Elements from Rat Adipose Tissue" *J Clin Invest*. 1968; 47: 2485-2498.

65. Stiles JW, Francendese AA, Masoro EJ. "Influence of age on size and number of fat cells in the epididymal depot" *Am J Physiol*. Dec 1975; 229(6); 1561-1568.

66. Dardick I, Poznanski WJ, Waheed I, Steerfield G. "Ultrastructural observations on differentiating human preadipocytes cultured *in vitro*" *Tissue & Cell*. 1976; 8(3): 561-571.

67. Bunnell BA, Estes BT, Guilak F Guilak, Gimble JM. "Differentiation of Adipose Stem Cells" *Met Mol Biol*. 2008; 456:155-171.

68. Li H, Zimmerlin L, Marra KG, Donnenberg VS, Donnenberg AD, Rubin JP. "Adipogenic potential of adipose stem cell subpopulations" *Plast Reconstr Surg*. Sept 2011; 128(3):663-672.

69. Emre Aksu A, Rubin JP, Dudas JR, Marra KG. "Role of Gender and Anatomical Region on Induction of Osteogenic Differentiation of Human Adipose-derived Stem Cells" *Ann Plast. Surg*. Mar 2008; 60(3); 306-320.

70. Sempere, J. M., et al. "Single cell-derived clones from human adipose stem cells present different immunomodulatory properties." *Clinical & Experimental Immunology* 176.2 (2014):255-265.

71. Blazquez, Rebeca, et al. "Immunomodulatory potential of human adipose mesenchymal stem cells derived exosomes on in vitro stimulated T cells." *Frontiers in immunology* 5(2014).

72. Mohammadzadeh, Adel, et al. "Immunomodulatory effects of adipose-derived mesenchymal stem cells on the gene expression of major transcription factors of T cell subsets." *International immunopharmacology* 20.2 (2014): 316-321.

73. Arribas MI, Jones J, Martinez S, Roche E. "Adipose cell-derived stem cells: neurogenic and immunomodulatory potentials." Adv Neuroimmune Biol 2012; 3:19–30.

74. Mazo M, Planat-Benard V, Abizanda G, Pelacho B, Leobon B, Gavira JJ, Penuelas I, Cemborain A, Penicaud L, Laharrague P, Joffre C, Boisson M, Ecay M, Collantes M, Barba J, Casteilla L, Prosper F. "Transplantation of adipose derived stromal cells is associated with functional improvement in a rat model of chronic myocardial infarction" Eur J Heart Fail. 2008; 10(5): 454-462.

75. Bel A, Planat-Benard V, Ssaito A, Bonnevie L, Bellamy V, Sabbah L, Bellabas L, Brinon B, Vanneaux V, Pradeau P, Peyrard S, Larghero J, Pouly J, Binder P, Garcia S, Shimizu T, Sawa Y, Okano T, Bruneval P, Desnos M, Hagege AA, Casteilla L, Puceat M, Menasche P. "Composite Cell Sheets: A Further Step Towards Safe and Effective Myocardial Regeneration by Cardiac Progenitors Derived from Embryonic Stem Cells" Circulat. 2010; 122: S118-S123.

76. Gershwin ME, Merchant B, Helfand MC, Vickers J, Steinberg AD, Hansen CT "The natural history and immunopathology of outbred athymic (nude) mice." 1975. Clin. Immunol. Immunopathol. 4, 324-340.

77. Pantelouris EM. "Athymic development in the mouse." 1973. Differentiation 1,437-450.

78. Rygaard J. "Thymus and self. Immunobiology of the mouse mutant nude." 1973. F.A.D.L. Copenhagen.

79. Rygaard J, Povlsen CO. "Effects of homozygosity of nude (nu) gene in three inbred strains of mice. A detailed study of mice of three genetic backgrounds (BALB/c, C3H, C57BL/6) with congenital absence of the thymus (nude mouse) at a stage in the gene transfer." 1974. Acta Pathol. Microbiol. Scand. 82, 48-70.

80. Cheers C, Waller R "Activated macrophages in congenitally athymic "nude mice" and in lethally irradiate mice." 1975. J. Immunol. 115, 844-847.

81. Rama Rao G, Rawls WE, Perey DYE, Tompkins WAF "Macrophage activation in congenitally athymic nude mice raised under conventional or germ-free conditions." 1977. Journal of the Reticuloendothelial Society 21, 13-20.

82. Bilodeau K, Mantovani D. Bioreactors for tissue engineering: focus on mechanical constraints. A comparative review. Tiss Eng. 2006;12(8):2367-2383.

83. Brayfield CA, Marra KG, Leonard JP, Cui XT, Gerlach JC (2008) Excimer laser channel creation in polyethersulfone hollow fibers for compartmentalized in vitro neuronal cell culture scaffolds. Acta Biomat. **4**(2):244-255.

84. Miki T, Ring A, Gerlach JC (2011) Three-Dimensional Dynamic Perfusion Culture Conditions Promote Hepatic Differentiation of Human Embryonic stem Cells. Tiss Engr Part C: Methods. **17**(5),557-68.

85. Gerlach JC, Hout M, Edsbagge J, Björquist P, Lübberstedt M, et al. (2010) Dynamic 3D culture promotes spontaneous embryonic stem cell differentiation *in vitro*. Tiss Engr: Part C: Methods. **16**(1), 115-121.

86. Gerlach JC, Lübberstedt M, Edsbagge J, Ring A, Hout M, et al. (2010) Interwoven four-compartment capillary membrane technology for 3D perfusion with decentral mass exchange to scale-up embryonic stem cell culture. Cells Tissues Organs. **192**(1), 39-49.

87. Ring A, Gerlach JC, Peters, G, Pazin B, Minervini C, et al. (2010) Hepatic maturation of human fetal hepatocytes in four-compartment 3D perfusion culture. Tiss Engr Part C: Methods. **16**(5), 835-45.

88. Schmelzer E, Triolo F, Turner ME, Thompson RL, Zeilinger K, et al. (2010) Three-dimensional perfusion bioreactor culture supports differentiation of human fetal liver cells. Tiss Engr Part A. **16**(6), 2007-16.

89. Stachelscheid H, Wulf-Goldenberg A, Eckert K, Jensen J, Edsbagge J, et al. (2012) Teratoma formation of human embryonic stem cells in three-dimensional perfusion culture bioreactors. J Tissue Eng Regen Med. **7**(9), 729-741.

90. Mauney JR, Nguyen T, Gillen K, Kirker-Head C, Gimble JM, et al (2007) Engineering adipose-like tissue in vitro and in vivo utilizing human bone marrow and adipose-derived mesenchymal stem cells with silk fibroin 3D scaffolds. Biomat. **28,** 5280-5290.

91. Unsworth BR & Lelkes PI. (1998). Growing tissues in microgravity. *Nature medicine*, *4*(8), 901-907.

92. Hwang YS, Cho J, Tay F, Heng JY, Ho R, Kazarian SG, et al., (2009). The use of murine embryonic stem cells, alginate encapsulation, and rotary microgravity bioreactor in bone tissue engineering. *Biomaterials*, *30*(4), 499-507.

93. Korossis SA, Bolland F, Kearney JN, Fisher J, Ingham E. Bioreactors in Tissue Engineering. Topics in Tiss Eng. 2005;2(8): 1-23.

94. Liao J, Guo X, Grande-Allen KJ, Kasper FK, Mikos AG. Bioactive polymer/extracellular matrix scaffolds fabricated with a flow perfusion bioreactor for cartilage tissue engineering. Biomat. 2010;31(34): 8911-8920.

95. Bancroft GN, Sikavitsas VI, Mikos AG. Design of a Flow Perfusion Bioreactor System for Bone Tissue-Engineering Applications. Tiss Eng. 2003;9(3): 549-554.

96. Irgang M, Sauer IM, Karlas A, Zeilinger K, Gerlach JC, Kurth R, Neuhaus P, Denner J. Porcine endogenous retroviruses: no infection in patients treated with a bioreactor based on porcine liver cells. J of Clin Virol. 2004;28(2): 141-154.

97. Miki T, Ring A, Gerlach JC. Hepatic Differentiation of Human Embryonic Stem Cells Is Promoted by Three-Dimensional Dynamic Perfusion Culture Conditions. Tiss Eng C: Methods. 2011;17(5): 557-568.

98. Martin I, Wendt D, Heberer M. (2004). The role of bioreactors in tissue engineering. *TRENDS in Biotechnology*, *22*(2), 80-86.

99. Mol A, Driessen NJ, Rutten MC, Hoerstrup SP, Bouten CV, Baaijens FP. (2005). Tissue engineering of human heart valve leaflets: a novel bioreactor for a strain-based conditioning approach. *Annals of biomedical engineering*, *33*(12), 1778-1788.

100. Moon DG, Christ G, Stitzel JD, Atala A, Yoo JJ. (2008). Cyclic mechanical preconditioning improves engineered muscle contraction. Tissue Engineering Part A, 14(4), 473-482.

101. Sorkin, Adam M., Kay C. Dee, and Melissa L. Knothe Tate. ""Culture shock" from the bone cell's perspective: emulating physiological conditions for mechanobiological investigations." American Journal of Physiology-Cell Physiology 287.6 (2004): C1527-C1536.

102. Matrix Membranes, 2014. www.matrixmembranes.com Accessed 7 February 2015.

103. Corning, 2015. www.corning.com Accessed 7 February 2015.

104. Becker, Jeanne L., and Glauco R. Souza. "Using space-based investigations to inform cancer research on Earth." *Nature Reviews Cancer* 13.5 (2013): 315-327.Cnop M, Welsh N, Jonas JC, Jörns A, Lenzen S, Eizirik DL. Mechanisms of Pancreatic β-Cell Death in Type 1 and Type 2 Diabetes: Many Differences, Few Similarities. *Diabetes*. 2005; 54(2): S97-107.

105.   Center for Disease Control and Prevention, "More than 29 million Americans have diabetes; 1 in 4 doesn't know;" U.S. Department of Health and Human Services, 10 June 2014, Press release.

106.   NASA Educational Brief. "NASA's Bioreactor: Growing Cells in a Microgravity Environment," EB-2002-12-187-MSFC.

107.   Wong J. (1997). Cells in space. *Nature medicine*, *3*(3), 259-259.

108.   Barzegari A & Saei AA. (2012). An update to space biomedical research: tissue engineering in microgravity bioreactors. *BioImpacts: BI*, *2*(1), 23.

109.   Song C, Duan XQ, Li X, Han LO, Xu P, Song CF, Jin LH. (2004). Experimental study of rat beta islet cells cultured under simulated microgravity conditions. *Acta biochimica et biophysica Sinica*, *36*(1), 47-50.

110.   Song C, Duan XQ, Zhou Y, Li X, Han LO, Xu P *et al.* (2004). Experimental Study on Islet Cells in Rats Under Condition of Three-Dimensional Microgravity. *Zhonghua Wai Ke Za Zhi,* 42(9), 559-561.

111.   Rutzky LP, Bilinski S, Kloc M, Phan T, Zhang H, Katz SM, Stepkowski SM. (2002). Microgravity culture condition reduces immunogenicity and improves function of pancreatic islets1. *Transplantation*, *74*(1), 13-21.

112.   Murray HE, Paget MB, Downing R. (2005). Preservation of glucose responsiveness in human islets maintained in a rotational cell culture system. *Molecular and cellular endocrinology*, *238*(1), 39-49.

113.   Samuelson L & Gerber DA. (2012). Improved function and growth of pancreatic cells in a three-dimensional bioreactor environment. *Tissue Engineering Part C: Methods*, *19*(1), 39-47.

114.   Tanaka H, Tanaka S, Sekine K, Kita S, Okamura A, et al. (2013). The generation of pancreatic B-cell spheroids in a simulated microgravity culture system. *Biomat*, *34*, 5785-5791.

115.   Stepkowski SM, Phan T, Zhang H, Bilinski S, Kloc M, et al. (2006). Immature Syngeneic Dendritic Cells Potentiate Tolerance to Pancreatic Islet Allografts Depleted of Donor Dendritic Cells in Microgravity Culture Condition. *Transplantation, 82*, 1756-1763.

116.   Hoesli CA., Luu M, Piret JM. (2009). A novel alginate hollow fiber bioreactor process for cellular therapy applications. *Biotechnology progress*, *25*(6), 1740-1751.

117.   Lu Y, Zhang G, Shen C, Uygun K, Yarmush ML, et al. (2012). A Novel 3D Organoid System for Elucidation of Hepatic Glucose Metabolism. *Biotech and Bioeng, 109*(2), 595-604.

118.   Chawla M, Bodnar CA, Sen A, Kallos MS, Behie LA. (2006). Production of Islet-Like Structures from Neonatal Porcine Pancreatic Tissue in Suspension Bioreactors. *Biotechnology progress*, *22*(2), 561-567.

119.   Dutt K, Sanford G, Harris-Hooker S, Brako L, Kumar R, et al. (2003). Three-dimensional model of angiogenesis: coculture of human retinal cells with bovine aortic endothelial cells in the NASA bioreactor. *Tissue engineering*, *9*(5), 893-908.

120.   Naughton G, Mansbridge J, Gentzkow G. (1997). A metabolically active human dermal replacement for the treatment of diabetic foot ulcers. *Artificial organs*, *21*(11), 1203-1210.

121.   Kemmerrer SV & Bagley DK. (2002). Dermagraft® scale-up case study. In *Engineering in Medicine and Biology, 2002. 24th Annual Conference and the Annual Fall Meeting of the Biomedical Engineering Society EMBS/ BMES Conference, 2002. Proceedings of the Second Joint* (Vol. 1, pp. 879-880). IEEE.

122.   Summers SA, Garza LA, Zhou H. Regulation of Insulin-Stimulated Glucose Transporter GLUT4 Translocation and Akt Kinase Activity by Ceramide. *Mol and Cell Biol.* 1998; 18(9):5457-5464.

123.   Sivakumar G, Medina-Bolivar F, Lay J, Dolan M, Condori J, et al. (2011). Bioprocess and bioreactor: next generation technology for production of potential plant-based antidiabetic and antioxidant molecules. *Current medicinal chemistry*, *18*(1), 79-90.

124.   Kanner J, & Lapidot T. (2001). The stomach as a bioreactor: dietary lipid peroxidation in the gastric fluid and the effects of plant-derived antioxidants. *Free Radical Biology and Medicine*, *31*(11), 1388-1395.

125.   Gorelik S, Ligumsky M, Kohen R, KannerJ. (2008). The stomach as a "bioreactor": when red meat meets red wine. *Journal of agricultural and food chemistry*, *56*(13), 5002-5007.

126.   Ho JAA, Wu LC, Fan NC, Lee MS, Kuo HY, et al. (2007). Development of a long-life capillary enzyme bioreactor for the determination of blood glucose. *Talanta*, *71*(1), 391-396.

127.   Jung E-S, Kim H-J, Oh D-K. (2005). Tagatose Production by Immobilized Recombinant Escherichia coli Cells Containing Geobacillus stearothermophilus L-Arabinose Isomerase Mutant in a Packed-Bed Bioreactor. Biotecnol. Prog., 21, 1335-1340.

128.   Minteer, Danielle M., Jorg C. Gerlach, and Kacey G. Marra. "Bioreactors Addressing Diabetes Mellitus." *Journal of diabetes science and technology* (2014): 1932296814548215.

129.   Sugihara, Hajime, et al. "Primary cultures of unilocular fat cells: characteristics of growth in vitro and changes in differentiation properties." *Differentiation* 31.1 (1986): 42-49.

130.   Zhang, H. H., et al. "Ceiling culture of mature human adipocytes: use in studies of adipocyte functions." *Journal of Endocrinology* 164.2 (2000): 119-128.

131.   Fernyhough, M. E., et al. "Primary adipocyte culture: adipocyte purification methods may lead to a new understanding of adipose tissue growth and development." *Cytotechnology* 46.2-3 (2004): 163-172.

132.   Flynn, Lauren, et al. "Adipose tissue engineering with naturally derived scaffolds and adipose-derived stem cells." *Biomaterials* 28.26 (2007): 3834-3842.

133.   Halbleib, Melanie, et al. "Tissue engineering of white adipose tissue using hyaluronic acid-based scaffolds. I: in vitro differentiation of human adipocyte precursor cells on scaffolds." *Biomaterials* 24.18 (2003): 3125-3132.

134.   Masuoka, Kazunori, et al. "Tissue engineering of articular cartilage with autologous cultured adipose tissue-derived stromal cells using atelocollagen honeycomb-shaped scaffold with a membrane sealing in rabbits." *Journal of Biomedical Materials Research Part B: Applied Biomaterials* 79.1 (2006): 25-34.

135.   Patrick Jr, C. W., et al. "Preadipocyte seeded PLGA scaffolds for adipose tissue engineering." *Tissue engineering* 5.2 (1999): 139-151.

136.   Kral, John G., and David L. Crandall. "Development of a human adipocyte synthetic polymer scaffold." *Plastic and reconstructive surgery* 104.6 (1999): 1732-1738.

137.   Rubin, J. Peter, et al. "Collagenous microbeads as a scaffold for tissue engineering with adipose-derived stem cells." *Plastic and reconstructive surgery* 120.2 (2007): 414-424.

138.   Green, Howard, and Mark Meuth. "An established pre-adipose cell line and its differentiation in culture." *Cell* 3.2 (1974): 127-133.

139.   Green, Howard, and Olaniyi Kehinde. "An established preadipose cell line and its differentiation in culture II. Factors affecting the adipose conversion." *Cell* 5.1 (1975): 19-27.

140.   Kang, Xihai, Yubing Xie, and Douglas A. Kniss. "Adipose tissue model using three-dimensional cultivation of preadipocytes seeded onto fibrous polymer scaffolds." *Tissue engineering* 11.3-4 (2005): 458-468.

141.   Kang, Xihai, et al. "Adipogenesis of murine embryonic stem cells in a three-dimensional culture system using electrospun polymer scaffolds." *Biomaterials* 28.3 (2007): 450-458.

142.   Li, Wan-Ju, et al. "Multilineage differentiation of human mesenchymal stem cells in a three-dimensional nanofibrous scaffold." *Biomaterials* 26.25 (2005): 5158-5166.

143.   Scherberich, Arnaud, et al. "Three-Dimensional Perfusion Culture of Human Adipose Tissue-Derived Endothelial and Osteoblastic Progenitors Generates Osteogenic Constructs with Intrinsic Vascularization Capacity." Stem cells 25.7 (2007): 1823-1829.

144.   Li, Wan-Ju, et al. "A three-dimensional nanofibrous scaffold for cartilage tissue engineering using human mesenchymal stem cells." *Biomaterials* 26.6 (2005): 599-609.

145.   Masuokab, Hidemi Hattoria Masato Satod Kazunori, et al. "Osteogenic potential of human adipose tissue-derived stromal cells as an alternative stem cell source." *Cells Tissues Organs* 178 (2004): 2-12.

146.   Li, Wan-Ju, et al. "Electrospun nanofibrous structure: a novel scaffold for tissue engineering." *Journal of biomedical materials research* 60.4 (2002): 613-621.

147.   Betre, Helawe, et al. "Chondrocytic differentiation of human adipose-derived adult stem cells in elastin-like polypeptide." *Biomaterials* 27.1 (2006): 91-99.

148.   Shen, Francis H., et al. "Osteogenic differentiation of adipose-derived stromal cells treated with GDF-5 cultured on a novel three-dimensional sintered microsphere matrix." *The Spine Journal* 6.6 (2006): 615-623.

149.   Shea, Lonnie D., et al. "Engineered bone development from a pre-osteoblast cell line on three-dimensional scaffolds." *Tissue engineering* 6.6 (2000): 605-617.

150.   Garreta, Elena, et al. "Osteogenic differentiation of mouse embryonic stem cells and mouse embryonic fibroblasts in a three-dimensional self-assembling peptide scaffold." *Tissue engineering* 12.8 (2006): 2215-2227.

151.   Clavijo-Alvarez JA, Rubin JP, Bennett J, Nguyen VT, Dudas J, Underwood C, Marra KG. "A novel perfluoroelastomer seeded with adipose-derived stem cells for soft-tissue repair" Plast Reconstr Surg 2006; 118: 1132.

152.   Patrick C, Uthamanthil R, Beahm E, Frye C. "Animal models for adipose tissue engineering" Tiss Eng Part B Rev 2008; 14: 167-178.

153.   Chick, William L., et al. "Cell culture device." U.S. Patent No. 4,242,459. 30 Dec. 1980.

154.   Reach, Gérard, and Michael Y. Jaffrin. "Kinetic modelling as a tool for the design of a vascular bioartificial pancreas: feedback between modelling and experimental validation." *Computer methods and programs in biomedicine* 32.3 (1990): 277-285.

155.   Todisco, S., V. Calabro, and G. Iorio. "A lumped parameter mathematical model of a hollow fiber membrane device for the controlled insulin release." *Journal of membrane science* 106.3 (1995): 221-232.

156.   Papas, Klearchos K., et al. "A stirred microchamber for oxygen consumption rate measurements with pancreatic islets." *Biotechnology and bioengineering* 98.5 (2007): 1071-1082.

157.   Center for Disease Control. "Adult Obesity Facts." August 13, 2012. Available from http://www.cdc.gov/obesity/data/adult.html. Accessed 06 November 2012.

158.   Center for Disease Control. "National Diabetes Fact Sheet, 2011." Available from http://www.cdc.gov/diabetes/pubs/pdf/ndfs_2011.pdf. Accessed 06 November 2012.

159.   Marcelino H, Veyrat-Durebex C, Summermatter S. et al. (2013) A Role for Adipose Tissue De Novo Lipogenesis in Glucose Homeostasis During Catch-up Growth. Diabetes, **62**(2), 362-372, 2013.

160.   Gerlach JC, Hout M, Edsbagge J, Björquist P, Lübberstedt M, et al. (2010) Dynamic 3D culture promotes spontaneous embryonic stem cell differentiation *in vitro*. Tiss Engr: Part C: Methods. **16**(1), 115-121.

161.   Gerlach JC, Lübberstedt M, Edsbagge J, Ring A, Hout M, et al. (2010) Interwoven four-compartment capillary membrane technology for 3D perfusion with decentral mass exchange to scale-up embryonic stem cell culture. Cells Tissues Organs. **192**(1), 39-49.

162.   Ring A, Gerlach JC, Peters, G, Pazin B, Minervini C, et al. (2010) Hepatic maturation of human fetal hepatocytes in four-compartment 3D perfusion culture. Tiss Engr Part C: Methods. **16**(5), 835-45.

163.   Schmelzer E, Triolo F, Turner ME, Thompson RL, Zeilinger K, et al. (2010) Three-dimensional perfusion bioreactor culture supports differentiation of human fetal liver cells. Tiss Engr Part A. **16**(6), 2007-16.

164.   Stachelscheid H, Wulf-Goldenberg A, Eckert K, Jensen J, Edsbagge J, et al. (2012) Teratoma formation of human embryonic stem cells in three-dimensional perfusion culture bioreactors. J Tissue Eng Regen Med. **7**(9), 729-741.

165.   Kissebah AH, Vydelingum N, Murray R, Evans DJ, Kalkhoff RD, et al. (1982) Relation of body fat distribution to metabolic complications of obesity. J Clin Endocrinol Metab. **54**, 254-260.

166.   Lofgren P, Hoffstedt J, Myden M, Thorne A, Holm C, et al. (2002) Major gender differences in the lipolytic capacity of abdominal subcutaneous fat cells in obesity observed before and after long-term weight reduction J Clin Endocrinol Metab. **87,** 764-771.

167.   Ramis J, Salinas R, Garcia-Sanz JM, Moreiro J, Proenza AM, et al. (2006) Depot- and gender-related differences in the lipolytic pathway of adipose tissue from severely obese patients Cell Phys Biochem. **17,** 173-180.

168.   Mikus CR, Oberlin DJ, Libla JL, Taylor AM, Booth FW et al. (2012) Lowering physical activity impairs glycemic control in healthy volunteers. Med Sci Sports Exerc. **44**(2): 225-31, 2012.

169.   Kelley, David E., et al. "Subdivisions of subcutaneous abdominal adipose tissue and insulin resistance." *American Journal of Physiology-Endocrinology And Metabolism* 278.5 (2000): E941-E948.

170.   Goodpaster, Bret H., F. Leland Thaete, and David E. Kelley. "Thigh adipose tissue distribution is associated with insulin resistance in obesity and in type 2 diabetes mellitus." *The American journal of clinical nutrition* 71.4 (2000): 885-892.

171.   Goodpaster, Bret H., et al. "Association between regional adipose tissue distribution and both type 2 diabetes and impaired glucose tolerance in elderly men and women." *Diabetes care* 26.2 (2003): 372-379.

172.   Kelley, David E., and Bret H. Goodpaster. "Skeletal muscle triglyceride an aspect of regional adiposity and insulin resistance." *Diabetes Care* 24.5 (2001): 933-941.

173.   Gallagher, Dympna, et al. "Adipose tissue in muscle: a novel depot similar in size to visceral adipose tissue." *The American journal of clinical nutrition* 81.4 (2005): 903-910.

174.   Goodpaster, Bret H., et al. "Subcutaneous abdominal fat and thigh muscle composition predict insulin sensitivity independently of visceral fat." *Diabetes* 46.10 (1997): 1579-1585.

175.   Kelley, David E., et al. "Plasma fatty acids, adiposity, and variance of skeletal muscle insulin resistance in type 2 diabetes mellitus." *The Journal of Clinical Endocrinology & Metabolism* 86.11 (2001): 5412-5419.

176.   Kanaya, Alka M., et al. "Adipocytokines attenuate the association between visceral adiposity and diabetes in older adults." *Diabetes Care* 27.6 (2004): 1375-1380.

177.   Amati, Francesca, et al. "Lower thigh subcutaneous and higher visceral abdominal adipose tissue content both contribute to insulin resistance." *Obesity* 20.5 (2012): 1115-1117.

178.   Ng, Jason M., et al. "PET imaging reveals distinctive roles for different regional adipose tissue depots in systemic glucose metabolism in nonobese humans." *American Journal of Physiology-Endocrinology and Metabolism* 303.9 (2012): E1134-E1141.

179.   Ouchi N, Parker JL, Lugus JL, Walsh K. "Adipokines in inflammation and metabolic disease" *Nature Rev Immunol*. Feb 2011; 11: 85-97.

180.   Summers SA. Ceramides in insulin resistance and lipotoxicity. *Prog in Lipid Res*. 2006; 45: 42-72.

181.   Gilbert, Thomas W., Tiffany L. Sellaro, and Stephen F. Badylak. "Decellularization of tissues and organs." *Biomaterials* 27.19 (2006): 3675-3683.

182.   Crapo, Peter M., Thomas W. Gilbert, and Stephen F. Badylak. "An overview of tissue and whole organ decellularization processes." *Biomaterials* 32.12 (2011): 3233-3243.

183.   Badylak, Stephen F., Doris Taylor, and Korkut Uygun. "Whole-organ tissue engineering: decellularization and recellularization of three-dimensional matrix scaffolds." *Annual review of biomedical engineering* 13 (2011): 27-53.

184.   Jackson DW, Grood ES, Arnoczky SP, Butler DL, Simon TM. Cruciate reconstruction using freeze dried anterior cruciate ligament allograft and a ligament augmentation device (LAD). An experi- mental study in a goat model. Am J Sports Med 1987;15:528–38.

185.   Jackson DW, Grood ES, Arnoczky SP, Butler DL, Simon TM. Freeze dried anterior cruciate ligament allografts. Preliminary studies in a goat model. Am J Sports Med 1987;15:295–303.

186.   Jackson DW, Grood ES, Cohn BT, Arnoczky SP, Simon TM, Cummings JF. The effects of in situ freezing on the anterior cruciate ligament. An experimental study in goats. J Bone Joint Surg Am 1991;73:201–13.

187.   Jackson DW, Grood ES, Wilcox P, Butler DL, Simon TM, Holden JP. The effects of processing techniques on the mechanical properties of bone–anterior cruciate ligament–bone allografts. An experimental study in goats. Am J Sports Med 1988;16:101–5.

188.   Jackson DW, Windler GE, Simon TM. Intraarticular reaction associated with the use of freeze-dried, ethylene oxide-sterilized bone–patella tendon–bone allografts in the reconstruction of the anterior cruciate ligament. Am J Sports Med 1990;18:1–10 [discussion 10-1].

189.   Roberts TS, Drez Jr D, McCarthy W, Paine R. Anterior cruciate ligament reconstruction using freeze-dried, ethylene oxide-sterilized, bone–patellar tendon–bone allografts. Two year results in thirty-six patients. Am J Sports Med 1991;19:35–41.

190.   Gulati AK. Evaluation of acellular and cellular nerve grafts in repair of rat peripheral nerve. J Neurosurg 1988;68:117–23.

191.   De Filippo RE, Yoo JJ, Atala A. Urethral replacement using cell seeded tubularized collagen matrices. J Urol 2002;168:1789–92 [discussion 1792-3].

192.   Falke G, Yoo JJ, Kwon TG, Moreland R, Atala A. Formation of corporal tissue architecture in vivo using human cavernosal muscle and endothelial cells seeded on collagen matrices. Tissue Eng 2003;9:871–9.

193.   Probst M, Dahiya R, Carrier S, Tanagho EA. Reproduction of functional smooth muscle tissue and partial bladder replacement. Br J Urol 1997;79:505–15.

194.   Yoo JJ, Meng J, Oberpenning F, Atala A. Bladder augmentation using allogenic bladder submucosa seeded with cells. Urology 1998;51:221–5.

195.   Hodde J, Hiles M. Virus safety of a porcine-derived medical device: evaluation of a viral inactivation method. Biotechnol Bioeng 2002;79:211–6.

196.   Pruss A, Kao M, Kiesewetter H, von Versen R, Pauli G. Virus safety of avital bone tissue transplants: evaluation of sterilization steps of spongiosa cuboids using a peracetic acid–methanol mixture. Biolo- gicals 1999;27:195–201.

197.   Brown B, Lindberg K, Reing J, Stolz DB, Badylak SF. The basement membrane component of biologic scaffolds derived from extracellular matrix. Tissue Eng 2005, in press.

198.   Hodde JP, Badylak SF, Brightman AO, Voytik-Harbin SL. Glycosaminoglycan content of small intestinal submucosa: a bioscaf- fold for tissue replacement. Tissue Eng 1996;2:209–17.

199.   Hodde J, Record R, Tullius R, Badylak S. Fibronectin peptides mediate HMEC adhesion to porcine-derived extracellular matrix. Biomaterials 2002;23:1841–8.

200.   Hodde JP, Record RD, Liang HA, Badylak SF. Vascular endothelial growth factor in porcine-derived extracellular matrix. Endothelium 2001;8:11–24.

201.   Voytik-Harbin SL, Brightman AO, Kraine MR, Waisner B, Badylak SF. Identification of extractable growth factors from small intestinal submucosa. J Cell Biochem 1997;67:478–91.

202.   Badylak S, Liang A, Record R, Tullius R, Hodde J. Endothelial cell adherence to small intestinal submucosa: an acellular bioscaffold. Biomaterials 1999;20:2257–63.

203.   Badylak SF, Record R, Lindberg K, Hodde J, Park K. Small intestinal submucosa: a substrate for in vitro cell growth. J Biomater Sci Polym Ed 1998;9:863–78.

204.   Hodde JP, Record RD, Tullius RS, Badylak SF. Retention of endothelial cell adherence to porcine-derived extracellular matrix after disinfection and sterilization. Tissue Eng 2002;8:225–34.

205.   McFetridge PS, Daniel JW, Bodamyali T, Horrocks M, Chaudhuri JB. Preparation of porcine carotid arteries for vascular tissue engineering applications. J Biomed Mater Res A 2004;70:224–34.

206.   Teebken OE, Bader A, Steinhoff G, Haverich A. Tissue engineering of vascular grafts: human cell seeding of decellularised porcine matrix. Eur J Vasc Endovasc Surg 2000;19:381–6.

207.   Voet D, Voet JG, Pratt CW. Fundamentals of biochemistry. New York: Wiley; 2002.

208.   Freyman T. Decellularized bone marrow extracellular matrix. USA, 2005

209.   Gamba PG, Conconi MT, Lo Piccolo R, Zara G, Spinazzi R, Parnigotto PP. Experimental abdominal wall defect repaired with acellular matrix. Pediatr Surg Int 2002;18:327–31.

210.   Gilbert, Thomas W., John M. Freund, and Stephen F. Badylak. "Quantification of DNA in biologic scaffold materials." *Journal of Surgical Research* 152.1 (2009): 135-139.

211.   Atala A, Bauer SB, Soker S, Yoo JJ, Retik AB. Tissue-engineered autologous bladders for patients needing cystoplasty. Lancet 2006;367:1241–1246.

212.   Barber FA, Herbert MA, Coons DA. Tendon augmentation grafts: biomechanical failure loads and failure patterns. Arthroscopy 2006;22:534–538.

213.   Brigido SA. The use of an acellular dermal regenerative tissue matrix in the treatment of lower extremity wounds: a prospective 16-week pilot study. Int Wound J 2006;3:181–187.

214.   Butler CE, Prieto VG. Reduction of adhesions with composite AlloDerm/polypropylene mesh implants for abdominal wall reconstruction. Plast Reconstr Surg 2004;114:464–473.

215.   Catena F, Ansaloni L, Leone A, De Cataldis A, Gagliardi S, Gazzotti F, Peruzzi S, Agrusti S, D'Alessandro L, Taffurelli M. Lichtenstein repair of inguinal hernia with Surgisis inguinal hernia matrix soft-tissue graft in immunodepressed patients. Hernia 2005;9:29–31.

216.   Coons DA, Alan Barber F. Tendon graft substitutes-rotator cuff patches. Sports Med Arthrosc 2006;14:185–190.

217.   Harper C. Permacol: clinical experience with a new biomaterial. Hosp Med 2001;62:90–95.

218.   Lee MS. GraftJacket augmentation of chronic Achilles tendon ruptures. Orthopedics 2004;27:s151– 153.

219.   Liyanage SH, Purohit GS, Frye JN, Giordano P. Anterior abdominal wall reconstruction with a Permacol implant. Br J Plast Surg. 2005

220.   Metcalf MH, Savoie FH, Kellum B. Surgical technique for xenograft (SIS) augmentation of rotator- cuff repairs. Oper Tech Orthop 2002;12:204–208.

221.   Parker DM, Armstrong PJ, Frizzi JD, North JH Jr. Porcine dermal collagen (Permacol) for abdominal wall reconstruction. Curr Surg 2006;63:255–258.

222.   Sclafani AP, Romo T 3rd, Jacono AA, McCormick S, Cocker R, Parker A. Evaluation of acellular dermal graft in sheet (AlloDerm) and injectable (micronized AlloDerm) forms for soft tissue augmentation. Clinical observations and histological analysis. Arch Facial Plast Surg 2000;2:130– 136.

223.   Smart N, Immanuel A, Mercer-Jones M. Laparoscopic repair of a Littre's hernia with porcine dermal collagen implant (Permacol). Hernia. 2007

224.   Ueno T, Pickett LC, de la Fuente SG, Lawson DC, Pappas TN. Clinical application of porcine small intestinal submucosa in the management of infected or potentially contaminated abdominal defects. J Gastrointest Surg 2004;8:109–112.

225.   Badylak, S. F., T. Hoppo, A. Nieponice, T. W. Gilbert, J. M. Davison, and B. A. Jobe. Esophageal preservation in five male patients after endoscopic inner-layer circumferential resection in the setting of superficial cancer: a regenerative medicine approach with a biologic scaffold. Tissue Eng Part A 17:1643–1650, 2011.

226.   Badylak, S. F., G. C. Lantz, A. Coffey, and L. A. Geddes. Small intestinal submucosa as a large diameter vascular graft in the dog. J Surg Res 47:74–80, 1989.

227.   Ho, K. L., M. N. Witte, and E. T. Bird. 8-ply small intestinal submucosa tension-free sling: spectrum of postoperative inflammation. J Urol 171:268–271, 2004.

228.   Petter-Puchner, A. H., R. H. Fortelny, R. Mittermayr, N. Walder, W. Ohlinger, and H. Redl. Adverse effects of porcine small intestine submucosa implants in experimental ventral hernia repair. Surg Endosc 20:942–946, 2006.

229.   Badylak, Stephen F. "Decellularized allogeneic and xenogeneic tissue as a bioscaffold for regenerative medicine: factors that influence the host response." *Annals of biomedical engineering* 42.7 (2014): 1517-1527.

230.   Zhang, Q., M. Raoof, Y. Chen, Y. Sumi, T. Sursal, et al. Circulating mitochondrial DAMPs cause inflammatory responses to injury. Nature 464:104–107, 2010.

231.   Crapo, P. M., T. W. Gilbert, and S. F. Badylak. An overview of tissue and whole organ decellularization processes. Biomaterials 32:3233–3243, 2011.

232.   Limana, F., A. Germani, A. Zacheo, J. Kajstura, A. Di Carlo, et al. Exogenous high-mobility group box 1 protein induces myocardial regeneration after infarction via enhanced cardiac C-kit+ cell proliferation and differentiation. Circ Res 97:e73–e83, 2005.

233.   Tian, J., A. M. Avalos, S. Y. Mao, B. Chen, K. Senthil, et al. Toll-like receptor 9-dependent activation by DNAcontaining immune complexes is mediated by HMGB1 and RAGE. Nat Immunol 8:487–496, 2007.

234.   Yang, D., Q. Chen, H. Yang, K. J. Tracey, M. Bustin, and J. J. Oppenheim. High mobility group box-1 protein induces the migration and activation of human dendritic cells and acts as an alarmin. J Leukoc Biol 81:59–66, 2007.

235.   Thomas, J. O. HMG1 and 2: architectural DNA-binding proteins. Biochem Soc Trans 29:395–401, 2001.

236.   Andrassy, M., H. C. Volz, J. C. Igwe, B. Funke, S. N. Eichberger, et al. High-mobility group box-1 in ischemia reperfusion injury of the heart. Circulation 117:3216–3226, 2008.

237.   Porto, A., R. Palumbo, M. Pieroni, G. Aprigliano, R. Chiesa, et al. Smooth muscle cells in human atherosclerotic plaques secrete and proliferate in response to high mobility group box 1 protein. FASEB J 20:2565–2566, 2006.

238.   Lolmede, K., L. Campana, M. Vezzoli, L. Bosurgi, R. Tonlorenzi, et al. Inflammatory and alternatively activated human macrophages attract vessel-associated stem cells, relying on separate HMGB1- and MMP-9-dependent pathways. J Leukoc Biol 85:779–787, 2009.

239.   Ranzato, E., M. Patrone, M. Pedrazzi, and B. Burlando. HMGb1 promotes scratch wound closure of HaCaT keratinocytes via ERK1/2 activation. Mol Cell Biochem 332:199–205, 2009.

240.   De Mori, R., S. Straino, A. Di Carlo, A. Mangoni, G. Pompilio, et al. Multiple effects of high mobility group box protein 1 in skeletal muscle regeneration. Arterioscler Thromb Vasc Biol 27:2377–2383, 2007.

241.   McPherson, T. B., H. Liang, R. D. Record, and S. F. Badylak. Galalpha(1,3)Gal epitope in porcine small intestinal submucosa. Tissue Eng 6:233–239, 2000.

242.   Daly, K., A. Stewart-Akers, H. Hara, M. Ezzelarab, C. Long, et al. Effect of the alphaGal epitope on the response to small intestinal submucosa

extracellular matrix in a nonhuman primate model. Tissue Eng. Part A. 15(12), 3877–3888, 2009.

243.   Anderson, J. M. Inflammatory response to implants. ASAIO Trans 34:101–107, 1988.

244.   Anderson, J. M., A. Rodriguez, and D. T. Chang. Foreign body reaction to biomaterials. Semin Immunol 20:86–100, 2008.

245.   Colorado, P. C., A. Torre, G. Kamphaus, Y. Maeshima, H. Hopfer, et al. Anti-angiogenic cues from vascular basement membrane collagen. Cancer Res 60:2520–2526, 2000.

246.   O'Reilly, M. S., T. Boehm, Y. Shing, N. Fukai, G. Vasios, et al. Endostatin: an endogenous inhibitor of angiogenesis and tumor growth. Cell 88:277–285, 1997.

247.   Ramchandran, R., M. Dhanabal, R. Volk, M. J. Waterman, M. Segal, et al. Antiangiogenic activity of restin, NC10 domain of human collagen XV: comparison to endostatin. Biochem Biophys Res Commun 255:735–739, 1999.

248.   Reing, J. E., L. Zhang, J. Myers-Irvin, K. E. Cordero, D.O. Freytes, et al. Degradation products of extracellular matrix affect cell migration and proliferation. Tissue Eng Part A 15:605–614, 2009.

249.   Gilbert, T. W., M. S. Sacks, J. S. Grashow, S. L. Woo, S. F. Badylak, and M. B. Chancellor. Fiber kinematics of small intestinal submucosa under biaxial and uniaxial stretch. J Biomech Eng 128:890–898, 2006.

250.   Musahl, V., S. D. Abramowitch, T. W. Gilbert, E. Tsuda, J. H. Wang, et al. The use of porcine small intestinal submucosa to enhance the healing of the

medial collateral ligament—a functional tissue engineering study in rabbits. J Orthop Res 22:214–220, 2004.

251.   Reing, J. E., B. N. Brown, D. A. Daly, J. M. Freund, T.W. Gilbert, et al. The effects of processing methods upon mechanical and biologic properties of porcine dermal extracellular matrix scaffolds. Biomaterials 31:8626–8633, 2010.

252.   Martin, P., and J. Lewis. Actin cables and epidermal movement in embryonic wound healing. Nature 360:179–183, 1992.

253.   Whitby, D. J., and M. W. Ferguson. The extracellular matrix of lip wounds in fetal, neonatal and adult mice. 112:651–668, 1991.

254.   Longaker, M. T., M. R. Harrison, T. M. Crombleholme, J.C. Langer, M. Decker, et al. Studies in fetal wound healing: A factor in fetal serum that stimulates deposition of hyaluronic acid. J Pediatr Surg 24:789–792, 1989.

255.   Sicari, B. M., S. A. Johnson, B. F. Siu, P. M. Crapo, K. A. Daly, et al. The effect of source animal age upon the in vivo remodeling characteristics of an extracellular matrix scaffold. Biomaterials 33:5524–5533, 2012.

256.   Tottey, S., S. A. Johnson, P. M. Crapo, J. E. Reing, L. Zhang, et al. The effect of source animal age upon extracellular matrix scaffold properties. Biomaterials 32:128–136, 2011.

257.   Brown, B. N., J. E. Valentin, A. M. Stewart-Akers, G. P. McCabe, and S. F. Badylak. Macrophage phenotype and remodeling outcomes in response to biologic scaffolds with and without a cellular component. Biomaterials 30:1482–1491, 2009.

258. Choi JS, Yang H-J, Kim BS, Kim JD, Kim JY, Yoo B, Park K, Lee HY and Cho YW, 2009. Human extracellular matrix (ECM) powders for injectable cell delivery and adipose tissue engineering *J. Control Release* (139) 2–7.

259. Turner AEB and Flynn LE, 2011. Design and characterization of tissue-specific extracellular matrix-derived microcarriers. *Tissue Eng.* C

260. Young DA, Ibrahim DO, Hu D and Christman KL. 2011 Injectable hydrogel scaffold from decellularized human lipoaspirate *Acta Biomaterialia* (7) 1040–9.

261. Young, D. Adam, and Karen L. Christman. "Injectable biomaterials for adipose tissue engineering." *Biomedical materials* 7.2 (2012): 024104.

262. Brown, Bryan N., et al. "Comparison of three methods for the derivation of a biologic scaffold composed of adipose tissue extracellular matrix." *Tissue Engineering Part C: Methods* 17.4 (2011): 411-421.

263. Fischbach C, Spru T, Weiser B, Neubauer M, Becker C, et al. (2004) Generation of mature fat pads in vitro and in vivo utilizing 3-D long-term culture of 3T3-L1 preadipocytes. Experiment Cell Res. **300**, 54-64.

264. Fujisaka, Shiho, et al. "Regulatory mechanisms for adipose tissue M1 and M2 macrophages in diet-induced obese mice." *Diabetes* 58.11 (2009): 2574-2582.

265. Lumeng, Carey N., et al. "Phenotypic switching of adipose tissue macrophages with obesity is generated by spatiotemporal differences in macrophage subtypes." *Diabetes* 57.12 (2008): 3239-3246.

266. Sadati, Kevin S., Anthony C. Corrado, and Robert W. Alexander. "Platelet-rich plasma (PRP) utilized to promote greater graft volume retention in

autologous fat grafting." *The American Journal of Cosmetic Surgery Vol* 23.4 (2006): 203.

267.   Jin, Rong, Lu Zhang, and Yu-Guang Zhang. "Does platelet-rich plasma enhance the survival of grafted fat? An update review." *International journal of clinical and experimental medicine* 6.4 (2013): 252.

268.   Kim, Deok-Yeol, et al. "Effects of Platelet-Rich Plasma, Adipose-Derived Stem Cells, and Stromal Vascular Fraction on the Survival of Human Transplanted Adipose Tissue." *Journal of Korean medical science* 29.Suppl 3 (2014): S193-S200.

269.   Gentile, Pietro, et al. "Breast reconstruction with autologous fat graft mixed with platelet-rich plasma." *Surgical innovation* 20.4 (2013): 370-376.

270.   Salgarello, Marzia, Giuseppe Visconti, and Antonio Rusciani. "Breast fat grafting with platelet-rich plasma: a comparative clinical study and current state of the art." *Plastic and reconstructive surgery* 127.6 (2011): 2176-2185.

271.   Oh, Dong Seok, et al. "Activated platelet-rich plasma improves fat graft survival in nude mice: a pilot study." *Dermatologic Surgery* 37.5 (2011): 619-625.

272.   Rodríguez-Flores, Jordi, et al. "Influence of platelet-rich plasma on the histologic characteristics of the autologous fat graft to the upper lip of rabbits." *Aesthetic plastic surgery* 35.4 (2011): 480-486.

273.   Fraga, Murillo Francisco Pires, et al. "Increased survival of free fat grafts with platelet-rich plasma in rabbits." *Journal of Plastic, Reconstructive & Aesthetic Surgery* 63.12 (2010): e818-e822.

274.   Nakamura, Shinichiro, et al. "Platelet-rich plasma (PRP) promotes survival of fat-grafts in rats." *Annals of plastic surgery* 65.1 (2010): 101-106.

275.   Por, Yong-Chen, et al. "Platelet-rich plasma has no effect on increasing free fat graft survival in the nude mouse." *Journal of Plastic, Reconstructive & Aesthetic Surgery* 62.8 (2009): 1030-1034.